THE EFFECT OF SLIDING INTERFACES AND INHOMOGENEOUS INTERPHASES ON THERMAL AND ELASTIC PROPERTIES OF COMPOSITES

by

Mohamed Wahid Kouider

A DISSERTATION

Submitted to

Michigan State University

in partial fulfillment of the requirements

for the degree of

DOCTOR OF PHILOSOPHY

Department of Metallurgy, Mechanics, and Materials Science

1992

ABSTRACT

The Effect of Sliding Interfaces and Inhomogeneous Interphases on Thermal and Elastic Properties of Composites

by

Mohamed Wahid Kouider

The transition zone between the matrix and the inclusion plays an important role in the transfer of loads, and it is a key factor affecting local stresses, displacement fields, and elastic and thermal properties of composites. In literature, this transition zone is assumed to be either the surface between matrix and inclusion called "interface" or an additional phase existing between matrix and inclusion called "interphase". In this dissertation these two cases are investigated by considering the following two problems.

In the first problem, a composite containing either aligned or randomly oriented short fibers of spheroidal shape is studied. The interface between matrix and fiber allows sliding such that shear tractions are specified to vanish. The fiber interaction is accounted for by using a Mori and Wakashima's (1990) successive iteration method based on a Mori-Tanaka's (1973) average field theory. In this problem

thermal stresses and thermal expansion coefficients of composites are determined by taking the matrix and the fiber to be isotropic in stiffness and transversely isotropic in thermal expansion coefficients. The effect of interface on thermal stresses and properties is investigated by comparing the results for the sliding case with the results for perfectly bonded case.

In the second problem, a composite containing aligned long fibers of cylindrical shape, which are distributed uniformly in the matrix, is studied. The interphase between matrix and inclusion is assumed to be inhomogeneous. Few functional forms are chosen to simulate the radial variation of the thermal and elastic properties in this region. The effect of this interphase on the local elastic fields and the overall thermal and elastic properties is studied. The thermal and elastic properties are assumed to be isotropic in the interphase and the matrix, and transversely isotropic in the inclusion. The perfect bonding is assumed at the matrix/interphase interface and the interphase/inclusion interface. The effective elastic constants and thermal expansion coefficients are derived by using the composite cylinders assemblage model (Hashin and Rosen, 1964) and the generalized self-consistent scheme (Kerner, 1956; Christensen and Lo, 1979).

DEDICATION

To my **Mother, Father,**

Wife,

Son, two Daughters,

and all my **Family**

ACKNOWLEDGEMENTS

I wish to acknowledge all those who assisted me in this undertaking and completion of this dissertation.

I am indepted to professor Iwona Jasiuk my advisor for her valuable time, assistance and encouragement, her kind consideration and understanding have been an incentive for the completion of this dissertation.

Sincere gratitude is extended to the other members of my guidance committee professor Nicholas Altiero, professor Dashin Liu and professor David Yen for their contribution, helpful discussions, and criticism.

Finally, I would like to thank my mother, and my father for my early education and their continuous support. Also, my heartfelt appreciation is extended to all the members of my familly for their constant encouragement and their moral support. My special gratitude goes to my wife Wahiba for her patience, care, and encouragement in each step I made towards the completion of this research. I would also express my deep appreciation to my son Hodhaifa and my two daughters Nousseiba and Alaa whose smiles and childish looks gave me the courage to accomplish my goals.

TABLE OF CONTENTS

TABLE OF CONTENTS (CONT)

TABLE OF CONTENTS (CONT)

LIST OF FIGURES

LIST OF FIGURES (CONT)

LIST OF FIGURES (CONT)

LIST OF FIGURES (CONT)

CHAPTER 1

INTRODUCTION

In composites the transition zone between the matrix and inclusion plays a very important role in the transfer of loads between the two constituents. This transition zone, which results from the bonding process during manufacturing, is seen as a critical area where stress concentrations arise due to the change in material properties. Therefore, it is a key factor affecting the local stresses, displacement fields, and the elastic and thermal properties of composites.

Many models for the transition zone have been proposed in literature to predict the local stress fields and the effective mechanical properties of composite materials. Two terms most commonly used to describe this transition zone are: interface and interphase (Hughes, 1991; Kerans et al., 1989; and Theocaris, 1983). When the transition zone is a two dimensional boundary separating the matrix and inclusions, it is called "interface". Whereas, when it is assumed to be an additional phase between the matrix and inclusion or a third layer, it is called "interphase" or "mesophase". The interphase region may be a coating, but is often a product of manufacturing processes. In fact, it is the region where the inclusion and the matrix phases are chemically and mechanically combined. This interphase may be a diffusion zone, a nucleation zone, a chemical reaction zone, or other.

In the past most of researchers assumed the interface between the matrix and the inclusion to be perfectly bonded. For a

comprehensive list of references, the reader is referred to a survey paper by Hashin (1983), and several books in this area (Christensen, 1979; Taya and Arsenault, 1989; Mura, 1982; Jones, 1975; Dvorak, 1990), among others.

However, microscopic examinations and experimental results indicate that a more complex state may exist at the interface between constituents (Drzal, 1983, 1986, 1987; Hughes, 1991; Theocaris, 1984, 1986, 1987). In reality the bonding may be imperfect due to the poor chemical bonding, or the presence of microcracks due to the thermal loading, for example. Such complicated situation does not allow researchers in this field to model the interface precisely with all parameters taken into consideration. However, simplified interfacial models are used in order to make this problem mathematically tractable. The effect of interfaces on the thermal and elastic behavior of composites has received a lot of attention in literature, especially in the past few years (Kerans et al., 1989; Hughes, 1991). However, the effects of interface are not yet fully understood.

One important model, which was adopted by many reseachers, is the so called "flexible interface model" (Jones and Whitter, 1967; Mal and Bose, 1974; Chatterjee and Kibler, 1979; Lene and Leguillon, 1982; Benveniste, 1984, 1985; Aboudi, 1987; Steif and Hoysan, 1986, 1987; Achenbach and Zhu, 1989, 1990; Jasiuk and Tong, 1989; Jasiuk et al., 1989, 1992; Hashin, 1990a, 1990b, 1991), among others.

This model is based on the simulation of the partial debonding between matrix and inclusion by a thin ficticious layer having a spring-like behavior, with the assumption that the continuity of tractions is maintained and jumps in the normal and tangential displacement are proportional to the corresponding traction components. Therefore, two parameters having the dimension of stress

divided by length, called interface parameters, are introduced to define the degree of bonding between matrix and inclusion in both tangential and normal directions. Specific interface condition can be simulated by a proper selection of those two parameters. For infinite values of these parameters, the displacement jumps vanish and therefore perfect bonding condition is assured at the interface. Whereas, when the values of those parameters vanish, the interface tractions are zero and the inclusion totaly disbonds from the matrix. The pure sliding case occurs when the tangential parameter is zero. The intermediate case when the inclusion is partially disbonded from the matrix is for a finite value of these parameters.

Another interfacial model, so called "interphase model", was adopted by many researchers. These researchers assume that an interphase usually exists between matrix and inclusion. This interphase may be a coating or a product of manufacturing processes. When the interphase is a coating, it is assumed to be a layer around the inclusion and have a known thickness. This interphase is made from different material, which is assumed to have constant thermal and elastic properties for simplicity. This model was used by Broutman and Agarwal (1974), Mikata and Taya (1985, 1986), Maurer et al. (1986, 1988), Luo and Weng (1987), Vedula et al. (1988), Pagano and Tandon (1988), Benveniste et al. (1989), Jasiuk et al. (1989), Dvorak and Chen (1989), Chen et al. (1990), Maurer (1990), Tong and Jasiuk (1990a, 1990b), Sullivan and Hashin (1990), and others.

It has been shown by Hashin (1991), that an interphase layer is equivalent to an imperfect interface provided that the interphase thickness is much smaller than the diameter of the fiber and that the interphase is very compliant in comparison with the properties of matrix and fibers. Hence, the interface parameters in the flexible

interface model can be determined in terms of the elastic properties and thickness of the interphase.

Some reseachers are using more general models in which the interphase is assumed to be inhomogeneous and to have property gradients in the radial direction. Composites with such interphase were studied by Theocaris (1984, 1986, 1987), who developed an interphase model, based on adhesion theory for polymer matrix composites, in which the interphase is assumed to be isotropic in nature with the elastic properties unfolding from those of the fiber to those of the matrix with a specific non-linear radial variation. In this study a composite cylinders assemblage model (Hashin and Rosen, 1964) was used. Sideridis (1988) investigated three models for the interphase shear modulus variation: linear, parabolic, and hyperbolic. The in-plane shear modulus of a unidirectional fiber reinforced composite was determined using the composite cylinders assemblage model. Papanicolaou et al. (1989) assumed an exponential law of variation of the elastic modulus in the interphase. They used the composite cylinders assemblage model to predict the elastic longitudinal modulus of a unidirectional fiber reinforced composite. In the above three models the stress fields were determined in an approximate way. The thermal stresses were determined in a rigorous way by Sottos et al. (1989) using a numerical method and by Jayaraman and Reifsnider (1990) and Jayaraman et al. (1991) using an analytical method. Sottos et al. (1989) assumed a linear variation in the radial direction for both thermal expansion coefficient and elastic modulus in the interphase. In this model the properties of the interphase near the fiber were the multiples of the bulk-matrix properties. The micro-thermal stresses were predicted using the Boundary Fitted Coordinate Technique. Jayaraman and Reifsnider (1990) investigated three models

for the interphase elastic modulus variation: power, reciprocal, and cubic variations. The composite cylinders assemblage model was used in this paper to determine the local stresses of continuous fiber composite. Jayaraman et al. (1991) used Mori-Tanaka average field concept (Benveniste, 1987) to determine thermal stresses of the same composite. In this paper the power variation relationship was used to simulate the change of the elastic modulus and the thermal expansion coefficient in the radial direction. In all of the above models Poisson's ratio in the interphase was assumed to be constant, for simplicity.

In this dissertation two different problems are considered: the pure sliding interface problem and the inhomogeneous interphase problem, in which the effect of interface on the elastic and thermal properties are investigated.

In the first problem, thermal stresses and thermal expansion coefficients of composites containing either aligned or randomly distributed in 2-D and 3-D space short fibers are analyzed. In this analysis the sliding at the fiber-matrix interface is allowed. The effect of friction is neglected for simplicity. The strain, induced by the mismatch of thermal expansion coefficients, is accounted for by introducing eigenstrains in the fibers. The solution for a single sliding spheroidal inclusion, given by Mura et al. (1985), is used to predict the average thermal expansion coefficients of a composite containing finite volume fraction of fibers. The interaction between fibers is accounted for by using Mori and Wakashima's (1990) successive iteration method, which is based on Mori and Tanaka's (1973) average field theory. This theory has been modified in this paper to account for the sliding at the inclusion-matrix interfaces and the fiber misorientation. For reference, the same study is done for a composite

with the fibers perfecly bonded to the matrix, and the effect of interface is investigated by comparing the pure sliding case with the perfectly bonded case. This work is a direct extension of Jasiuk et al. (1988) paper, in which a similar composite system was considered. However, in the present study an alternate method is used and the results are applicable for higher fiber volume fractions. Also, the effect of fiber orientation is investigated. This study is presented in Chapter 3.

In the second problem, the elastic constants and the thermal expansion coefficients of a composite containing long fibers of cylindrical shape uniformly distributed in the matrix are studied. The interphase between matrix and inclusion is assumed to be inhomogeneous and having elastic and thermal properties changing in the radial direction. This study is an extension to the work done by Jayaraman and Reifsnider (1990) and by Jayaraman et al. (1991) who evaluated thermal stresses using three models for the interphase elastic modulus variation: power, reciprocal, and cubic variations, while Poisson's ratio in the interphase was kept constant for simplicity. The above results are extended by evaluating the elastic moduli and thermal expansion coefficients in a closed form by using a power variation relationship simulating the variation of the thermal and elastic modulus in the interphase. Furthermore, the same work is done for few other variation relationships in the radial direction. The solutions for local stresses and thermal and elastic properties are obtained using infinite series. Also, in this study the effect of Poisson's ratio changing in the radial direction in the interphase is investigated. Few variation relationships are assigned to the Poisson's ratio value in the interphase in order to determine its effect on stresses and thermal and elastic properties. It is shown

that the variation in Poisson's ratio property of the interphase has a considerable effect on the local stress fields and the effective elastic and thermal properties. This work is discussed in Chapter 4.

A similar study was done by Sullivan and Hashin (1990) and others for interphase having constant elastic properties to determine the effective axial elastic modulus, axial Poisson's ratio, axial and transverse shear modulus.

The discussion of the above mentioned problems is preceeded by a short discussion of effective medium theories which is included in Chapter 2.

CHAPTER 2

BACKGROUND

In this chapter the effective medium theories used in this dissertation are briefly described in order to give a background to the reader on the methods used. Three theories, the composite cylinders assemblage, the generalized self-consistent scheme, and Mori-Tanaka average field concept are presented.

2.1 COMPOSITE SPHERES AND CYLINDERS MODEL

The composite spheres assemblage model was introduced by Hashin (1962), while the composite cylinders assemblage model was introduced by Hashin and Rosen (1964). In this model the composite is composed of a size gradation of spheres or cylinders embedded in a matrix such that each individual composite has the same ratio of radii, a/c, where a is the fiber radius and c is the outer radius of the matrix for each individual composite cylinder as seen in Fig. 2.1a. This model is modified in this dissertation by introducing a third layer between the fiber and the matrix of outer radius b as seen in Fig. 2.1b (Sullivan and Hashin, 1990). The composite cylinders assemblage model gives an exact solution for the effective axisymmetric properties (effective axial Young's modulus, effective axial Poisson's ratio, and effective transverse plane strain bulk modulus) and the effective axial shear modulus. In Chapter 4 the displacement boundary conditions are used to obtain the four properties mentioned above. Alternatively, rather than imposing displacement boundary conditions, traction boundary conditions

can be imposed. Christensen (1979) stated that the bounds coincide and the results for the above four properties are the same regardless of the type of boundary conditions imposed. In contrast, the composite cylinders assemblage model does not yield the exact solution for the effective transverse shear modulus. The shear modulus solution for displacement boundary conditions for the composite cylinders assemblage model leads to an upper bound for the effective transverse shear modulus, while the solution for shearing traction boundary conditions for the same model leads to the lower bound. The reason why these bounds do not coincide is because in the case where simple shear type displacement components are prescribed on the surface of the composite cylinder, the resulting boundary stresses are not those corresponding to a state of simple shear stress. Correspondingly, when the simple shear stresses are prescribed on a boundary, the resulting surface deformation state is not that of simple shear deformation (Christensen, 1979). Therefore, the composite cylinder cannot be replaced by an equivalent homogeneous cylinder (Hashin, 1983), and the replacement method which leads to equal upper and lower bounds is not applicable.

In Chapter 4, the composite cylinders assemblage model is used for a transversely isotropic composite reinforced by unidirectional long fibers to determine the three axisymmetric effective properties and the effective axial shear property. This model is used because it is a very simple mathematical model. However, since this model does not yield a single solution for the effective transverse shear modulus, an alternate method, the generalized self-consistent scheme (Kerner, 1956; Christensen and Lo, 1979), is used instead for this case (see Section 2.2).

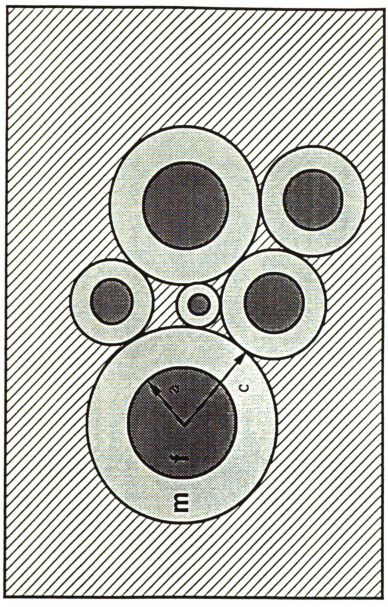

Fig. 2.1a Composite spheres and cylinders assemblage model.

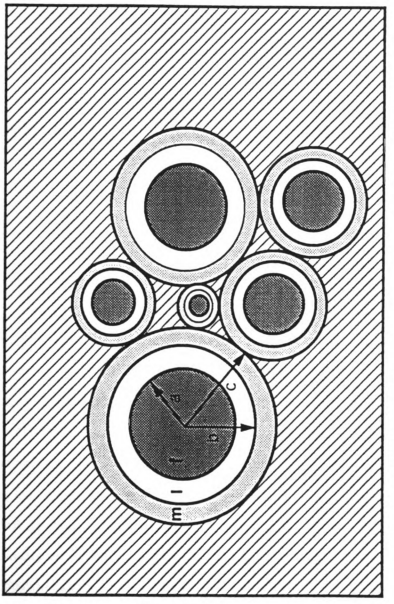

Fig. 2.1b Modified composite spheres and cylinders assemblage model.

2.2 GENERALIZED SELF-CONSISTENT SCHEME

In the self-consistent scheme (Budiansky, 1965; Hill, 1965) an inclusion is assumed to be embedded in a homogeneous body which has the unknown properties of the effective medium (see Fig. 2.2). This defines a boundary value problem which can be solved easily for any perfectly bonded ellipsoidal inclusion by using Eshelby (1957) solution. Hill (1965) showed that the expressions derived by this method give reliable values at low inclusion volume fraction, reasonable values at intermediate volume fractions, and unreliable values at high ones when applied to composite materials. Also, Christensen (1979) commented that this method is suitable for polycrystalline materials but not for composites.

The modification of the self-consistent method is the generalized self-consistent scheme (Kerner, 1956; Christensen and Lo, 1979) in which the inclusion is not embedded directly in the effective medium like in the self-consistent scheme, but it is embedded in a matrix shell, which is in turn embedded in the effective medium to which the effective properties to be determined are assigned (see Fig. 2.3a) Hashin (1983) stated that this method appears to give a more realistic approximation for the effective properties of composite materials since the inclusion is now embedded in a matrix shell instead of being embedded in the effective medium directly. This model satisfies the MMM principle of Hashin (1983), while the self-consistent scheme does not. Furthermore, this model permits a full packing with the volume fraction of inclusions approaching the value one due to the fact that it allows the gradation of sizes of inclusions.

The generalized self-consistent scheme, also called three phase model, gives exact solutions for the five independent effective elastic

properties of a transversely isotropic composite (Christensen, 1979), but the mathematics is more difficult since it is necessary to solve a three-phase boundary value problem to get the stress field around the inclusion. This model is modified by introducing an interphase between the fiber and the matrix (see Fig. 2.3b). In Chapter 4 this model is used to obtain the effective transverse shear modulus. The predicted value of the effective transverse shear modulus lies within Hashin-Shtrikman's (1963) upper and lower bounds.

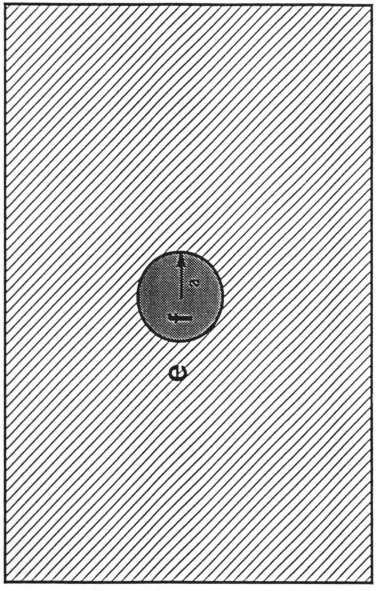

Fig. 2.2 Self-consistent scheme.

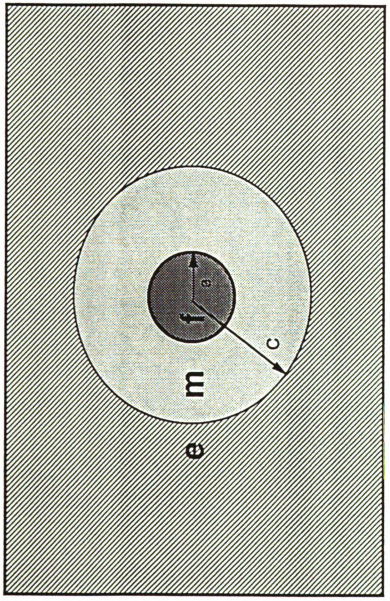

Fig. 2.3a Generalized self-consistent scheme.

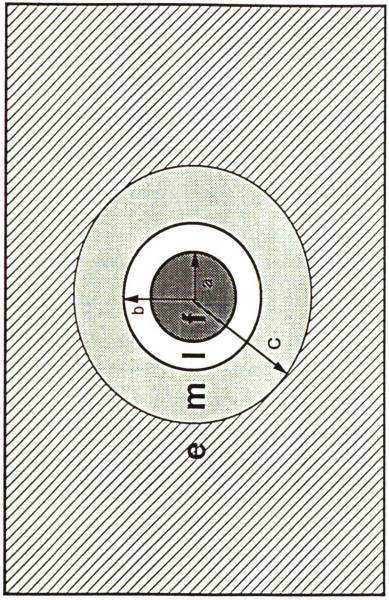

Fig. 2.3b Modified generalized self-consistent scheme.

2.3 MORI-TANAKA AVERAGE FIELD CONCEPT

Another approach is the average field concept of Mori and Tanaka (1973), which is one of the models that account for the interaction between inclusions. To summarize this concept, a composite domain denoted by D is considered, in which inclusions occupy a domain denoted by Ω and the matrix, the remaining domain, denoted by D-Ω. The composite is assumed to be reinforced by a small volume fraction of inclusions f. The bold face letters denote vectors and tensors in this section. If a stress $\boldsymbol{\sigma}^{(0)}$ is applied at infinity, the average total stress in the matrix is $\langle \boldsymbol{\sigma}^{(0)} + \boldsymbol{\sigma} \rangle_{D-\Omega}$, where $\boldsymbol{\sigma}$ is the stress disturbance. Now assume a single inclusion in the infinite medium subjected to the same stress at infinity. Then, the average stress disturbance in this single inclusion is defined as $\langle \boldsymbol{\sigma}^{\infty} \rangle_{\Omega}$. The later quantity was obtained by Eshelby (1957) for the perfect bonding case. If a new single inclusion is introduced to the composite, this addition does not affect the volume fraction f. Then, the average stress in the inclusion is the sum of the average stress disturbance in a single inclusion present in the infinite medium and the total average stress in the matrix, which can be written as

$$\langle \boldsymbol{\sigma}^{(0)} + \boldsymbol{\sigma} \rangle_{\Omega} = \langle \boldsymbol{\sigma}^{(0)} + \boldsymbol{\sigma} \rangle_{D-\Omega} + \langle \boldsymbol{\sigma}^{\infty} \rangle_{\Omega} \tag{2.1}$$

The above relation can be simplified by using the stress disturbance only as

$$\langle \sigma \rangle_{\Omega} = \langle \sigma \rangle_{D-\Omega} + \langle \sigma^{\infty} \rangle_{\Omega} \tag{2.2}$$

The average stress disturbance in the composite must vanish. Therefore,

$$f \langle \sigma \rangle_{\Omega} + (1-f) \langle \sigma \rangle_{D-\Omega} = 0 \tag{2.3}$$

Using equations (2.2) and (2.3), the average stress disturbance in the matrix is obtained as

$$\langle \sigma \rangle_{D-\Omega} = -f \langle \sigma^{\infty} \rangle_{\Omega} \tag{2.4}$$

and, in the inclusion as

$$\langle \sigma \rangle_{\Omega} = (1-f) \langle \sigma^{\infty} \rangle_{\Omega} \tag{2.5}$$

It is to be noted that Mori-Tanaka average field concept gives a good approximation when the volume fraction of inclusions is small. However for large volume fraction of inclusions, the basic results given by Eshelby (1957) need to be modified to account for fibers interaction. The modification was first given by Wakashima et al. (1974) who analyzed thermal expansion of composites. They used Eshelby's solution (1957) of an ellipsoidal inclusion and Mori-Tanaka's concept (1973) of average stress in the matrix. This method was also used by (Taya and Chou, 1981; Taya and Mura, 1981; Weng, 1984; Takao and Taya, 1985; Tandon and Weng, 1986a, 1986b; Takahashi and Chou, 1988; Zhao et al., 1988; Luo and Weng, 1987, 1989; Norris, 1989;

Shibata et al., 1990; Tong and Jasiuk, 1988, 1990a, 1990b), and others.

A recent different interpretation of Mori-Tanaka (1973) is the successive iteration method proposed by Mori and Wakashima (1990). The formulation of this method is the same as given in Wakashima et al. (1974) and recently in Benveniste (1987) but the appraoch is different. The new approach is used to evaluate the average values of stresses and displacements in inhomogeneities and a surrounding matrix, also, it can treat any boundary condition at inclusion-matrix interface provided that the solution for an isolated inclusion is known . Therefore, this method is chosen to solve this problem and is modified to account for sliding and fibers misorientation. The successive iteration method consists of evaluating the stress disturbance in a single representative inclusion. Then, the contribution of the other inclusions is taken into account using Mori-Tanaka's average field concept. This process is repeated infinite number of times, so that the equivalent eigenstrain is expressed in the form of series, which converges under a certain condition to a closed form expression. This method is applicable for high fiber volume fractions and more details about it are presented in Mori-Wakashima's paper (1990). The works which follow this approach are of Tong and Jasiuk (1990a, 1990b) and Shibata et al. (1990), among others.

In Chapter 3, thermal stresses and thermal expansion coefficients of composites containing either aligned or randomly oriented short fibers of spheroidal shape in 2-D and 3-D space are analysed. The sliding is allowed at fiber-matrix interfaces.

CHAPTER 3

THERMAL EXPANSION COEFFICIENTS OF COMPOSITES WITH SLIDING INTERFACES

3.1 INTRODUTION

In this chapter thermal stresses and thermal expansion coefficients of composites containing either aligned or misoriented in 2-D and 3-D space short fibers are analysed. The fibers are assumed to be spheroidal in shape. The sliding is allowed at fiber-matrix interfaces such that shear tractions are specified to vanish. The fiber interaction is accounted for by using successive iteration method (Mori and Wakashima, 1990) based on Mori-Tanaka's average field theory (Mori and Tanaka, 1973).

Composite materials deform and undergo thermal stresses when subjected to temperature change. These thermal stresses are induced because of the mismatch of thermal expansion coefficients of constituents. These thermal stresses may cause stress concentrations around the inclusions, which may initiate yielding, cracking, or debonding. Therefore, it is important to know and to control the magnitude of these stresses. Also, for design purposes, it is important to know thermal expansion coefficients of composites.

The problem of predicting thermal stresses and effective thermal expansion coefficients has received a lot of attention in literature, but most of the papers assumed perfect bonding at the inclusion-matrix interfaces (Budiansky, 1970; Rosen and Hashin, 1970; Laws, 1973;

Wakashima et al., 1974; Ishikawa et al., 1978; Takao and Taya, 1985). For more complete list of references see Taya and Arsenault (1989) and Hashin (1983). The inclusions with sliding interface were studied by Mura and Furuhashi (1984), Jasiuk et al. (1988), Shibata et al. (1990), among others. The composites with fibers misoriented in the matrix have been investigated by Cooper (1965), Wu (1966), Christensen and Waals (1972), Takao et al. (1982), Craft and Christensen (1984), Hatta and Taya (1985), Takao (1985), Tandon and Weng (1986), Pagano and Tandon (1988), Ferrari and Johnson (1989), Taya et al. (1990).

The present work is an extension of Jasiuk et al. (1988) paper. However, in this work an alternate method is used and the results are applicable for higher fiber volume fraction. Also, the fiber orientation is accounted for in this section.

3.2 METHOD OF SOLUTION

3.2.1 ALIGNED FIBERS

In this study the matrix and the inclusions (fibers) are taken to be isotropic in stiffness **L** and transversely isotropic in thermal expansion coefficients $\boldsymbol{\alpha}$. In the notation used, the quantities referring to the matrix and the fibers are specified by superscript m and f, respectively. For the simplicity of notation the vectors and tensors are denoted by bold face letters whenever possible. Otherwise, the indicial notation is used.

The fibers are represented by spheroidal inclusions as shown in Fig. 3.1. They are assumed in this section to be distributed uniformly in the matrix and aligned. The sliding is allowed at the fiber-matrix interfaces such that the shear tractions are specified to vanish. The solutions for stresses and strains illustrated in this section are determined using the spheroidal coordinate system as shown in Fig. 3.2.

The domain of composite is denoted as D, the domain of inclusions as Ω. Therefore, the domain of the matrix is given by $D-\Omega$. The fiber-matrix interface is given by $|\Omega|$. The composite is subjected to a uniform temperature change ΔT. Then, the average total strain in the composite is defined as

$$\langle\tilde{\epsilon}\rangle = \frac{1}{D}\int_D \tilde{\epsilon}\, dV \qquad (3.1)$$

In the notation used, "~" denotes the total quantities and "< >" the volume average quantities. The average strain, given in (3.1), can be written as (Jasiuk et al., 1988)

$$\langle \tilde{\epsilon}_{ij} \rangle = \frac{1}{D} \left(\int_{D-\Omega} \tilde{\epsilon}_{ij} \, dV + \int_{\Omega} \tilde{\epsilon}_{ij} \, dV \right.$$

$$\left. + \int_{|\Omega|} ([u_i]n_j + [u_j]n_i) \, dS \right) \tag{3.2}$$

where

$$\tilde{\epsilon} = \mathbf{e} + \boldsymbol{\alpha}^{*m} \quad \text{in } D-\Omega$$

$$\tilde{\epsilon} = \mathbf{e} + \boldsymbol{\alpha}^{*f} \quad \text{in } \Omega \tag{3.3}$$

$\tilde{\mathbf{u}}$ is the total displacement, $[\tilde{\mathbf{u}}] = \tilde{\mathbf{u}}^m - \tilde{\mathbf{u}}^f$ is the jump in the displacement, $\mathbf{n}$ is the unit normal vector on $|\Omega|$, $\mathbf{e}$ is the elastic strain, and $\boldsymbol{\alpha}^{*m}$ and $\boldsymbol{\alpha}^{*f}$ are the thermal strains of the matrix and fiber, respectively, defined as

$$\boldsymbol{\alpha}^{*m} = \boldsymbol{\alpha}^{m} \Delta T$$

$$\boldsymbol{\alpha}^{*f} = \boldsymbol{\alpha}^{f} \Delta T \tag{3.4}$$

The elastic strain is related to stress by Hooke's law as

$$\mathbf{e} = \mathbf{M}^{m}\boldsymbol{\sigma} \quad \text{in } D-\Omega$$

$$\mathbf{e} = \mathbf{M}^{f}\boldsymbol{\sigma} \quad \text{in } \Omega \tag{3.5}$$

where **M** is a compliance tensor such that $\mathbf{M} = \mathbf{L}^{-1}$. Using (3.1) and the fact that the volume average of the internal stresses vanishes, (3.2) is written as

$$\langle \tilde{\epsilon}_{ij} \rangle = \frac{f}{\Omega} (M^{f}_{ijk\ell} - M^{m}_{ijk\ell}) \int_{\Omega} \tilde{\sigma}_{k\ell} \, dV$$

$$+(1-f)\alpha^{*m}_{ij} + f\,\alpha^{*f}_{ij} + \frac{f}{\Omega} \int_{|\Omega|} (\,[\tilde{u}_i] n_j + [\tilde{u}_i] n_j) \, dS \tag{3.6}$$

The average total strain in the composite can also be expressed in terms of an average ficticious eigenstrain ϵ^* obtained via Eshelby's equivalent inclusion method (Tong and Jasiuk, 1990a) as

$$\langle \tilde{\epsilon} \rangle = \alpha^{*m} + f\,\epsilon^* \tag{3.7}$$

In this situation the present composite is a homogeneous material subjected to the eigenstrain ϵ^* in the inclusions, which accounts for the sliding and the mismatch in stiffness and thermal expansion coefficients of constituents.

By comparing equations (3.6) and (3.7) the idea of Eshelby's "equivalent inclusion method" is employed and ϵ^* can be found. Since the actual stress in the inclusion is not known, the single inclusion solution is used to solve for an eigenstrain $\epsilon^{*(0)}$ which will be refered to as zero order approximation (Mori and Wakashima, 1990).

$$\epsilon^{*(0)}_{ij} = \frac{1}{\Omega} (M^{f}_{ijk\ell} - M^{m}_{ijk\ell}) \int_{\Omega} \tilde{\sigma}_{k\ell} \, dV + (\alpha^{*f}_{ij} - \alpha^{*m}_{ij}) \tag{3.8}$$

$$+ \frac{1}{\Omega} \int_{|\Omega|} ([\tilde{u}_i] \, n_j + [\tilde{u}_i] \, n_j) \, dS$$

For simplicity of notation (3.8) is written as

$$\epsilon^{*(0)} = \eta \, \Delta T = \eta_1 (\alpha^f - \alpha^m) \, \Delta T \tag{3.9}$$

where η_1 is a 6x6 matrix and η is a 6x1 vector

The average stress in the isolated sliding inclusion due to a uniform temperature change in the composite is

$$\Delta\sigma^{(0)} = \langle \tilde{\sigma} \rangle_\Omega = \frac{1}{\Omega} \int_\Omega \tilde{\sigma} \, dV = \gamma \, \Delta T \tag{3.10}$$

where γ is a 6x1 vector, $\Delta\sigma$ denotes the average stress disturbance in the absence of applied stress, and $\Delta\sigma^{(0)}$ represents the average stress disturbance of the zeroth order solution, in which only a single sliding inclusion is considered. The corresponding average displacement disturbance is defined by $\Delta u^{(0)}$.

For a finite concentration of inclusions, some correction needs to be made to account for the interaction between inclusions. Since this isolated inclusion solution of stresses in composite is either an overestimate or underestimate depending on whether the inclusions are stiffer or more compliant than the matrix. Therefore, Mori and Wakashima's method (Mori and Wakashima, 1990) is employed to account for the inclusions interaction. The inclusions with the eigenstrain of the zeroth order produce an average stress in the matrix which is given by Mori-Tanaka's theory (Mori and Tanaka, 1973) as in equation (2.4)

$$\boldsymbol{\sigma}^{(1)} = - f \, \Delta\boldsymbol{\sigma}^{(0)} \tag{3.11}$$

According to Mori-Wakashima's method, this average stress in the matrix has the same effect as an applied loading at infinity, which induces additional disturbance in the inclusion's neighborhood. To determine this additional disturbance the second boundary value problem consisting of the isolated sliding inclusion subjected to stresses at infinity needs to be solved.

This second problem involves a body which is subjected to $\boldsymbol{\sigma}^{(1)}$ stress at infinity and $\mathbf{u}^{(1)}$ is the displacement due to the applied load when no inclusion exists. The total stress and displacement field are

$$\begin{aligned} \tilde{\boldsymbol{\sigma}}^{(1)} &= \boldsymbol{\sigma}^{(1)} + \Delta\boldsymbol{\sigma}^{(1)} \\ \tilde{\mathbf{u}}^{(1)} &= \mathbf{u}^{(1)} + \Delta\mathbf{u}^{(1)} \end{aligned} \tag{3.12}$$

where $\Delta\boldsymbol{\sigma}^{(1)}$ and $\Delta\mathbf{u}^{(1)}$ are the average stress and displacement disturbances. $\Delta\boldsymbol{\sigma}^{(1)}$ satisfies the equilibrium equations and the traction free condition at infinity.

The elastic strain energy produced by the applied stress $\boldsymbol{\sigma}^{(1)}$ is

$$W = \frac{1}{2} \int_D [\boldsymbol{\sigma}^{(1)} + \Delta\boldsymbol{\sigma}^{(1)}][\boldsymbol{\epsilon}^{(1)} + \Delta\boldsymbol{\epsilon}^{(1)}] dV \tag{3.13}$$

The elastic strain energy given in (3.13) can also be written as

$$W = \frac{1}{2} \int_D \boldsymbol{\sigma}^{(1)} \boldsymbol{\epsilon}^{(1)} dV - \frac{1}{2} \int_\Omega \tilde{\boldsymbol{\sigma}}^{(1)} \boldsymbol{\epsilon}^{(1)} dV + \frac{1}{2} \int_\Omega \boldsymbol{\sigma}^{(1)} \tilde{\boldsymbol{\epsilon}}^{(1)} dV$$

$$+ \frac{1}{2} \int_{|\Omega|} \boldsymbol{\sigma}^{(1)} \mathbf{n} \, [\tilde{\mathbf{u}}]^{(1)} dS \tag{3.14}$$

or using Hooke's law as

$$W = \frac{1}{2} \int_D \boldsymbol{\sigma}^{(1)} \boldsymbol{\epsilon}^{(1)} \, dV - \frac{1}{2} \int_\Omega (\mathbf{L}^f - \mathbf{L}^m) \tilde{\boldsymbol{\epsilon}}^{(1)} \boldsymbol{\epsilon}^{(1)} dV$$

$$+ \frac{1}{2} \int_{|\Omega|} \boldsymbol{\sigma}^{(1)} \mathbf{n} \, [\tilde{\mathbf{u}}]^{(1)} dS \tag{3.15}$$

Note that the second integral vanishes if there is no mismatch in stiffness of the constituents and the third integral is zero if there is no jump in the displacement. Suppose now that the same work is done by the applied load $\boldsymbol{\sigma}^{(1)}$ at infinity on the homogeneous material with ficticious eigenstrains $\boldsymbol{\epsilon}^{*(1)}$ in the inclusions. Then, the elastic strain energy
is

$$W = \frac{1}{2} \int_D \boldsymbol{\sigma}^{(1)} \boldsymbol{\epsilon}^{(1)} dV + \frac{1}{2} \int_\Omega \boldsymbol{\sigma}^{(1)} \boldsymbol{\epsilon}^{*(1)} dV \tag{3.16}$$

By equating equations (3.15) and (3.16), the average eigenstrain for the first order correction is evaluated as

$$\epsilon_{ij}^{*(1)} = \frac{1}{\Omega} \left(M_{ijk\ell}^f - M_{ijk\ell}^m \right) \int_\Omega \tilde{\sigma}_{k\ell}^{(1)} dV$$

$$+ \frac{1}{\Omega} \int_{|\Omega|} \left([u_i] n_j + [u_j] n_i \right) dS \tag{3.17}$$

For the simplicity of notation (3.17) can be written written as

$$\epsilon^{*(1)} = \boldsymbol{\beta}\, \sigma^{(1)} \tag{3.18}$$

where $\boldsymbol{\beta}$ is a 6x6 matrix.

The average stress in the sliding inclusion is

$$\Delta\sigma^{(1)} = \langle\tilde{\sigma}^{(1)}\rangle_{\Omega} - \sigma^{(1)} = \frac{1}{\Omega}\int_{\Omega}\tilde{\sigma}^{(1)}dV - \sigma^{(1)} = \boldsymbol{\lambda}\,\sigma^{(1)} \tag{3.19}$$

where $\boldsymbol{\lambda}$ is a 6x6 tensor.

The second order correction is similarly performed using again Mori-Tanaka's average concept. The stress disturbance $\Delta\sigma^{(1)}$ induces the additional average stress $\sigma^{(2)}$ in the matrix which acts as applied load at infinity. Then,

$$\sigma^{(2)} = -\,f\,\Delta\sigma^{(1)} \tag{3.20}$$

$$\Delta\sigma^{(2)} = \boldsymbol{\lambda}\,\sigma^{(2)} = -\,f\,\boldsymbol{\lambda}\,\Delta\sigma^{(1)} = -\,f\,\boldsymbol{\lambda}^2\,\sigma^{(1)} \tag{3.21}$$

$$\begin{aligned}\epsilon^{*(2)} &= \boldsymbol{\beta}\,\sigma^{(2)} = -\,f\,\boldsymbol{\beta}\,\Delta\sigma^{(1)} = -\,f\,\boldsymbol{\beta}\,\boldsymbol{\lambda}\,\sigma^{(1)} \\ &= -\,f\,\boldsymbol{\beta}\,\boldsymbol{\lambda}\,\boldsymbol{\beta}^{-1}\boldsymbol{\beta}\,\sigma^{(1)} = -\,f\,\boldsymbol{\lambda}_1\,\epsilon^{(1)}\end{aligned} \tag{3.22}$$

where

$$\boldsymbol{\lambda}_1 = \boldsymbol{\beta}\,\boldsymbol{\lambda}\,\boldsymbol{\beta}^{-1} \tag{3.23}$$

and λ_1 is a 6x6 tensor.

The nth-order correction is given as

$$\sigma^{(n)} = - f \Delta\sigma^{(n-1)} \tag{3.24}$$

$$\Delta\sigma^{(n)} = - f \lambda^2 \Delta\sigma^{(n-1)} \tag{3.25}$$

$$\epsilon^{*(n)} = - f \lambda_1 \epsilon^{*(n-1)} \tag{3.26}$$

The procedure is repeated infinite number of times. Then, the total equivalent eigenstrain is the eigenstrains from every iteration

$$\epsilon^* = \epsilon^{*(0)} + \epsilon^{*(1)} + \epsilon^{*(2)} + \ldots \tag{3.27}$$

Using equations (3.22) and (3.26), equation (3.27) yields

$$\epsilon^* = \epsilon^{*(0)} + \epsilon^{*(1)}(\mathbf{I} - f \lambda_1 + f^2\lambda_1^2 \ldots) \tag{3.28}$$

where **I** is a 6x6 identity tensor.

The convergence condition for the series given in (3.28) is that the magnitude of every eigenvalue of $-f \lambda_1$ is less than one (Mori and Wakashima, 1990). Under this condition, the eigenstrain ϵ^* is expressed in a closed form as

$$\epsilon^* = \epsilon^{*(0)} + [I + f\,\lambda_1]^{-1}\,\epsilon^{*(1)} \tag{3.29}$$

It can be shown that

$$\gamma\,\eta^{-1} = \Delta\sigma^{(0)}[\epsilon^{*(0)}]^{-1} = \Delta\sigma^{(1)}[\epsilon^{*(1)}]^{-1} = \lambda\,\beta^{-1} \tag{3.30}$$

and

$$\lambda_1 + I = \eta_1 \tag{3.31}$$

Then, the total eigenstrain ϵ^* is

$$\epsilon^* = [I + f\,\lambda_1]^{-1}\epsilon^{*(0)} = [I + f\,\lambda_1]^{-1}\eta\,\Delta T \tag{3.32}$$

or,

$$\epsilon^* = [(1-f)I + f\eta_1]^{-1}\eta_1(\alpha^f - \alpha^m)\,\Delta T \tag{3.33}$$

The effective thermal expansion coefficients are defined as the average strains due to a unit temperature rise for a traction free composite

$$\alpha^c = \frac{1}{\Delta T}\,\langle\tilde{\epsilon}\rangle_D \tag{3.34}$$

Equation (3.34) can also be written as

$$\boldsymbol{\alpha}^c = \boldsymbol{\alpha}^m + \frac{f}{\Delta T}\,\boldsymbol{\epsilon}^* \tag{3.35}$$

Finally, the thermal expansion coefficients of composite can be expressed as

$$\boldsymbol{\alpha}^c = \boldsymbol{\alpha}^m + f\,[(1-f)\mathbf{I} + f\boldsymbol{\eta}_1]^{-1}\boldsymbol{\eta}_1(\boldsymbol{\alpha}^f - \boldsymbol{\alpha}^m) \tag{3.36}$$

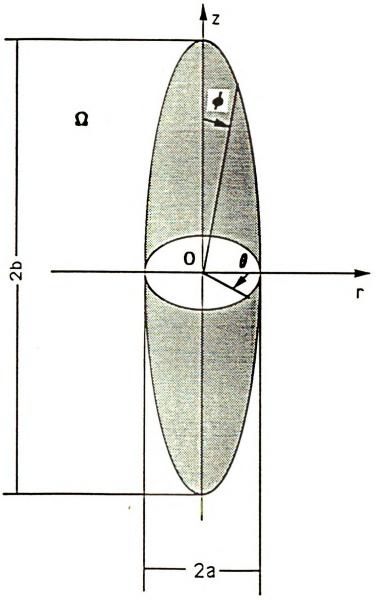

Fig. 3.1 Spheroidal inclusion.

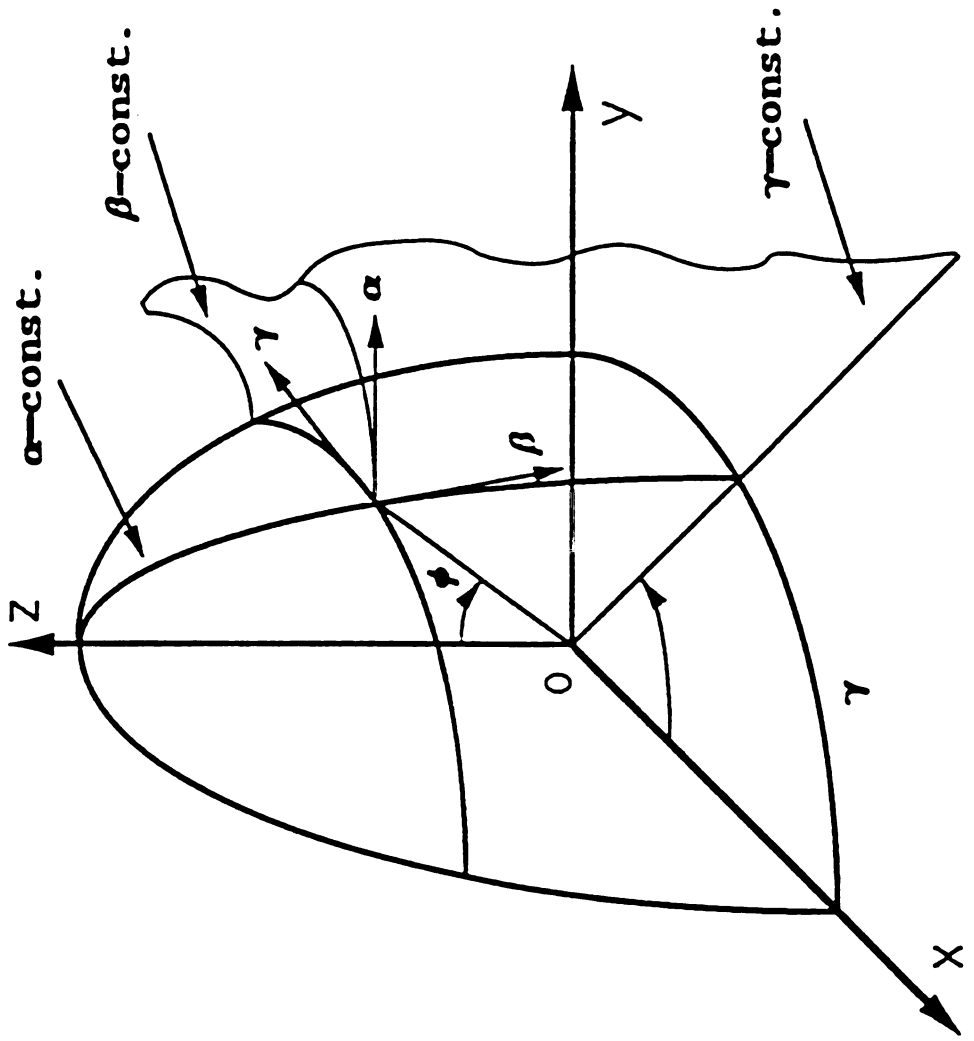

Fig. 3.2 Spheroidal coordinate system.

3.2.2 2-D AND 3-D MISORIENTED FIBERS

In most of the short fiber reinforced composites the orientation of fibers is random. In this section the effect of the orientation is studied. When the fibers are randomly oriented in 3-D space (see Fig. 3.3), the composite as a whole is macroscopically isotropic. While, when the fibers are randomly oriented in 2-D (see Fig. 3.4), the composite as a whole is transversely isotropic.

It is convenient to introduce a local set of axes x_1', x_2', and x_3' to describe any chosen fiber by assuming that x_3' axis is set to coincide with the fiber's longitudinal axis (see Fig. 3.3). The orientation of the fiber is defined by two angles ϕ and θ.

For 2-D misorientation ϕ is set equal to $\pi/2$ to have the fibers randomly oriented in plane x_1-x_2.

The coordinate tranformation tensor **T** is given as (Hatta and Taya, 1985)

$$\mathbf{T} = \begin{vmatrix} \cos\phi\cos\theta & -\sin\theta & \sin\phi\cos\theta \\ \cos\phi\sin\theta & \cos\theta & \sin\phi\sin\theta \\ -\sin\phi & 0 & \cos\phi \end{vmatrix} \tag{3.37}$$

Recall that a second order tensor follows the transformation rule

$$Y'_{ij} = T_{im}T_{jn}\,Y_{mn} \tag{3.38}$$

where the primes indicate quantities referred to the local coordinate system and Y'_{ij} and Y_{mn} are 3x3 tensors. A symmetric second order tensor **Y** (3x3) can be written in the contracted notation (6x1) as

$$\mathbf{Y} = [Y_{11}\ Y_{22}\ Y_{33}\ Y_{23}\ Y_{13}\ Y_{12}]^T \tag{3.39}$$

If Y'_{ij} and Y_{mn} in equation (3.38) are written in contracted notation (6x1) as shown in equation (3.39), equation (3.38) is transformed to

$$Y'_{ij} = Z_{ijmn}\ Y_{mn} \tag{3.40}$$

where Z_{ijmn} is a fourth rank tensor which can be represented in a contracted form by a 6x6 matrix.

Equation (3.38) is compared to equation (3.40) to give the following indicial equation (Taya et al., 1990)

$$Z_{ijmn} = T_{im}\ T_{jn} \tag{3.41}$$

Z tensor is used to transform any quantity written in contracted notation from local to global coordinates.

It is postulated that the effect of the random orientation of fibers upon determining any quantity **Y** is analytically equivalent to finding the average value of this quantity for the fiber direction axis

x_3' taking all possible orientations to fixed axes x_i (Christensen and Waals, 1972), where, i = 1, 2, or 3.

The average value of the quantity **Y**, denoted by <**Y**>, is given by

$$\langle \mathbf{Y} \rangle = \frac{1}{2\pi} \int_0^{\pi} \int_0^{\pi} \mathbf{Z}\,\mathbf{Y} \sin\phi \; d\theta \; d\phi \qquad \text{for 3-D}$$

$$\langle \mathbf{Y} \rangle = \frac{1}{\pi} \int_0^{\pi} \mathbf{Z}\,\mathbf{Y} \; d\theta \qquad \text{for 2-D} \tag{3.42}$$

Since the quantity **Y** from previous section for aligned fibers is independent of ϕ and θ then, <**Y**> can be written as

$$\langle \mathbf{Y} \rangle = \mathbf{A}_{id}\,\mathbf{Y} \qquad i = 2 \text{ or } 3 \tag{3.43}$$

where $$\mathbf{A}_{3d} = \frac{1}{2\pi} \int_0^{\pi} \int_0^{\pi} \mathbf{Z} \sin\phi \; d\theta \; d\phi$$

(3.44)

and $$\mathbf{A}_{2d} = \frac{1}{\pi} \int_0^{\pi} \mathbf{Z} \; d\theta$$

Finally, the thermal expansion coefficients given by equation (3.36) for composite reinforced with unidirectioal short fibers are written for a composite reinforced with misoriented short fibers as

$$\boldsymbol{\alpha}^c = \boldsymbol{\alpha}^m + f\,[(1-f)\mathbf{I} + f\boldsymbol{\eta}_1']^{-1}\boldsymbol{\eta}_1'(\boldsymbol{\alpha}^f - \boldsymbol{\alpha}^m) \tag{3.45}$$

where

$$\eta_1' = A_{id}\, \eta_1\, A_{id}^{-1} \qquad i = 2 \text{ or } 3 \tag{3.46}$$

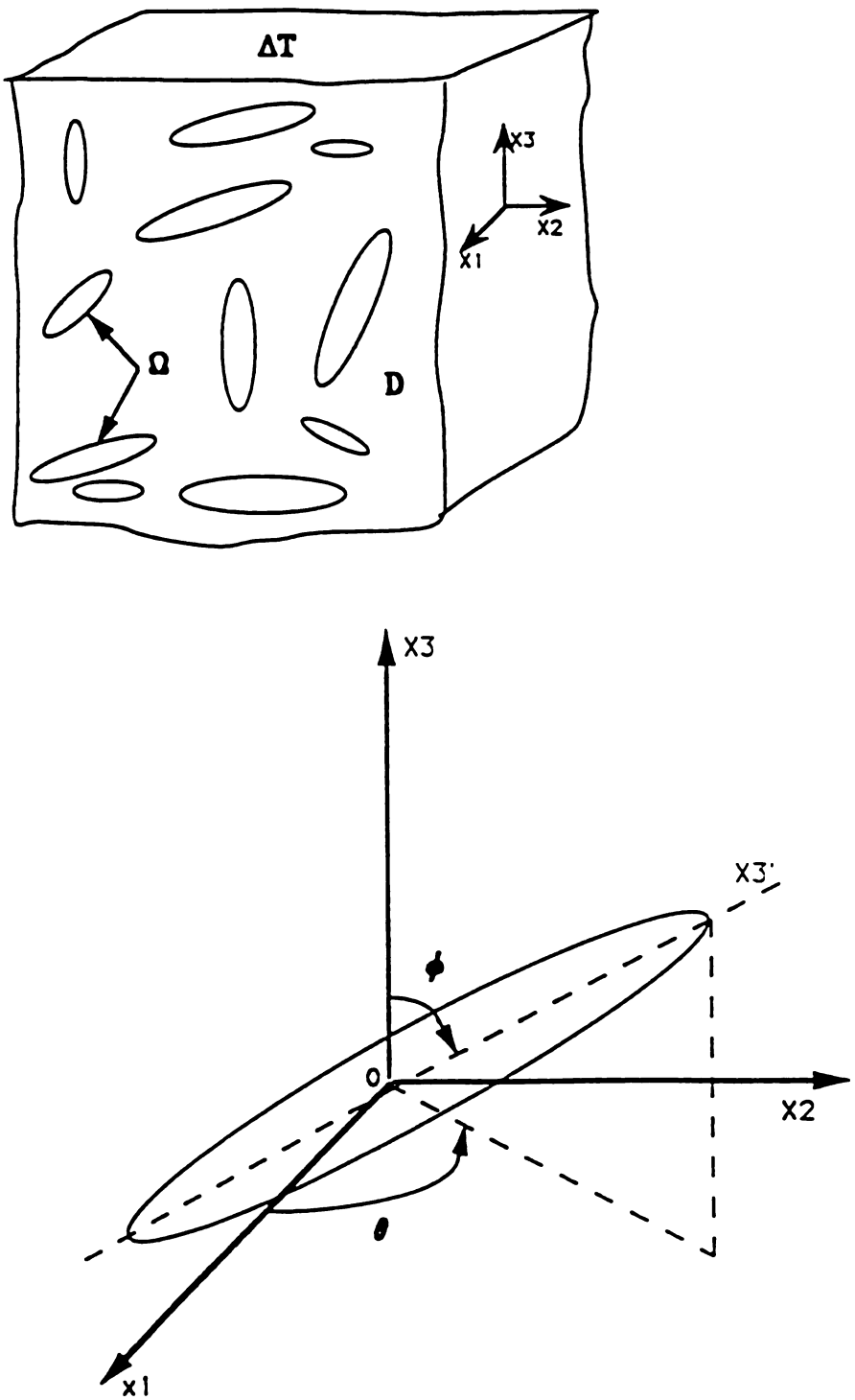

Fig. 3.3 3-D misoriented short fiber composite system.

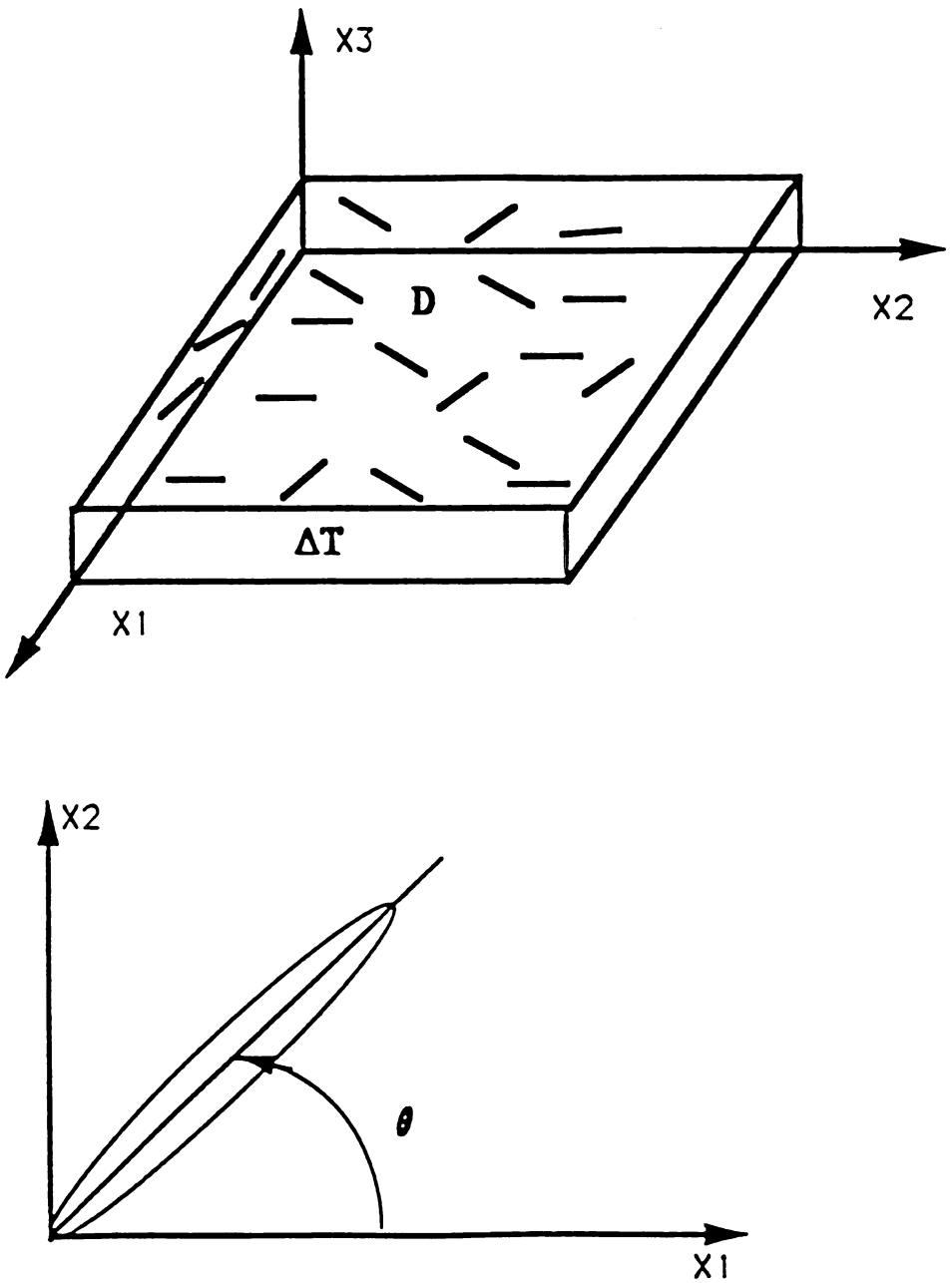

Fig. 3.4 2-D misoriented short fiber composite system.

3.3 NUMERICAL RESULTS AND DISCUSSION

In this section the effect of sliding interface and fiber misorientation on the thermal expansion coefficients and thermal stresses for composites reinforced with short fibers of spheroidal shape is studied. The fibers and matrix are assumed to be isotropic in stiffness and transversely isotropic in thermal expansion coefficients.

Figs. 3.5-3.6 present the effect of fiber volume fraction on the normalized thermal expansion coefficients α_A^c/α^m and α_T^c/α^m for both sliding case denoted by (SL) and perfect bonding case denoted by (PB), where A implies the axial direction and T implies the transverse direction. These graphs are done for inclusions isotropic in both stiffness and thermal expansion coefficients. The stiffness ratio $\Gamma = E^f/E^m = 5$, the aspect ratio $s = b/a = 5$ (see Fig. 3.1), the Poisson's ratios $\nu^f = \nu^m = 0.3$, and the thermal expansion coefficient ratio $\rho = \alpha^f/\alpha^m = 0.2$, 0.4, 0.6 and 0.8. It is seen from Figs. 3.5-3.6 that α_A increases due to sliding while α_T decreases. This is due to the fact the sliding allows matrix, which has a higher coefficient of thermal expansion to expand more freely in the axial direction. However it restrains the expansion in the transverse direction since the sliding should not cause volume change.

The results predicted by the successive iteration method presented here are more accurate than the results predicted by Jasiuk et al. (1988) because in this method the correction which accounts for fiber interaction is repeated infinite number of times, while in the previous paper by Jasiuk et. al. (1988), the analysis of the fiber interaction was limited to the first order correction only. Because of that the

present method is applicable for higher fiber volume fractions. For the extreme value of fiber volume fraction equal to one which is possible since the gradation of sizes is allowed, this present method predicts reasonable results for both perfect bonding and pure sliding cases. The thermal expansion coefficients predicted for fiber volume fraction equal to one are equal to the thermal expansion coefficients of the inclusions as expected. Physically, for this volume fraction of fibers the inclusions and the matrix are the same material, and if this composite undergoes thermal stresses, the expansion is stress free and no sliding between matrix and inclusions occurs. For perfect bonding the thermal expansion coefficients predicted by the present method match with Wakashima et al. (1974) and Benveniste (1987) predictions, which is expected, since the governing equations for these three methods are the same. The difference is in the problem formulation and the actual numerical evaluation. The present method is flexible to be used for sliding and may be easily extended to other boundary conditions.

Figs. 3.7 and 3.8 show the effect of fibers misoriented in 2-D and 3-D space on thermal expansion coefficients. These two graphs were done for glass-fiber-reinforced plastics with the following properties $E^f=69GN/m^2$, $E^m=3.4GN/m^2$, $\nu^f=0.2$, $\nu^m=0.38$, $\alpha^f=5x10^{-6}/°C$, and $\alpha^m=66x10^{-6}/°C$ (Uemura et al. 1979). For the case of composite with sliding interfaces the glass fibers are assumed to be lubricated to assure a very poor interfacial adhesion between the matrix and the fibers.

The variation of thermal expansion coefficients versus fiber volume fraction is shown for 2-D and 3-D fiber misorientation for both perfect bonding and pure sliding cases. For 2-D misorientation the

composite as a whole is transversely isotropic, the thermal expansion coefficient in plane x_1-x_2 is denoted α_{12}^c while the one in x_3 direction is denoted by α_3^c. For 3-D misorientation the composite as a whole is macroscopically isotropic, the thermal expansion coefficient is denoted by α^c.

It is seen that for 2-D random orientation the effect of sliding interfaces on thermal expansion coefficients is significant. It is seen that α_{12}^c increases since a matrix which has higher coefficient of thermal expansion expands more freely. However, it decreases α_3^c because sliding does not cause volume change. For 3-D random orientation the effect of sliding is negligible, and this can be explained by two facts: first for 3-D random orientation the composite as a whole is regarded as an isotropic material, and second, that the sliding does not cause volume change. The 3-D random orientation has an important effect on α^c and this effect is more pronounced when the aspect ratio s increases.

The results predicted by the present method for 2-D and 3-D misoriented fibers for perfect bonding case agree with the results predicted by Takao (1985) for the same composite system.

When composite reinforced with unidirectional short fibers is subjected to a temperature change ΔT, the maximum stresses appear at the poles of the fibers. The effect of fiber volume fraction on the normalized stresses in z-direction at the poles $\sigma_{zz}/2\mu^m\epsilon_{zz}^*$ is shown in Fig. 3.9, in which both sliding and perfect bonding cases are shown. This graph is done for inclusions isotropic in thermal expansion and

having aspect ratios s = 5 and 10 and a stiffness ratio $\Gamma = E^f/E^m = 5$. The stresses are higher for sliding case than for perfect bonding and this difference is more pronounced for higher aspect ratios. It is also seen that the increase in fiber volume fraction decreases these stresses for both interfacial cases, and for the extreme value of fiber volume fraction equal to one, these stresses vanish for both perfect bonding and pure sliding cases. Physically, for this case the matrix and the fiber are the same material, and if the composite is subjected to thermal stresses, the expansion is stress free.

Fig. 3.10 shows the relation between the normalized effective stress and the shape of the spheroid for the following stiffness ratios $\Gamma = 1$, 10 and 20. The effective stress as defined by Von Mises (1928) in cartesian coordinates is

$$\sigma_{eff} = \{[(\sigma_{xx}-\sigma_{yy})^2 + (\sigma_{yy}-\sigma_{zz})^2 + (\sigma_{zz}+\sigma_{xx})^2 + 6(\sigma_{xy}^2+\sigma_{yz}^2+\sigma_{zx}^2)]/2\}^{1/2} \tag{3.47}$$

This indicates that plastic deformation will be initiated first in the composites with sliding interfaces at the poles of fibers.

The composite with sliding interfaces is not a ficticious composite. Many designers are using such composites, especially when they are dealing with reinforcements which bond poorly to the matrix such as the silicone carbide-fiber reinforced aluminum, metal-fiber reinforced epoxy and other composites. In such composites as discussed in this chapter it is very important to address the sliding effect on the elastic and thermal properties of the composite. An interesting

experimental work in this area was done by Dekkers (1985), in which the polycarbonate-glassbead composite was considered with two different interfacial adhesions:

a) Excellent interfacial adhesion obtained with γ-aminopropylsilane.

b) Poor interfacial adhesion obtained with silicone oil.

In this work the tensile deformation behaviour of glass bead-filled glassy polymers was investigated. The attention was mainly focused on the relation between the local microscopic deformation mechanisms and the local stresses and the relation between the microscopic deformation mechanisms and the macroscopic tensile behaviour of the composites.

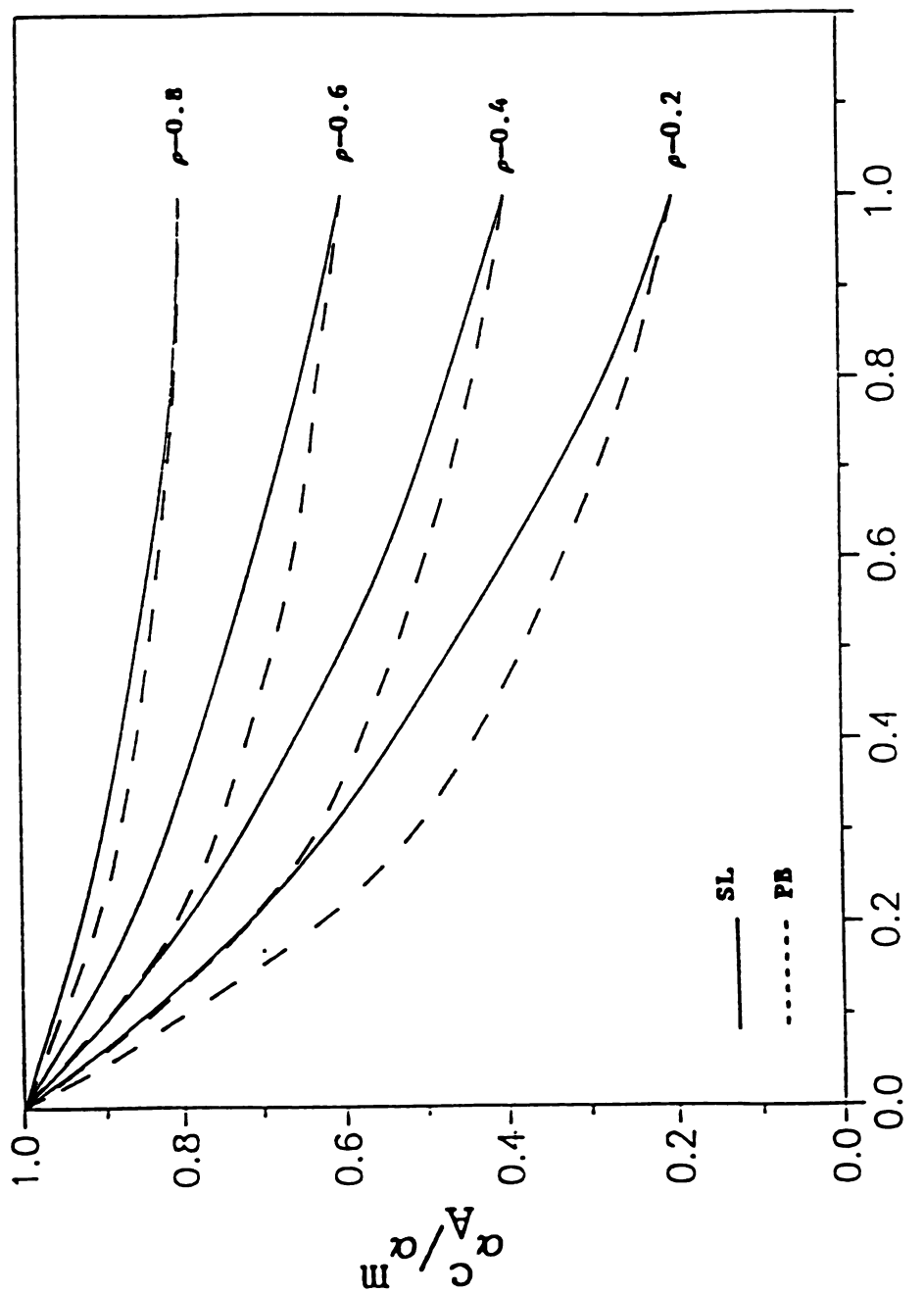

Fig. 3.5 α_A^c/α^m vs. f for SL & PB for various ρ when s = 5, Γ = 5, and $\nu^f = \nu^m = 0.3$.

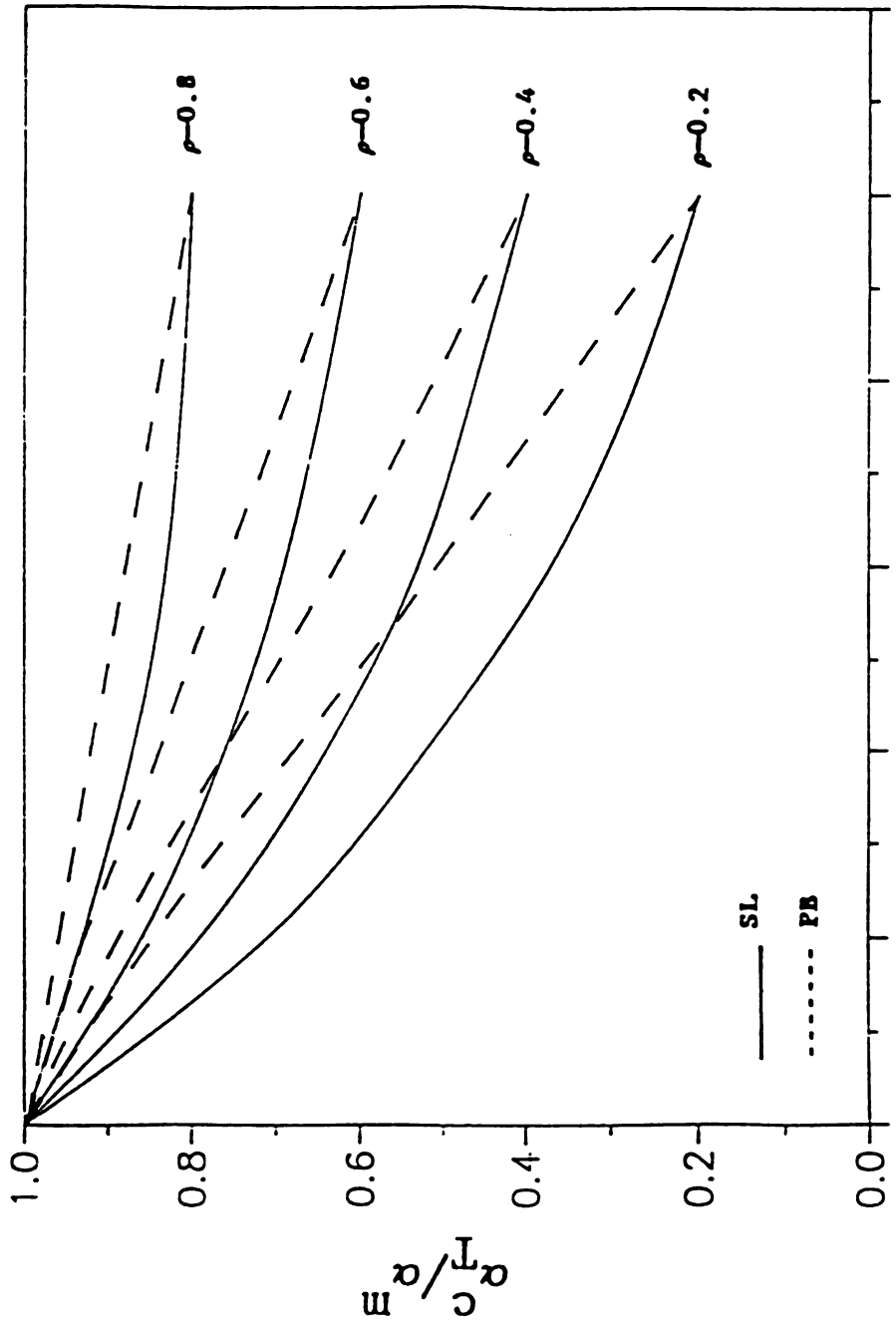

Fig. 3.6 α_T^c/α^m vs. f for SL & PB for various ρ when $s = 5$, $\Gamma = 5$, and $\nu^f = \nu^m = 0.3$.

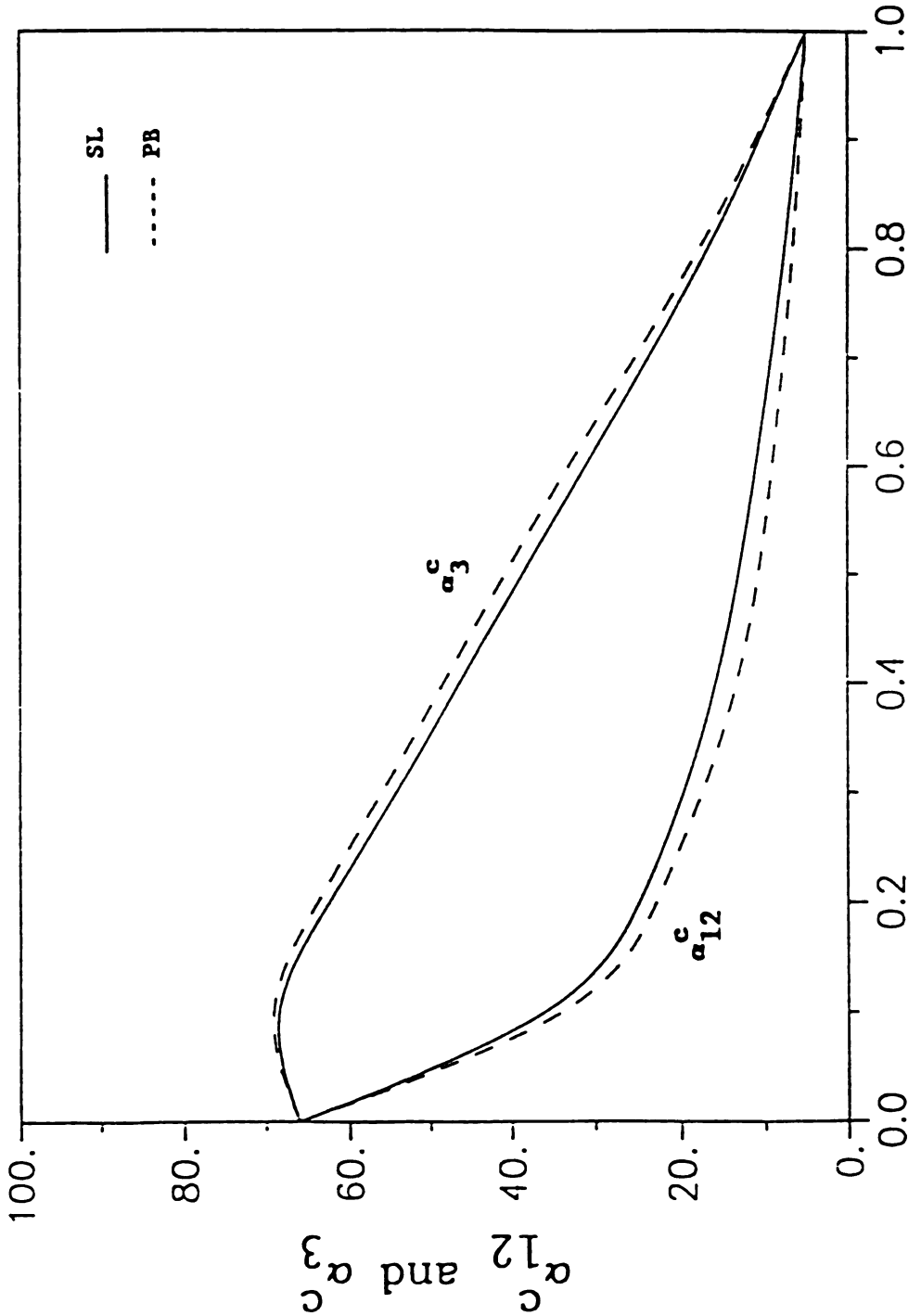

Fig. 3.7 α_{12}^c and α_3^c vs. f for SL & PB for 2-D misoriented glass-plastics composite when s = 10.

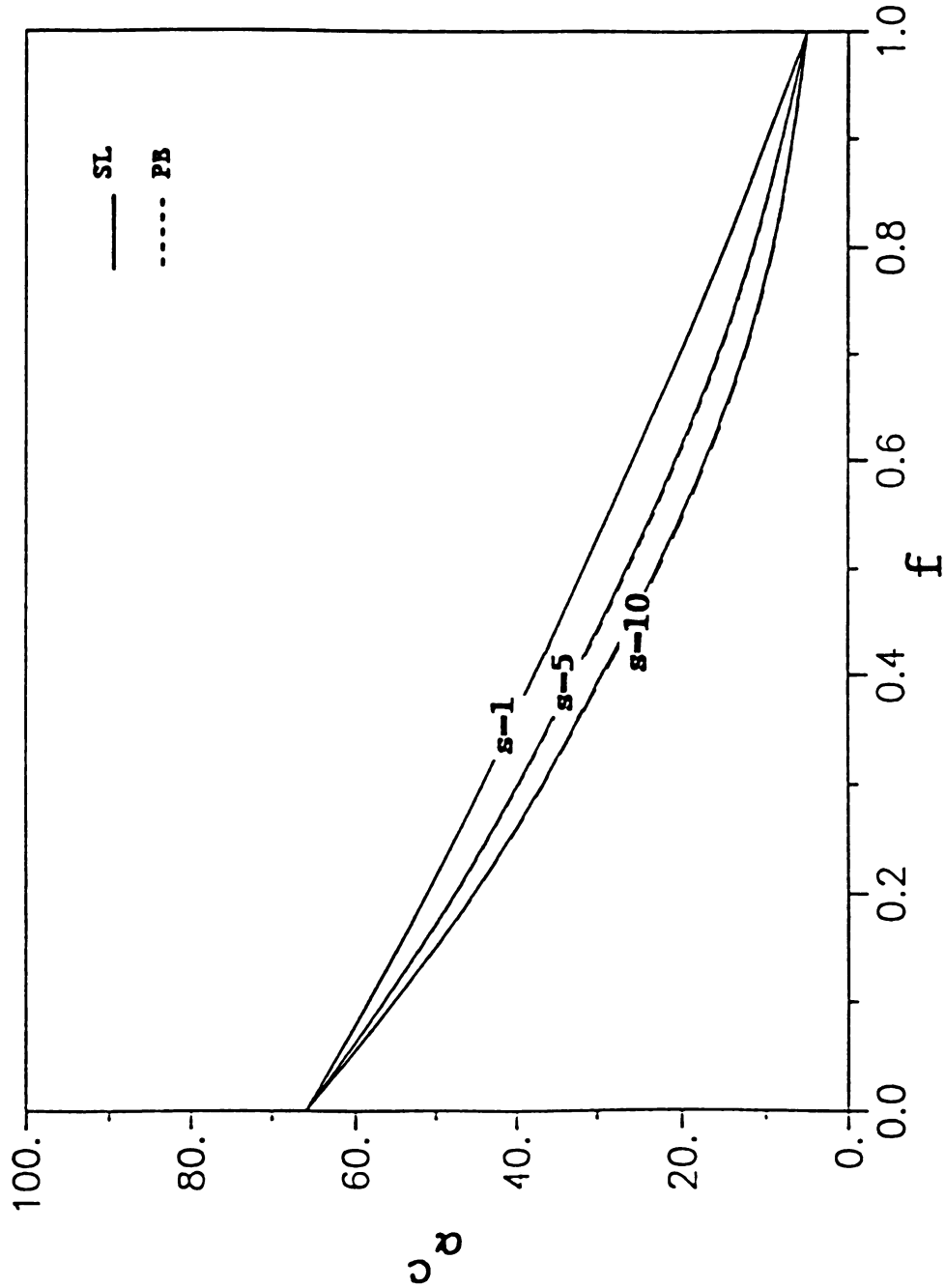

Fig. 3.8 α^c vs. f for SL & PB for 3-D misoriented glass-plastics composite for various s.

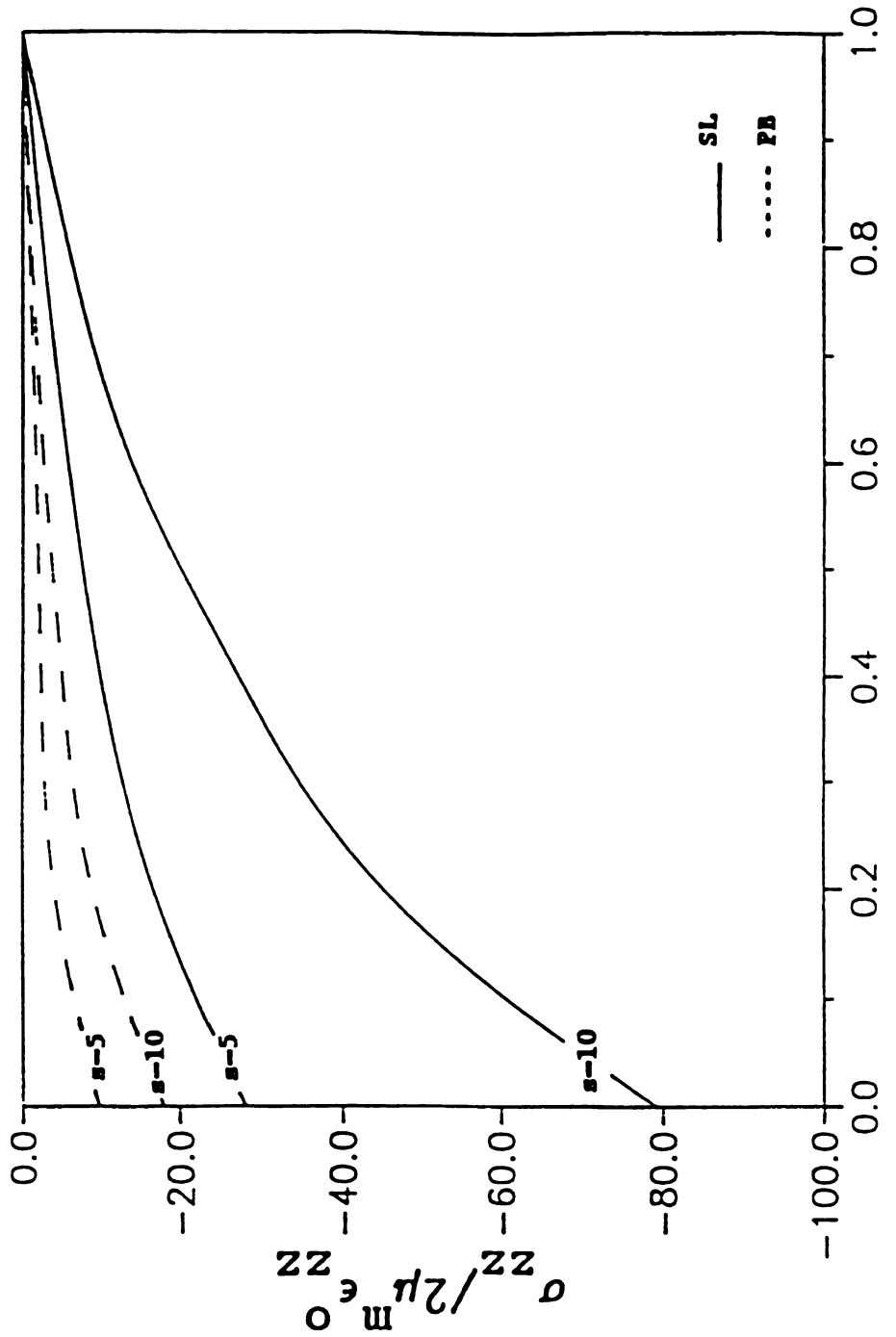

Fig. 3.9 $\sigma_{zz}/2\mu^m\epsilon^o_{zz}$ at the poles vs. f for SL & PB when s = 5 & 10.

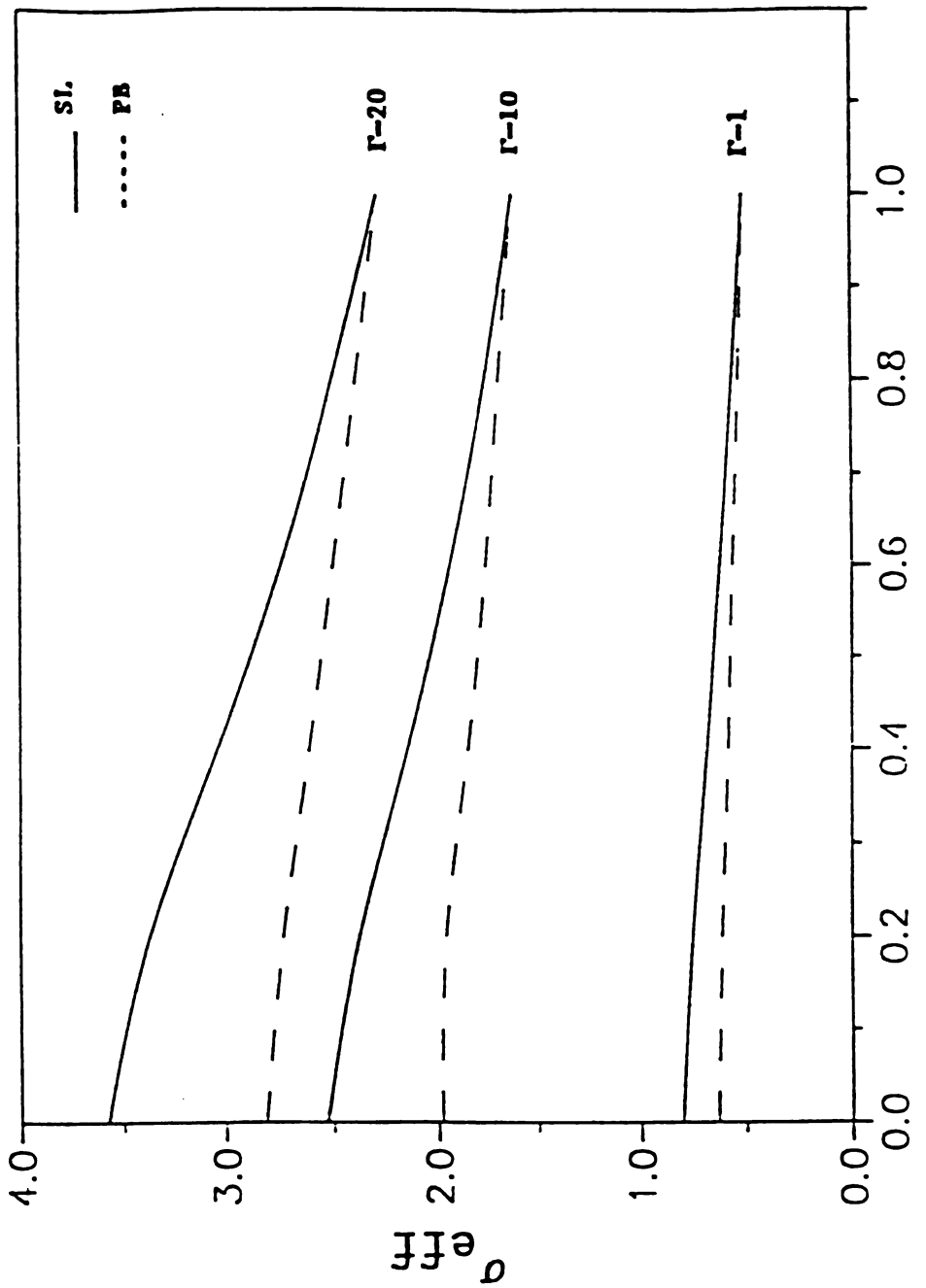

Fig. 3.10 σ_{eff} at the poles vs. 1/s for SL & PB when Γ = 1, 10, and 20.

CHAPTER 4

ELASTIC CONSTANTS AND THERMAL EXPANSION COEFFICIENTS OF TRANSVERSELY ISOTROPIC COMPOSITES HAVING INHOMOGENEOUS INTERPHASE

4.1 INTRODUCTION

In this chapter, a composite reinforced with aligned long cylindrical fibers is investigated. The interphase between matrix and inclusion is assumed to be inhomogeneous and having elastic properties changing in the radial direction. The effect of the interphase on the local elastic fields and the overall elastic constants and thermal expansion coefficients of this composite are studied. These quantities are derived using the composite cylinders assemblage model (see Section 2.1) and the generalized self-consistent scheme (see Section 2.2).

The interphase region may be a coating but is often a product of the manufacturing processes. When it is a coating it is assumed to be a layer around the inclusion made from different material and having its own thermal and elastic properties. The thermal and elastic properties in this interphase are assumed to be constant. In case the interphase is a product of manufacturing processes, it has nonuniform properties varying from location to location, and this variation is related to the chemical and thermodynamic nature of the bonding between the inclusion and the matrix.

Researchers in this field are interested in studing the micro-details of the interphase. Some of them are assuming that the thermal

and elastic properties of the interphase vary in the radial direction following a chosen mathematical variation relationship (more details about the mathematical models adopted by researchers are included in Chapter 1). This inhomogeneous interphase has been modeled by Theocaris (1984, 1985, 1987), among others. His work however did not address the elasticity solution properly. The stress field was determined in an approximate way. The thermal stresses were determined in a more rigorous way by Sottos et al. (1989) using a numerical method and by Jayaraman and Reifsnider (1990) and Jayaraman et al. (1991) using an analytical method. Jayaraman and Reifsnider (1990) investigated three models for the interphase elastic modulus variation: power, reciprocal, and cubic variations. The composite cylinder assemblage model was used to determine the micromechanical stresses of continuous fiber composite. In Jayaraman et al. (1991) the power variation relationship was used to simulate the variation in the radial direction of both elastic modulus and thermal expansion coefficient. Mori-Tanaka average field concept was used to determine the elastic and thermal stresses of the same composite. In all of the above models Poisson's ratio in the interphase was assumed to be constant, for simplicity.

In this chapter the work done by Jayaraman and Reifsnider (1990) and Jayaraman et al. (1991) is extended. The elastic moduli and thermal expansion coefficients are evaluated in closed forms by using a power variation relationship simulating the variation of the thermal and elastic properties in the interphase. Furthermore, the same work is done for few other variation relationships in the radial direction. The solutions for local stresses and thermal and elastic properties are obtained using infinite series. Also, in this study the effect of Poisson's ratio changing in the radial direction in the interphase is

studied. Few variation relationships are assigned to the Poisson's ratio value in the interphase in order to determine its effect on stresses, and thermal and elastic properties. It is shown that a variation of Poisson's ratio in the interphase has a considerable effect on the local stress fields and the effective elastic and thermal properties.

4.2 FORMULATION

In this study a composite reinforced with aligned long fibers (see Fig. 4.1) and having an interphase region between fiber and matrix (see Fig. 4.2) is considered. A cylindrical coordinate system (r, θ, z) is adopted (see Fig. 4.2), where z is the axial coordinate and r-θ is the transverse plane which corresponds to x-y plane of Fig. 4.1. The quantities referring to fiber, interphase, matrix, and the composite are prescribed by superscripts or subscripts f, 1, m, and c, respectively. The analysis is done assuming the interphase having radially varying elastic and thermal properties.

The objective of this work is to predict the effective elastic constants and thermal expansion coefficients of a composite, which has an isotropic interphase and matrix, and transversely isotropic inclusion. The same study can be extended to the case when the matrix is transversely isotropic matrix without further difficulties. This composite can be idealized as being effectively homogeneous in order to determine its effective elastic and thermal properties. Further, it is characterized as being transversely isotropic, with elastic properties defined by five constants. It is convenient to represent the elastic constants of this transversely isotropic material by the constants E_A^c, ν_A^c, G_A^c, G_T^c, and K_T^c, and the thermal expansion coefficients by the constants α_A^c and α_T^c.

where

E_A: axial Young's modulus

ν_A: axial Poisson's ratio

G_A: axial shear modulus

G_T: transverse shear modulus

K_T: transverse plane strain bulk modulus

α_A: axial thermal expansion coefficient

α_T: transverse thermal expansion coefficient

The other elastic constants, a transverse elastic modulus (E_T) and a transverse Poisson's ratio (ν_T) can be obtained via

$$\nu_T = \frac{K_T - mG_T}{K_T + mG_T}$$

$$E_T = 2(1 + \nu_T)G_T \tag{4.1}$$

where $$m = 1 + \frac{4K_T\nu_A^2}{E_A}$$

Before proceeding with the analysis, for completeness the stress-strain relations for isotropic and transversely isotropic materials, the strain-displacements relations, and the equations of equilibrium expressed in cylindrical coordinates are included here.

The stress-strain relations for a transversely isotropic material are

$$\sigma_{rr} = (K_T + G_T)\,\epsilon_{rr} + (K_T - G_T)\,\epsilon_{\theta\theta} + 2K_T\nu_A\,\epsilon_{zz}$$

$$\sigma_{\theta\theta} = (K_T - G_T)\,\epsilon_{rr} + (K_T + G_T)\,\epsilon_{\theta\theta} + 2K_T\nu_A\,\epsilon_{zz}$$

$$\sigma_{zz} = 2K_T\nu_A\,\epsilon_{rr} + 2K_T\nu_A\,\epsilon_{\theta\theta} + (E_A + 4K_T\nu_A^2)\,\epsilon_{zz} \qquad (4.2a)$$

$$\sigma_{r\theta} = 2G_T\,\epsilon_{r\theta}$$

$$\sigma_{\theta z} = 2G_A\,\epsilon_{\theta z}$$

$$\sigma_{rz} = 2G_A\,\epsilon_{rz}$$

The stress-strain relations given by equations (4.2a) for a transversely isotropic material are transformed for an isotropic material to

$$\sigma_{rr} = \frac{E}{(1-2\nu)(1+\nu)}\,[(1-\nu)\,\epsilon_{rr} + \nu\,(\epsilon_{\theta\theta} + \epsilon_{zz})]$$

$$\sigma_{\theta\theta} = \frac{E}{(1-2\nu)(1+\nu)}\,[\nu\,\epsilon_{rr} + (1-\nu)\,\epsilon_{\theta\theta} + \nu\,\epsilon_{zz}]$$

$$\sigma_{zz} = \frac{E}{(1-2\nu)(1+\nu)}\,[\nu\,(\epsilon_{rr} + \epsilon_{\theta\theta}) + (1-\nu)\,\epsilon_{zz}] \qquad (4.2b)$$

$$\sigma_{r\theta} = \frac{E}{1+\nu}\,\epsilon_{r\theta}$$

$$\sigma_{rz} = \frac{E}{1+\nu} \epsilon_{rz}$$

$$\sigma_{\theta z} = \frac{E}{1+\nu} \epsilon_{\theta z}$$

using the following relations

$$E_A = E$$

$$\nu_A = \nu$$

$$G_A = G \tag{4.3a}$$

$$G_T = G$$

$$K_T = \frac{G}{1-2\nu}$$

where

$$G = \frac{E}{2(1+\nu)} \tag{4.3b}$$

The strain-displacement equations in cylindrical coordinate system are given by

$$\epsilon_{rr} = \frac{\partial u_r}{\partial r} \quad ; \quad \epsilon_{\theta\theta} = \frac{u_r}{r} + \frac{\partial u_\theta}{r\partial\theta} \quad ; \quad \epsilon_{zz} = \frac{\partial u_z}{\partial z}$$

$$\epsilon_{r\theta} = \frac{1}{2}\left(\frac{\partial u_r}{r\partial\theta} + \frac{\partial u_\theta}{\partial r} - \frac{u_\theta}{r}\right) \tag{4.4}$$

$$\epsilon_{rz} = \frac{1}{2}\left(\frac{\partial u_r}{\partial z} + \frac{\partial u_z}{\partial r}\right); \quad \epsilon_{z\theta} = \frac{1}{2}\left(\frac{\partial u_\theta}{\partial z} + \frac{\partial u_z}{r\partial\theta}\right)$$

where u_r, u_θ and u_z are the displacement components.

The equations of equilibrium expressed in cylindrical coordinates are

$$\frac{\partial\sigma_{rr}}{\partial r} + \frac{1}{r}\frac{\partial\sigma_{r\theta}}{\partial\theta} + \frac{\partial\sigma_{rz}}{\partial z} + \frac{\sigma_{rr} - \sigma_{\theta\theta}}{r} = 0 \tag{4.5a}$$

$$\frac{\partial\sigma_{rz}}{\partial r} + \frac{1}{r}\frac{\partial\sigma_{\theta z}}{\partial\theta} + \frac{\partial\sigma_{zz}}{\partial z} + \frac{\sigma_{rz}}{r} = 0 \tag{4.5b}$$

$$\frac{\partial\sigma_{r\theta}}{\partial r} + \frac{1}{r}\frac{\partial\sigma_{\theta\theta}}{\partial\theta} + \frac{\partial\sigma_{\theta z}}{\partial z} + 2\frac{\sigma_{r\theta}}{r} = 0 \tag{4.5c}$$

Now, the analysis proceeds in order to evaluate the local fields and the effective elastic constants and thermal expansion coefficients. Two methods are employed. The composite cylinders assemblage model is used to determine the effective axial Young's modulus, axial Poisson's ratio, axial shear modulus, plane strain bulk modulus, and thermal expansion coefficients. The generalized self consistent scheme is used to determine the effective transverse shear modulus. A short description of both methods is included in Chapter 2 for completeness; for more details see Christensen (1979, 1990) and Sullivan and Hashin (1990).

The thermal and the elastic properties in the interphase zone are first simulated by a power variation relationship in Sections 4.3-4.6. This leads to closed form results for the thermal and elastic properties and for the stresses as discussed by Lekhnitskii (1981) and illustrated by Jayaraman and Reifsnider (1990) and Jayaraman et al. (1991). The Poisson's ratio in these Sections 4.3-4.6 is kept constant for simplicity. Later, in Section 4.7 few other variation relationships are adopted to simulate the radial variation of the thermal and elastic properties including Poisson's ratio (see Appendix G). In Section 4.7 the governing equilibrium equations in the interphase zone are included. The results for stresses and displacements for this case are written in a form of infinite series.

The power variation relationship used in Sections 4.3-4.6 to simulate the elastic modulus and the thermal expansion coefficient changing in the radial direction in the interphase is written as

$$E^{\ell}(r) = P\, r^{Q}$$

$$\alpha^{\ell}(r) = M\, r^{N} \tag{4.6}$$

where r is the radial coordinate, P, Q, M and N are four constants to be determined. In this dissertation the thermal expansion coefficient and elastic modulus in the interphase are chosen to vary from the properties of the fiber at r = a to the properties of the matrix at r = b. However, any other value $E^{\ell}(a)$, $E^{\ell}(b)$, $\alpha^{\ell}(a)$ and $\alpha^{\ell}(b)$ can be specified. For example the conditions chosen for elastic modulus are written as

at $r = a \quad E_T^f = P\ a^Q$

at $r = b \quad E^m = P\ b^Q$ (4.7a)

which gives us

$$Q = [\ln(E_T^f/E^m)]/[\ln(a/b)]$$

$$P = E_T^f/a^Q \quad (4.7b)$$

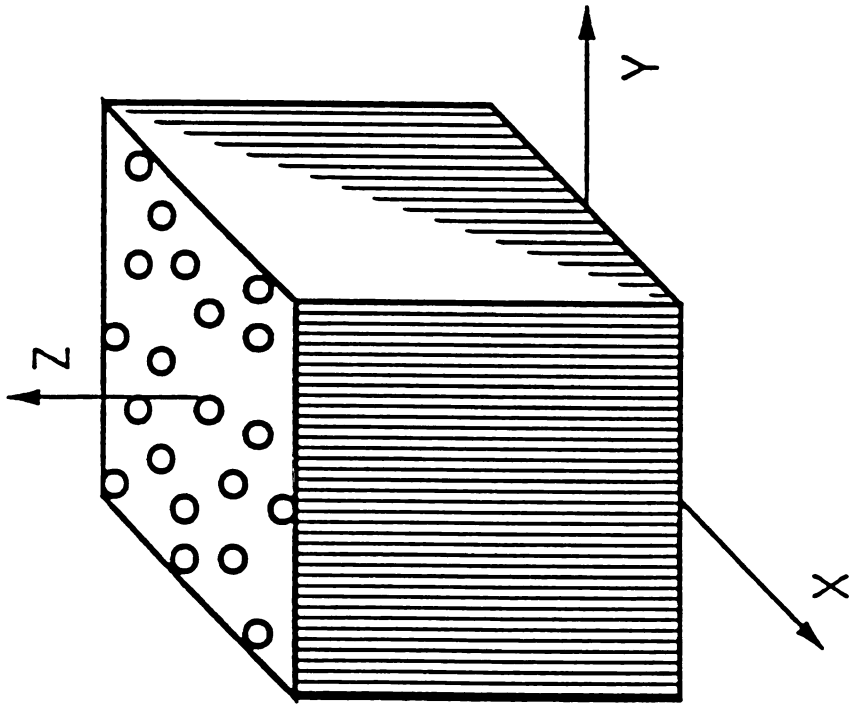

Fig. 4.1 Unidirectional long fiber composite system.

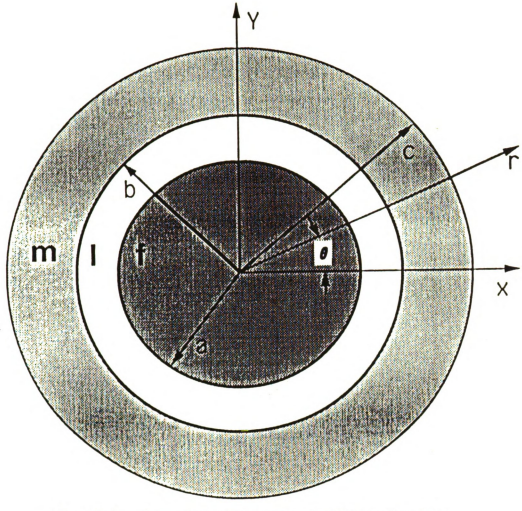

Fig. 4.2 Cross-section of a composite cylinder.

4.3 AXISYMMETRIC PROPERTIES

4.3.1 EFFECTIVE AXIAL YOUNG'S MODULUS AND AXIAL POISSON'S RATIO

In this section the composite cylinders assemblage model (Hashin and Rosen, 1964) is used to obtain the effective axial Young's modulus and axial Poisson's ratio.

An axially symmetric state defined by the following is considered

$$u_r = u(r)$$

$$u_\theta = 0 \qquad (4.8)$$

$$u_z = \epsilon^o_{zz}\, z$$

where ϵ^o_{zz} = constant.

The strain displacement relations given in (4.4) reduce to

$$\epsilon_{rr} = \frac{du(r)}{dr} \quad ; \quad \epsilon_{\theta\theta} = \frac{u(r)}{r} \quad ; \quad \epsilon_{zz} = \epsilon^o_{zz}$$

$$\epsilon_{r\theta} = \epsilon_{rz} = \epsilon_{\theta z} = 0 \qquad (4.9)$$

The stresses given in (4.2a), expressed in terms of displacements for a transversely isotropic case are

$$\sigma_{rr} = (K_T + G_T)\, u' + (K_T - G_T)\, \frac{u}{r} + 2K_T\, \nu_A\, \epsilon^o_{zz}$$

$$\sigma_{\theta\theta} = (K_T - G_T)\, u' + (K_T + G_T)\, \frac{u}{r} + 2K_T\, \nu_A\, \epsilon^o_{zz} \qquad (4.10a)$$

$$\sigma_{zz} = 2K_T\nu_A(u' + \frac{u}{r}) + (E_A + 4K_T\nu_A^2)\epsilon^o_{zz}$$

$$\sigma_{r\theta} = \sigma_{rz} = \sigma_{\theta z} = 0$$

where " ' " denotes the derivative with respect to r.

Similarly, the stresses for isotropic case given in (4.2b) are

$$\sigma_{rr} = \frac{E}{(1-2\nu)(1+\nu)} [(1-\nu)\, u' + \nu(\frac{u}{r} + \epsilon^o_{zz})]$$

$$\sigma_{\theta\theta} = \frac{E}{(1-2\nu)(1+\nu)} [\nu\, u' + (1-\nu)\, \frac{u}{r} + \nu\epsilon^o_{zz}] \qquad (4.10b)$$

$$\sigma_{zz} = \frac{E}{(1-2\nu)(1+\nu)} [\nu(u' + \frac{u}{r}) + (1-\nu)\, \epsilon^o_{zz}]$$

$$\sigma_{r\theta} = \sigma_{rz} = \sigma_{\theta z} = 0$$

The equations of equilibrium (4.5) for the axisymmetric case reduce to a single equation given as follows

$$\frac{d\sigma_{rr}}{dr} + \frac{\sigma_{rr} - \sigma_{\theta\theta}}{r} = 0 \qquad (4.11)$$

Equations (4.10) are introduced into (4.11) to obtain the differential equation in terms of displacements for each of the three phases.

a) Transversely isotropic fiber

The differential equation (4.11) is written as

$$r^2 u'' + r u' - u = 0 \tag{4.12}$$

The general solution is

$$u(r) = A_f r + B_f/r \tag{4.13}$$

where A_f and B_f are the unknown constants. $B_f = 0$ for finite solution at $r = 0$

b) Isotropic interphase

The governing differential equation is

$$u'' + \frac{Q+1}{r} u' + \frac{\frac{Q\nu^{\ell}}{1-\nu^{\ell}} - 1}{r^2} u + \frac{Q}{r} \left(\frac{\nu^{\ell}}{1-\nu^{\ell}} \right) \epsilon_{zz}^{o} = 0 \tag{4.14}$$

where Q is given by equation (4.7b)

The solution of equation (4.14) is written as

$$u(r) = A_{\ell} r^{s_1} + B_{\ell} r^{s_2} - \epsilon_{zz}^{o} \nu^{\ell} r \tag{4.15}$$

where

$$s_1,\ s_2 = \frac{1}{2}\left[-Q \pm \left(Q^2 - \frac{4\nu^{\ell}Q}{1-\nu^{\ell}} + 4\right)^{1/2}\right] \tag{4.16}$$

ν^{ℓ} is the layer's Poisson's ratio, which is assumed to be uniform.

c) Isotropic matrix

The differential equation is written as

$$r^2 u'' + r u' - u = 0 \tag{4.17}$$

The general solution is

$$u(r) = A_m r + B_m/r \tag{4.18}$$

To find the stress components in the three phases, the corresponding displacement solutions are substituted in equations (4.10). The unknown constants A_f, A_{ℓ}, B_{ℓ}, A_m, and B_m are evaluated by using the boundary conditions assumed in the composite cylinders assemblage model, which are the continuity of radial displacement and radial stress across each interface at r = a and r = b

at r = a $\qquad u_r^f(a) = u_r^{\ell}(a)$ (4.19a)

$$A_f a = A_{\ell} a^{s_1} + B_{\ell} a^{s_2} - \epsilon_{zz}^{o} \nu^{\ell} a \tag{4.19b}$$

$$\sigma_{rr}^f(a) = \sigma_{rr}^{\ell}(a) \tag{4.20a}$$

$$2K_T^f A_f + 2\,K_T^f \nu_A^f \epsilon_{zz}^o = \frac{E_T^f}{(1-2\nu^\ell)(1+\nu^\ell)} \{[(1-\nu^\ell)\,s_1+\nu^\ell]A_\ell a^{s_1-1}$$

$$+ [(1-\nu^\ell)s_2+\nu^\ell]\,B_\ell a^{s_2-1}\} \tag{4.20b}$$

at r = b $$u_r^\ell(b) = u_r^m(b) \tag{4.21a}$$

$$A_\ell b^{s_1} + B_\ell b^{s_2} - \epsilon_{zz}^o \nu^\ell b = A_m b + B_m/b \tag{4.21b}$$

$$\sigma_{rr}^\ell(b) = \sigma_{rr}^m(b) \tag{4.22a}$$

$$\frac{E^m}{(1-2\nu^\ell)(1+\nu^\ell)} \{[(1-\nu^\ell)s_1 + \nu^\ell]A_\ell b^{s_1-1}$$

$$+ [(1-\nu^\ell)s_2 + \nu^\ell]B_\ell b^{s_2-1}\} \tag{4.22b}$$

$$= \frac{E^m}{(1-2\nu^m)(1+\nu^m)} \left[A_m - (1-2\nu^m)\,\frac{B_m}{b^2} + \nu^m \epsilon_{zz}^o\right]$$

and the imposed condition at r = c is given as

$$\sigma_{rr}^m(c) = 0 \tag{4.23a}$$

$$A_m - (1-2\nu^m)\frac{B_m}{c^2} + \nu^m \epsilon_{zz}^o = 0 \qquad (4.23b)$$

where a is the outer radius of the inclusion, b is the outer radius of the interphase, and c the outer radius of the matrix as indicated in Figure 4.2.

Equations (4.19)-(4.23) are five equations with five unknowns A_f, A_ℓ, B_ℓ, A_m, and B_m, which are to be determined. The expressions for these constants are given in the Appendix B.

4.3.1.1 EFFECTIVE AXIAL YOUNG'S MODULUS

The effective axial Young's modulus of the composite E_A^c is found using the fact (Christensen, 1979), that the average axial stress in the composite $\bar{\sigma}_{zz}$ is given as

$$\bar{\sigma}_{zz} = E_A^c \, \epsilon_{zz}^o \tag{4.24a}$$

It can also be written as

$$\frac{1}{A} \iint_A \sigma_{zz}(r) \, dA = E_A^c \, \epsilon_{zz}^o \tag{4.24b}$$

Then, the effective elastic modulus is

$$E_A^c = \frac{1}{\epsilon_{zz}^o} \frac{1}{A} \iint_A \sigma_{zz}(r) \, dA \tag{4.25a}$$

or,

$$E_A^c = \frac{1}{\epsilon_{zz}^o c^2} \left([4K_T^f \nu_A^f A_f + (E_A^f + 4K_T^f \nu_A^{f\,2}) \, \epsilon_{zz}^o] a^2 \right.$$

$$\left. + \frac{2\nu^\ell}{(1-2\nu^\ell)(1+\nu^\ell)} \left[A_\ell \frac{s_1+1}{s_1+Q+1} (E^m b^{s_1+1} - E_T^f a^{s_1+1}) \right. \right. \tag{4.25b}$$

$$+ B_{\ell} \frac{s_2+1}{s_2+Q+1} (E^m b^{s_2+1} - E_T^f a^{s_2+1})] + \frac{2\epsilon_{zz}^o}{(Q+2)} (E^m b^2 - E_T^f a^2)$$

$$+ \frac{E^m}{(1-2\nu^m)(1+\nu^m)} [2\nu^m A_m + (1-\nu^m)\epsilon_{zz}^o](c^2 - b^2))$$

4.3.1.2 EFFECTIVE AXIAL POISSON'S RATIO

The effective axial Poisson's ratio ν_A^c is determined using the fact that the displacement at r = c due to the Poisson's effect (Christensen, 1979) is

$$u_r^m(c) = - \nu_A^c \epsilon_{zz}^o c \tag{4.26}$$

Then, the effective Poisson's ratio is

$$\nu_A^c = - \frac{u_r^m(c)}{\epsilon_{zz}^o c} \tag{4.27a}$$

or,

$$\nu_A^c = - \frac{1}{\epsilon_{zz}^o} \left(A_m + \frac{B_m}{c^2} \right) \tag{4.27b}$$

4.3.2 EFFECTIVE PLANE STRAIN BULK MODULUS

To predict the effective plane strain bulk modulus K_T^c again the composite cylinders assemblage model is used.

A single composite cylinder is subjected to the boundary displacement

$$u_r(c) = \epsilon_{rr}^o \, c$$

$$u_\theta(c) = u_z(c) = 0 \tag{4.28}$$

where ϵ_{rr}^o is a constant applied strain at the outer boundary at $r = c$.

The displacement solution is of the form

$$u_r = u(r)$$

$$u_\theta = 0 \tag{4.29}$$

$$u_z = 0$$

The equation of equilibrium to be satisfied for this type of deformation is as in equation (4.11). This equation is solved for the three constituents.

a) Transversely isotropic fiber.

Equations (4.10a) are introduced into (4.11) to get the governing differential equation in terms of displacements

$$r^2 u'' + r u' - u = 0 \tag{4.30}$$

This differential equation has the following solution

$$u(r) = A_f r + B_f/r \tag{4.31}$$

where $B_f = 0$ at the origin for finite solution.

b) Isotropic interphase.

Equations (4.10b) are introduced into (4.11) to get the following governing equation

$$r^2 u'' + r(1+Q) u' + \left(Q \frac{\nu^\ell}{1-\nu^\ell} - 1\right) u = 0 \tag{4.32}$$

The solution to this equation is

$$u(r) = A_\ell r^{s_1} + B_\ell r^{s_2} \tag{4.33}$$

where

$$s_1, s_2 = \frac{1}{2}\left[- Q \pm \left(Q^2 - \frac{4\nu^\ell Q}{1-\nu^\ell} + 4\right)^{1/2}\right] \tag{4.34}$$

c) Isotropic matrix

Equations (4.10b) are introduced into (4.11) to get the following differential equation

$$r^2 u'' + r u' - u = 0 \tag{4.35}$$

This differential equation has the following solution

$$u(r) = A_m r + B_m/r \tag{4.36}$$

Using the boundary conditions of the composite cylinder model, the continuity of radial displacement and radial stress across each interface must exist to assure a perfect bonding across the interfaces. Also, the condition at the outer boundary should be satisfied. Then,

at $r = a$ $\quad u_r^f(a) = u_r^\ell(a)$ (4.37a)

$$A_f a = A_\ell a^{s_1} + B_\ell a^{s_2} \tag{4.37b}$$

$$\sigma_{rr}^f(a) = \sigma_{rr}^\ell(a) \tag{4.38a}$$

$$2K_T^f A_f = \frac{E_T^f}{(1-2\nu^\ell)(1+\nu^\ell)} \{[(1-\nu^\ell)s_1+\nu^\ell]A_\ell a^{s_1-1} + [(1-\nu^\ell)s_2+\nu^\ell]B_\ell a^{s_2-1}\} \tag{4.38b}$$

at $r = b$ $\quad u_r^\ell(b) = u_r^m(b)$ (4.39a)

$$A_\ell b^{s_1} + B_\ell b^{s_2} = A_m b + B_m/b \tag{4.39b}$$

$$\sigma^\ell_{rr}(b) = \sigma^m_{rr}(b) \tag{4.40a}$$

$$\frac{E^m}{(1-2\nu^\ell)(1+\nu^\ell)} \{[(1-\nu^\ell)\, s_1 + \nu^\ell]A_\ell b^{s_1-1}$$

$$+ [(1-\nu^\ell)s_2+\nu^\ell]B_\ell b^{s_2-1}\} \tag{4.40b}$$

$$= \frac{E^m}{(1-2\nu^m)(1+\nu^m)} [A_m - (1-2\nu^m)\frac{B_m}{b^2}]$$

at r = c the imposed condition, $u_r(c) = \epsilon^o_{rr}\, c$, is written as

$$u_r(c) = A_m c + \frac{B_m}{c} = \epsilon^o_{rr} c \tag{4.41}$$

The five equations (4.37)-(4.41) with 5 unknowns are solved for the constants A_f, A_ℓ, B_ℓ, A_m, and B_m, which are given in the Appendix C.

The average strain state at the outer boundaries of the composite cylinder and the equivalent homogeneous cylinder subjected to the same displacement are equated. This procedure results in the solution of the effective plane strain bulk modulus of the single composite cylinder K^c_T, which is the same as the effective plane strain bulk

modulus of the composite as stated by Christensen (1979). The equality of the average strain in the composite cylinder and in the homogeneous cylinder (Christensen, 1979) is written as

$$\frac{\sigma_{rr}^{m}(c)}{2K_{T}^{c}} = \epsilon_{rr}^{o} \tag{4.42}$$

Then, the effective transverse plane strain bulk modulus is

$$K_{T}^{c} = \frac{\sigma_{rr}^{m}(c)}{2\epsilon_{rr}^{o}} \tag{4.43a}$$

or,

$$K_{T}^{c} = \frac{1}{2\epsilon_{rr}^{o}} \quad \frac{E^{m}}{(1-2\nu^{m})(1+\nu^{m})} \left[A_{m} - (1-2\nu^{m})\frac{B_{m}}{c^{2}}\right] \tag{4.43b}$$

4.4 EFFECTIVE AXIAL SHEAR MODULUS

To evaluate the effective axial shear modulus G_A^c, the composite cylinders assemblage model is again used. The composite cylinder is subjected to the following deformation

$$u_r = \epsilon_{xz}^o z \cos\theta$$

$$u_\theta = - \epsilon_{xz}^o z \sin\theta \tag{4.44}$$

$$u_z = u_z(r,\theta)$$

where ϵ_{xz}^o is a constant.

The strain components are

$$\epsilon_{rz} = \epsilon_{xz}^o \cos\theta + \frac{\partial u_z}{\partial r}$$

$$\epsilon_{\theta z} = - \epsilon_{xz}^o \sin\theta + \frac{1}{r} \frac{\partial u_z}{\partial \theta} \tag{4.45}$$

$$\epsilon_{rr} = \epsilon_{\theta\theta} = \epsilon_{zz} = \epsilon_{r\theta} = 0$$

The equilibrium equation to be satisfied is

$$\frac{\partial \sigma_{rz}}{\partial r} + \frac{1}{r}\frac{\partial \sigma_{\theta z}}{\partial \theta} + \frac{\sigma_{rz}}{r} = 0 \tag{4.46}$$

This equilibrium equation is solved for the three phases.

a) Transversely isotropic fiber

The governing differential equation (4.46) is given by

$$\frac{\partial^2 u_z}{\partial r^2} + \frac{1}{r}\frac{\partial u_z}{\partial r} + \frac{1}{r^2}\frac{\partial^2 u_z}{\partial \theta^2} = 0 \tag{4.47}$$

Using the separation of variables method the solution is

$$u_z(r,\theta) = (A_f r + B_f/r)\ \epsilon_{xz}^{o} \cos\theta \tag{4.48}$$

where $B_f = 0$ for finite solution at $r = 0$.

b) Isotropic layer

The governing differential equation (4.46) is written as

$$\frac{\partial^2 u_z}{\partial r^2} + \frac{Q+1}{r}\frac{\partial u_z}{\partial r} + \frac{1}{r^2}\frac{\partial^2 u_z}{\partial \theta^2} + \frac{Q}{r}\epsilon_{xz}^{o} \cos\theta = 0 \tag{4.49}$$

The general solution to the differential equation (4.49) is

$$u_z(r,\theta) = (A_\ell r^{s_1} + B_\ell r^{s_2} - r)\ \epsilon_{xz}^{o} \cos\theta \tag{4.50}$$

where

$$s_1, s_2 = \frac{1}{2}[- Q \pm (Q^2 + 4)^{1/2}] \tag{4.51}$$

c) Isotropic matrix

The governing differential equation is

$$\frac{\partial^2 u_z}{\partial r^2} + \frac{1}{r}\frac{\partial u_z}{\partial r} + \frac{1}{r^2}\frac{\partial^2 u_z}{\partial \theta^2} = 0 \tag{4.52}$$

The solution to this differential equation is

$$u_z(r,\theta) = (A_m\, r + B_m/r)\, \epsilon_{xz}^{o} \cos\theta \tag{4.53}$$

The axial displacement and axial shear stress should be continuous across each interface to assure the perfect bonding interfaces assumed in the composite cylinders model

at r = a $\qquad u_z^f(a) = u_z^\ell(a)$ (4.54a)

$$A_f a = A_\ell a^{s_1} + B_\ell a^{s_2} - a \tag{4.54b}$$

$$\sigma_{rz}^f(a) = \sigma_{rz}^\ell(a) \tag{4.55a}$$

$$2G_A^f(A_f+1) = 2G_A^f(A_\ell s_1 a^{s_1-1} + B_\ell s_2 a^{s_2-1}) \tag{4.55b}$$

at r = b $\qquad u_z^{\ell}(b) = u_z^{m}(b)$ (4.56a)

$$A_{\ell} b^{s_1} + B_{\ell} b^{s_2} - b = A_m b + B_m/b \tag{4.56b}$$

$$\sigma_{rz}^{\ell}(b) = \sigma_{rz}^{m}(b) \tag{4.57a}$$

$$2G^m(A_{\ell} s_1 b^{s_1-1} + B_{\ell} s_2 b^{s_2-1}) = 2G^m(A_m + 1 - B_m/b^2) \tag{4.57b}$$

The imposed boundary condition at r = c is

$$u_z^m(c,\theta) = \epsilon_{xz}^o \, c \cos\theta = (A_m c + B_m/c)\, \epsilon_{xz}^o \cos\theta \tag{4.58}$$

The five equations (4.54)-(4.58) are solved for A_f, A_{ℓ}, B_{ℓ}, A_m and B_m. The solutions are given in the Appendix D.

The shear stress at the exterior surface at r = c is equated to the one on the boundary of a homogeneous transversely isotropic cylinder with an axial shear modulus G_A^c (Sullivan and Hashin, 1990). Therefore, the effective axial shear modulus is

$$G_A^c = \frac{\sigma_{rz}^m(c,\theta)}{2\epsilon_{rz}^o} \tag{4.59}$$

where $\epsilon_{rz}^o = \epsilon_{xz}^o \cos\theta$ (4.60)

or,

$$G_A^c = \frac{G^m}{2} (A_m + 1 - B_m/c^2) \tag{4.61}$$

4.5 EFFECTIVE TRANSVERSE SHEAR MODULUS

The generalized self-consistent scheme is used (Christensen and Lo, 1979) to obtain the effective transverse shear modulus. In this model, the inclusion surrounded by the interphase is embedded in a matrix shell which is embedded in the infinite medium. This medium has the effective properties to be determined.

The following boundary displacement is prescribed at infinity

$$u_r = \epsilon_{xy}^{o} \, r \sin 2\theta$$

$$u_\theta = \epsilon_{xy}^{o} \, r \cos 2\theta \qquad (4.62)$$

$$u_z = 0$$

where ϵ_{xy}^{o} is a constant.

A plane strain deformation is assumed in the following form

$$u_r(r,\theta) = u(r) \sin 2\theta$$

$$u_\theta(r,\theta) = v(r) \cos 2\theta \qquad (4.63)$$

The strain components are

$$\epsilon_{rr} = u' \sin 2\theta$$

$$\epsilon_{\theta\theta} = (u - 2v) \sin 2\theta \, / r$$

(4.64)

$$\epsilon_{r\theta} = (2u/r + v' - v/r)\cos 2\theta /2$$

$$\epsilon_{zz} = \epsilon_{rz} = \epsilon_{\theta z} = 0$$

where " ' " are derivatives with respect to the radial coordinate r.

The equilibrium equations to be satisfied are

$$\frac{\partial \sigma_{rr}}{\partial r} + \frac{1}{r}\frac{\partial \sigma_{r\theta}}{\partial \theta} + \frac{\sigma_{rr} - \sigma_{\theta\theta}}{r} = 0 \tag{4.65}$$

$$\frac{\partial \sigma_{r\theta}}{\partial r} + \frac{1}{r}\frac{\partial \sigma_{\theta\theta}}{\partial \theta} + 2\frac{\sigma_{r\theta}}{r} = 0 \tag{4.66}$$

These coupled equilibrium equations are expressed in terms of displacements for each constituent.

a) Transversely isotropic fiber

The governing differential equations (4.65) and (4.66) are given as

$$r^2 u''(K_T^f + G_T^f) + ru'(K_T^f + G_T^f) - u(K_T^f + 5G_T^f)$$

(4.67)

$$- rv'(2K_T^f) + v(2K_T^f + 4G_T^f) = 0$$

$$r^2 v'' G_T^f + rv' G_T^f - v(4K_T^f + 5G_T^f)$$

(4.68)

$$+ ru'(2K_T^f) + u(2K_T^f + 4G_T^f) = 0$$

The solution to these two coupled differential equations is obtained by the reduction of order method given in Kaplan (1980) as

$$u(r) = A_f r + B_f/r + C_f r^3 + D_f/r^3 \tag{4.69}$$

$$v(r) = K_1 A_f r + K_2 B_f/r + K_3 C_f r^3 + K_4 D_f/r^3 \tag{4.70}$$

where

$$K_1 = 1;\ K_2 = \frac{G_T^f}{K_T^f + G_T^f}\ ;\ K_3 = \frac{2K_T^f + G_T^f}{K_T^f - G_T^f}\ ;\ K_4 = -1 \tag{4.71}$$

The same solution has been found in Sullivan and Hashin (1990) for the case of constant elastic properties in the interphase.

For finite values of displacements at $r = 0$ $B_f = D_f = 0$.

Then, equations (4.69) and (4.70) are written as

$$u_r = (A_f r + C_f r^3) \sin 2\theta \tag{4.72}$$

$$u_\theta = (K_1 A_f r + K_3 C_f r^3) \cos 2\theta \tag{4.73}$$

b) Isotropic interphase

The coupled differential equations are given as

$$r^2u''(1-\nu^{\ell}) + ru'(Q+1)(1-\nu^{\ell}) + u[-3+(Q+5)\nu^{\ell}] \tag{4.74}$$
$$- rv' + v[3-2(Q+2)\nu^{\ell}] = 0$$

$$r^2v''(1-2\nu^{\ell}) + rv'(Q+1)(1-2\nu^{\ell}) + v[-(Q+9)+2(Q+5)\nu^{\ell}] \tag{4.75}$$
$$+ 2ru' + u[2(Q+3)-4(Q+2)\nu^{\ell}] = 0$$

The solution to this system of two coupled equations is given for real values of $\lambda_1,\lambda_2,\lambda_3,\lambda_4,Q_1,Q_2,Q_3$, and Q_4 as.

$$u_r = (A_{\ell}r^{\lambda_1} + B_{\ell}r^{\lambda_2} + C_{\ell}r^{\lambda_3} + D_{\ell}r^{\lambda_4}) \sin 2\theta \tag{4.76}$$

$$u_{\theta} = (Q_1A_{\ell}r^{\lambda_1} + Q_2B_{\ell}r^{\lambda_2} + Q_3C_{\ell}r^{\lambda_3} + Q_4D_{\ell}r^{\lambda_4}) \cos 2\theta \tag{4.77}$$

where $\lambda_1,\lambda_2,\lambda_3,\lambda_4,Q_1,Q_2,Q_3$, and Q_4 are given in Appendix E. In the case of complex values of $\lambda_1,\lambda_2,\lambda_3,\lambda_4,Q_1,Q_2,Q_3$, and Q_4 the solution for displacements and stresses is also given in the Appendix E

c) Isotropic matrix

The coupled differential equilibrium equations are given as

$$r^2u''(1-\nu^m) + ru'(1-\nu^m) - u(3-5\nu^m) - rv'$$

$$+ v(3-4\nu^m) = 0 \tag{4.78}$$

$$r^2v''(1-2\nu^m) + rv'(1-2\nu^m) - v(9-10\nu^m) + 2ru'$$

$$+ u[2(3-4\nu^m)] = 0 \tag{4.79}$$

The solution to this system of two coupled equations is given as

$$u_r = (A_m r + B_m/r + C_m r^3 + D_m/r^3) \sin 2\theta \tag{4.80}$$

$$u_\theta = (P_1 A_m r + P_2 B_m/r + P_3 C_m r^3 + P_4 D_m/r^3) \cos 2\theta \tag{4.81}$$

where

$$P_1 = 1 \; ; \; P_2 = \frac{1 - 2\nu^m}{2(1 - \nu^m)} \; ; \; P_3 = \frac{3 - 2\nu^m}{2\nu^m} \; ; \; P_4 = -1 \tag{4.82}$$

The displacement and traction continuity conditions across each interface should be satisfied to assure perfect bonding at interfaces

at $r = a$ $\qquad u_r^f(a,\theta) = u_r^\ell(a,\theta)$

$$u_\theta^f(a,\theta) = u_\theta^\ell(a,\theta)$$

(4.83)

$$\sigma_{rr}^{f}(a,\theta) = \sigma_{rr}^{\ell}(a,\theta)$$

$$\sigma_{r\theta}^{f}(a,\theta) = \sigma_{r\theta}^{\ell}(a,\theta)$$

at $r = b$

$$u_{r}^{\ell}(b,\theta) = u_{r}^{m}(b,\theta)$$

$$u_{\theta}^{\ell}(b,\theta) = u_{\theta}^{m}(b,\theta)$$

(4.84)

$$\sigma_{rr}^{\ell}(b,\theta) = \sigma_{rr}^{m}(b,\theta)$$

$$\sigma_{r\theta}^{\ell}(b,\theta) = \sigma_{r\theta}^{m}(b,\theta)$$

at $r = c$

$$u_{r}^{m}(c,\theta) = u_{r}^{c}(c,\theta)$$

$$u_{\theta}^{m}(c,\theta) = u_{\theta}^{c}(c,\theta)$$

(4.85)

$$\sigma_{rr}^{m}(c,\theta) = \sigma_{rr}^{c}(c,\theta)$$

$$\sigma_{r\theta}^{m}(c,\theta) = \sigma_{r\theta}^{c}(c,\theta)$$

The displacement solution for the equivalent composite is

$$u(r) = A_c r + B_c/r + C_c r^3 + D_c/r^3 \tag{4.86}$$

$$v(r) = D_1 A_c r + D_2 B_c/r + D_3 C_c r^3 + D_4 D_c/r^3 \tag{4.87}$$

where

$$D_1 = 1;\ D_2 = \frac{G_T^c}{K_T^c + G_T^c}\ ;\ D_3 = \frac{2K_T^c + G_T^c}{K_T^c - G_T^c}\ ;\ D_4 = -1 \tag{4.88}$$

The displacement boundary conditions at infinity are

$$\begin{aligned} u(r) &= \epsilon_{xy}^o\, r \\ v(r) &= \epsilon_{xy}^o\, r \end{aligned} \tag{4.89}$$

Then, $A_c = \epsilon_{xy}^o$ since $D_1 = 1$, and $C_c = 0$.

The average transverse shear stress at the outer boundary **r=c is** equated to the one of the homogeneous transversely isotropic **composite** subjected to the same pure shear strain.

The average stress in the composite is evaluated from

$$\begin{aligned} \bar{\sigma}_{xy} = 2G_T^c\, \epsilon_{xy}^o = \frac{1}{\Pi c^2} \int_{r=c} [\sigma_{rr}^c(c,\theta)\cos\theta \\ - \sigma_{r\theta}^c(c,\theta)\sin\theta]c^2 \sin\theta\, d\theta \end{aligned} \tag{4.90}$$

where G_T^c is the effective transverse shear modulus of the composite. Then, equation (4.90) is written as

$$G_T^c[2\epsilon_{xy}^o - \frac{K_T^c}{K_T^c+G_T^c} B_c/c^2] = 2G_T^c \epsilon_{xy}^o \tag{4.91}$$

which is satisfied when $B_c = 0$.

Equations (4.83) to (4.85) are 12 equations with 12 unknowns A_f, C_f, A_ℓ, B_ℓ, C_ℓ, D_ℓ, A_m, B_m, C_m, D_m, D_c, and G_T^c. Ten of these equations are linear whereas two equations are non-linear. Therefore, these 12 equations are solved by using an iteration method.

The solution for the transverse shear modulus G_T^c is

$$G_T^c = \frac{G_m}{2\epsilon_{xy}^o} [2A_m - \frac{B_m}{2(1-\nu_m)} /c^2 + \frac{3C_m}{2\nu_m} c^2] \tag{4.92}$$

4.6 EFFECTIVE THERMAL EXPANSION COEFFICIENTS

The thermal expansion coefficients for a composite reinforced with unidirectional long fibers are determined using the composite cylinders model. In this study the interphase is assumed to be inhomogeneous having properties changing in the radial direction. The power variation relationship is used to simulate the variation of both the axial Young's modulus and thermal expansion coefficients. In this section Poisson's ratio is assumed to be constant for simplicity.

The elastic axial Young's modulus and the thermal expansion coefficients are given by

$$E^{\ell}(r) = P\, r^{Q}$$

$$\alpha^{\ell}(r) = M\, r^{N} \tag{4.93}$$

where P, Q, M, and N are constants which are evaluated by assuming the following conditions

$$E^{\ell}(a) = E_T^f \qquad \alpha^{\ell}(a) = \alpha_T^f \qquad \text{at } r = a$$

$$E^{\ell}(b) = E^m \qquad \alpha^{\ell}(b) = \alpha^m \qquad \text{at } r = b \tag{4.94}$$

The conditions (4.94) are adopted in this dissertation, however, any other conditions can be used without further difficulties.

The composite is subjected to a uniform temperature change ΔT . Consider an axially symmetric state defined by the following

$$u_r = u(r)$$

$$u_\theta = 0 \tag{4.95}$$

$$u_z = \epsilon^o_{zz}\, z$$

where ϵ^o_{zz} is a constant to be determined.

The strain-displacement relations given in (4.4) reduce to

$$\epsilon_{rr} = u'(r) \quad ; \quad \epsilon_{\theta\theta} = \frac{u(r)}{r} \quad ; \quad \epsilon_{zz} = \epsilon^o_{zz}$$

$$\epsilon_{r\theta} = \epsilon_{rz} = \epsilon_{\theta z} = 0 \tag{4.96}$$

Hooke's law expressed in terms of displacements for transversely isotropic case is

$$\sigma_{rr} = (K_T+G_T)\, u' + (K_T-G_T)\, \frac{u}{r} - 2K_T\alpha_T\Delta T + 2K_T\nu_A(\epsilon^o_{zz} - \alpha_A\Delta T)$$

$$\sigma_{\theta\theta} = (K_T-G_T)\, u' + (K_T+G_T)\, \frac{u}{r} - 2K_T\alpha_T\Delta T + 2K_T\nu_A(\epsilon^o_{zz} - \alpha_A\Delta T)$$

$$\sigma_{zz} = 2K_T\nu_A(u' + \frac{u}{r} - 2\alpha_T\Delta T) + (E_A + 4K_T\nu_A^2)(\epsilon^o_{zz} - \alpha_A\Delta T)$$

$$\sigma_{r\theta} = \sigma_{rz} = \sigma_{\theta z} = 0 \tag{4.97a}$$

The stresses for isotropic case are expressed as

$$\sigma_{rr} = \frac{E}{(1-2\nu)(1+\nu)} [(1-\nu)\, u' + \nu \frac{u}{r} - (1+\nu)\alpha\Delta T + \nu\epsilon^{o}_{zz})]$$

$$\sigma_{\theta\theta} = \frac{E}{(1-2\nu)(1+\nu)} [\nu\, u' + (1-\nu) \frac{u}{r} - (1+\nu)\alpha\Delta T + \nu\epsilon^{o}_{zz}]$$

$$\sigma_{zz} = \frac{E}{(1-2\nu)(1+\nu)} [\nu(u' + \frac{u}{r} - 2\alpha\Delta T) + (1-\nu)(\epsilon^{o}_{zz} - \alpha\Delta T)]$$

$$\sigma_{r\theta} = \sigma_{rz} = \sigma_{\theta z} = 0 \qquad (4.97b)$$

The equations of equilibrium (4.5) reduce to the single equation given by (4.11). Equations (4.97) are introduced into (4.11) to obtain the differential equation in terms of displacements. This equation is written for each constituent.

a) Transversely isotropic fiber and isotropic matrix

The differential equation (4.11) for inclusion and matrix is written as

$$\frac{d^2u^i}{dr^2} + \frac{1}{r}\frac{du^i}{dr} - \frac{1}{r^2} u^i = 0 \qquad i = f, m \qquad (4.98)$$

The general solution is

$$u^i(r) = A_i r + B_i/r \qquad i = f, m \qquad (4.99)$$

where A_i and B_i are constants to be determined using the boundary conditions, B_f is set to zero for finite solution at $r = 0$.

b) Isotropic interphase

The governing differential equation is

$$u'' + \frac{1}{r}(Q+1)\,u' + \frac{1}{r^2}\left(\frac{Q\nu^{\ell}}{1-\nu^{\ell}} - 1\right) u$$

$$+ \frac{1}{r}\left[\frac{Q\nu^{\ell}}{1-\nu^{\ell}}\,\epsilon^{o}_{zz} - \frac{1+\nu^{\ell}}{1-\nu^{\ell}}\,(Q+N)\alpha^{\ell}\Delta T\right] = 0 \qquad (4.100)$$

The general solution to equation (4.100) is

$$u(r) = A_{\ell} r^{s_1} + B_{\ell} r^{s_2} - \epsilon^{o}_{zz}\,\nu^{\ell} r + \frac{\left[M(Q+N)\Delta T\,\frac{1+\nu^{\ell}}{1-\nu^{\ell}}\right] r^{N+1}}{N^2 + 2N + QN + Q\,\frac{1}{1-\nu^{\ell}}} \qquad (4.101)$$

where

$$s_1, s_2 = \frac{1}{2}\left[-Q \pm \left(Q^2 - \frac{4Q\nu^{\ell}}{1-\nu^{\ell}} + 4\right)^{1/2}\right] \qquad (4.102)$$

which is the same as equation (4.16).

The stress components in the three phases are determined by substituting the corresponding displacement solutions in equations (4.97).

The unknown constants A_f, A_ℓ, B_ℓ, A_m, B_m, and ϵ_{zz}^o are determined by using the boundary conditions. The continuity of radial displacement and radial stress across each interface at r = a and r = b is due to the perfect bonding assumption in the composite cylinder model. These continuity equations are written as

$$\text{at } r = a \quad u_r^f(a) = u_r^\ell(a) \tag{4.103}$$

$$\sigma_{rr}^f(a) = \sigma_{rr}^\ell(a) \tag{4.104}$$

$$\text{at } r = b \quad u_r^\ell(b) = u_r^m(b) \tag{4.105}$$

$$\sigma_{rr}^\ell(b) = \sigma_{rr}^m(b) \tag{4.106}$$

The boundary condition at r = c is

$$\sigma_r^m(c) = 0 \tag{4.107}$$

The additional equation is

$$\sigma_{zz}^f(\text{area of fiber}) + \sigma_{zz}^\ell(\text{area of interphase})$$

$$+ \sigma_{zz}^m(\text{area of matrix}) = \int_0^c \sigma_{zz} r \, dr = 0 \tag{4.108}$$

where a, b, and c are shown in Fig. 4.2.

Equations (4.103) to (4.108) are six equation with six unknowns A_f, A_ℓ, B_ℓ, A_m, B_m, and ϵ^o_{zz} to be determined. The expressions for these six constants are given in the Appendix F.

The effective thermal expansion coefficients are defined as the average strains due to a unit temperature rise for a traction free composite. Therefore α^c_A and α^c_T are given as in (Uemura et al., 1979; Tong, 1990).

$$\alpha^c_A = \frac{\epsilon^o_{zz}}{\Delta T} \tag{4.109}$$

$$\alpha^c_T = \frac{u^m(c)}{c\Delta T} = \frac{A_m + B_m/c^2}{\Delta T} \tag{4.110}$$

4.7 POISSON'S RATIO GRADIENTS PROBLEM

In the previous sections Poisson's ratio of the interphase was assumed to be constant for simplicity. In this section the effect of variation in Poisson's ratio value in the interphase on the thermal and elastic properties of composites is investigated. Therefore, different variations for Poisson's ratio value, elastic modulus and thermal expansion coefficients in the interphase are adopted to show its effect on the effective thermal and elastic properties (see Appendix G). In this section the elastic modulus, Poisson's ratio and thermal expansion coefficient of the interphase are denoted respectively by E_ℓ, ν_ℓ and α_ℓ, the subscript is used instead of superscript to avoid confusion with the derivative with respect to r denoted by " ' " and the power.

The models used in Sections 4.7.1-4.7.4 are as follows

Model 1 $$E_\ell = P\, r^{Q} \tag{4.111}$$

$$\nu_\ell = S\, r + T$$

Model 2 $$E_\ell = P\, r^{Q} \tag{4.112}$$

$$\nu_\ell = S + \frac{T}{r}$$

Model 3 $$E_\ell = P\, r^{Q} \tag{4.113}$$

$$\nu_\ell = \frac{S}{r - T}$$

Model 4 $$E_\ell = P\ r^Q \qquad (4.114)$$

$$\nu_\ell = S\ r^2 + T\ r + W$$

Model 5 $$E_\ell = P\ r + Q \qquad (4.115)$$

$$\nu_\ell = S\ r + T$$

Model 6 $$E_\ell = P\ r + Q \qquad (4.116)$$

$$\nu_\ell = S + \frac{T}{r}$$

Model 7 $$E_\ell = P\ r + Q \qquad (4.117)$$

$$\nu_\ell = \frac{S}{r - T}$$

Model 8 $$E_\ell = P + \frac{Q}{r} \qquad (4.118)$$

$$\nu_\ell = S + \frac{T}{r}$$

Model 9 $$E_\ell = P\ r^2 + Q\ r + R \qquad (4.119)$$

$$\nu_\ell = S\ r + T$$

Model 10 $$E_\ell = R\ r^2 + P\ r + Q \qquad (4.120)$$

$$\nu_\ell = S$$

where P, Q, S, and T are four constants to be determined using the assumed conditions at r = a and r = b. R in the quadratic variation relationship is a free parameter, which allows us to have a wide range of distributions.

For all of the above models the homogeneous part of the governing differential equation in terms of displacements in the interphase for plane strain axisymmetric boundary displacements is written in the following form

$$u'' + M(r)\ u' + N(r)\ u = 0 \qquad (4.121)$$

where M(r) and N(r) are two functions of the radial coordinate r which are given in Appendix H for each model for axisymmetric deformations. These two functions are determined using a symbolic manipulation program called MACSYMA (1990).

The series solution method (Johnson and Johnson, 1982) is used to solve equation (4.121). This method states that if r = 0 is a regular singular point, that is r M(r) and r^2 N(r) both have Taylor's series expansions about r = 0, then, a convergent series solution exists of the form

$$u_k(r) = \sum_{n=0}^{\infty} a_n r^{n+k} \tag{4.122}$$

The coefficients a_n are determined by making (4.122) satisfy the differential equation (4.121). Two values of k are obtained using the indicial equation of order zero given as

$$k^2 + (m_o - 1)\, k + n_o = 0 \tag{4.123}$$

where m_o and n_o are the first terms of the Taylor's series expansions about r = 0 of M(r) and N(r), respectively.

Therefore, the displacement solution in the interphase is written in terms of series expansions as

$$u(r) = A_\ell \sum_{n=0}^{\infty} a_n r^{n+k_1} + B_\ell \sum_{n=0}^{\infty} a_n r^{n+k_2} + u_p(r) \tag{4.124}$$

where $u_p(r)$ is a particular solution.

The displacement and stress solutions in the inclusion and the matrix are the same as the ones obtained in Sections 4.3-4.6 where the effective thermal and elastic properties were discussed. In Sections 4.7.1-4.7.5 the effect of Poisson's ratio radial variation in the interphase is studied. The governing differential equations in the interphase will be presented for each case.

4.7.1 EFFECTIVE AXIAL ELASTIC MODULUS & POISSON'S RATIO

In this section the composite cylinders assemblage model is used to evaluate the effective axial Young's modulus and the axial Poisson's ratio of composite.

A single three phase cylinder, which undergoes the axially symmetric state of deformation at its boundary is considered. In this section we follow the same procedure as in Section 4.3.1 to get the effective axial elastic modulus and effective Poisson's ratio except that Poisson's ratio in the interphase is now changing in the radial direction. The solutions for stresses and displacements are written using infinite series following the method discussed in Section 4.7.

The governing differential equation in the inhomogeneous (isotropic) interphase is written as

$$
\begin{aligned}
& E_\ell(1-2\nu_\ell)(1-\nu_\ell)\, u'' \\
& + \{E_\ell(1-2\nu_\ell)(1-\nu_\ell^2) + E_\ell\nu_\ell'(1-\nu_\ell)(1+4\nu_\ell) \\
& + E_\ell(1-2\nu_\ell)(1+\nu_\ell)\left(\frac{1-\nu_\ell}{r} - \nu_\ell'\right)\} u' \\
& + \{E_\ell'(1-2\nu_\ell)(1+\nu_\ell)\frac{\nu_\ell}{r} + E_\ell\nu_\ell'\frac{\nu_\ell}{r}(1+4\nu_\ell) \\
& + E_\ell(1-2\nu_\ell)(1+\nu_\ell)\left(\frac{\nu_\ell'}{r} - \frac{1-\nu_\ell}{r^2}\right)\} u
\end{aligned}
\qquad (4.125)
$$

$$+ \{E_{\ell}'(1-2\nu_{\ell})(1+\nu_{\ell})\nu_{\ell} + E_{\ell}\nu_{\ell}'\nu_{\ell}(1+4\nu_{\ell})$$

$$+ E_{\ell}(1-2\nu_{\ell})(1+\nu_{\ell})\ \nu_{\ell}'\}\ \epsilon_{zz}^{0} = 0.$$

Here, both E_{ℓ} and ν_{ℓ} are assumed to be functions of r.

If the case when both the elastic modulus and Poisson's ratio have a parabolic distribution, equation (4.125) is of the form

$$r^2\ P_1(r)\ u'' + r\ P_2(r)\ u' + P_3(r)\ u + r\ P_4(r) = 0, \qquad (4.126)$$

where

$$P_i(r) = A_i r^8 + B_i r^7 + C_i r^6 + D_i r^5 + E_i r^4 + F_i r^3 + G_i r^2 + H_i r + I_i$$

for $i = 1, 2, 3, 4.$ (4.127)

The homogeneous part of the differential equation (4.125) is written using the symbolic manipulation program MACSYMA (1990) as

$$u'' + M(r)\ u' + N(r)\ u = 0 \qquad (4.128)$$

where the explicit solution for the homogeneous part is given in Section 4.7 in an infinite series form.

The particular solution for each model is also given in the infinite series form.

1.b EFFECTIVE PLANE STRAIN BULK MODULUS

To predict the effective plane strain bulk modulus, the composite cylinders assemblage model is again used. In this section we follow the same procedure as in Section 4.3.2

A single composite cylinder is subjected to the boundary displacement given by (4.29)

For the inhomogeneous interphase the governing equation is written as

$$
\begin{aligned}
& E_\ell(1-2\nu_\ell)(1-\nu_\ell^2)\, u'' + \\
& + \{E_\ell'(1-2\nu_\ell)(1-\nu_\ell^2) + E_\ell\nu_\ell'(1-\nu_\ell)(1+4\nu_\ell) \\
& + E_\ell(1-2\nu_\ell)(1+\nu_\ell)\left(\frac{1-\nu_\ell}{r} - \nu_\ell'\right)\} u' \qquad (4.129) \\
& + \{E_\ell'(1-2\nu_\ell)(1+\nu_\ell)\frac{\nu_\ell}{r} + E_\ell\nu_\ell'\frac{\nu_\ell}{r}(1+4\nu_\ell) \\
& + E_\ell(1-2\nu_\ell)(1+\nu_\ell)\left(\frac{\nu_\ell'}{r} - \frac{1-\nu_\ell}{r^2}\right)\} u = 0.
\end{aligned}
$$

The solution to this differential equation is obtained using the same procedure as in Section 4.7.1.

4.7.3 EFFECTIVE AXIAL SHEAR MODULUS

To predict the effective axial shear modulus again the composite cylinders model is used. In this section we follow the same procedure as in Section 4.4.

The composite is subjected to the same boundary displacement as in equation (4.44).

The equilibrium equation governing the inhomogeneous interphase written in terms of displacements is

$$E_\ell(1+\nu_\ell)\frac{\partial^2 u_z}{\partial r^2} + [E'_\ell(1+\nu_\ell)-E_\ell\nu'_\ell+E_\ell(1+\nu_\ell)/r]\frac{\partial u_z}{\partial r}$$

$$+ \frac{1}{r^2}E_\ell(1+\nu_\ell)\frac{\partial^2 u_z}{\partial \theta} + [E'_\ell(1+\nu_\ell)-E_\ell\nu'_\ell]\epsilon^o_{xz}\cos\theta = 0 \qquad (4.130)$$

Equation (4.130) is solved using the separation of variables method as in Section 4.4, and then the series solution technique described in Section 4.7.

4.7.4 EFFECTIVE TRANSVERSE SHEAR MODULUS

To obtain the effective transverse shear modulus, the generalized self-consistent scheme is used (Christensen and Lo, 1979). In this model the inclusion surrounded by the interphase is embedded in a matrix shell which is embedded in the infinite medium which has the effective properties to be determined (see Fig. 2.3). Consider the composite to be subjected to the boundary displacement prescribed at infinity as given by equation (4.62).

For the inhomogeneous isotropic interphase the coupled differential equations for the case when both the elastic modulus and Poisson's ratio changing in the radial direction reduce to

$$E_\ell(1-2\nu_\ell)(1-\nu_\ell^2)\,u'' \tag{4.131}$$

$$+ [E_\ell'(1-2\nu_\ell)(1-\nu_\ell^2) + E_\ell\nu_\ell'(1+4\nu_\ell)(1-\nu_\ell) - E_\ell\nu_\ell'(1-2\nu_\ell)(1+\nu_\ell)$$

$$+ E_\ell\nu_\ell(1-2\nu_\ell)(1+\nu_\ell)/r + E_\ell(1+\nu_\ell)(1-2\nu_\ell)^2/r]\,u'$$

$$+ [E_\ell'\nu_\ell(1-2\nu_\ell)(1+\nu_\ell)/r + E_\ell\nu_\ell'\nu_\ell(1+4\nu_\ell)/r$$

$$+ E_\ell\nu_\ell'(1-2\nu_\ell)(1+\nu_\ell)/r - E_\ell\nu_\ell(1-2\nu_\ell)(1+\nu_\ell)/r^2$$

$$- 3E_\ell(1+\nu_\ell)(1-2\nu_\ell)^2/r^2]\,u$$

$$+ [-2E_\ell\nu_\ell(1-2\nu_\ell)(1+\nu_\ell) - E_\ell(1+\nu_\ell)(1-2\nu_\ell)^2/r]\ v'$$

$$+ [-2E'_\ell\nu_\ell(1-2\nu_\ell)(1+\nu_\ell)/r - 2E_\ell\nu_\ell\nu'_\ell(1+4\nu_\ell)/r$$

$$- 2E_\ell\nu'_\ell(1-2\nu_\ell)(1+\nu_\ell)/r + 2E_\ell\nu_\ell(1-2\nu_\ell)(1+\nu_\ell)/r^2$$

$$+ 3E_\ell(1+\nu_\ell)(1-2\nu_\ell)^2/r^2]\ v = 0$$

$$E_\ell(1+\nu_\ell)(1-2\nu_\ell)\ v'' \qquad (4.132)$$

$$+ [E'_\ell(1+\nu_\ell)(1-2\nu_\ell) - E_\ell\nu'_\ell(1-2\nu_\ell) + E_\ell(1+\nu_\ell)(1-2\nu_\ell)/r]\ v'$$

$$+ [-E'_\ell(1+\nu_\ell)(1-2\nu_\ell)/r + E_\ell\nu'_\ell(1-2\nu_\ell)/r$$

$$+ E_\ell(1+\nu_\ell)(1-2\nu_\ell)/r^2 - 8E_\ell(1-\nu_\ell^2)/r^2$$

$$- 2E_\ell(1+\nu_\ell)(1-2\nu_\ell)/r^2]\ v$$

$$+ [2E_\ell(1+\nu_\ell)(1-2\nu_\ell)/r + 4E_\ell\nu_\ell(1+\nu_\ell)/r]\ u'$$

$$+ [2E'_\ell(1+\nu_\ell)(1-2\nu_\ell)/r - 2E_\ell\nu'_\ell(1-2\nu_\ell)/r$$

$$+ 2E_\ell(1+\nu_\ell)(1-2\nu_\ell)/r^2 + 4E_\ell(1-\nu_\ell^2)/r^2]\ u = 0$$

where E_ℓ and ν_ℓ are function of the radial coordinate r.

The solution for stresses and displacements are determined using the same method as in Section 4.5.

4.7.6 EFFECTIVE THERMAL EXPANSION COEFFICIENTS

The thermal expansion coefficients for a composite reinforced with unidirectional long fibers are determined using again the composite cylinders assemblage model. The parabolic variation is chosen here to simulate the variation of the axial Young's modulus, Poisson's ratio, and thermal expansion coefficients. The solution for stresses and displacements requires infinite series (see Section 4.7).

The governing differential equation in the inhomogeneous interphase is written as

$$
\begin{aligned}
& E_\ell(1-2\nu_\ell)(1-\nu_\ell^2)\, u'' \\
& + [E_\ell'(1-2\nu_\ell)(1-\nu_\ell^2) + E_\ell\nu_\ell'(1+4\nu_\ell)(1-\nu_\ell) \\
& + E_\ell(1-2\nu_\ell)(1+\nu_\ell)(\frac{\nu_\ell}{r} - \nu') + \frac{E_\ell}{r}(1-2\nu_\ell)^2(1+\nu_\ell)]\, u' \\
& + [\frac{E_\ell'}{r}(1-2\nu_\ell)(1+\nu_\ell)\nu_\ell + \frac{E_\ell}{r}\nu_\ell\nu_\ell'(1+4\nu_\ell) \\
& - \frac{E_\ell}{r}(1-2\nu_\ell)(1+\nu_\ell)(\frac{\nu_\ell}{r} - \nu') - \frac{E_\ell}{r^2}(1-2\nu_\ell)^2(1+\nu_\ell)]\, u \qquad (4.133) \\
& + [-E_\ell'(1-2\nu_\ell)(1+\nu_\ell)^2\alpha_\ell\Delta T + E_\ell'(1-2\nu_\ell)(1+\nu_\ell)\nu_\ell\epsilon_{zz}^o \\
& - E_\ell\nu_\ell'(1+4\nu_\ell)(1+\nu_\ell)\alpha_\ell\Delta T + E_\ell\nu_\ell'\nu_\ell(1+4\nu_\ell)\epsilon_{zz}^o
\end{aligned}
$$

$$- E_\ell(1-2\nu_\ell)(1+\nu_\ell)\nu'_\ell\alpha_\ell\Delta T - E_\ell(1-2\nu_\ell)(1+\nu_\ell)^2\alpha'_\ell\Delta T$$

$$+ E_\ell(1-2\nu_\ell)(1+\nu_\ell)\nu'_\ell\epsilon^o_{zz}] = 0$$

For parabolic variation relationship the Young's modulus , Poisson's ratio, and thermal expansion coefficients are given as

$$E_\ell(r) = M\, r^2 + P\, r + Q$$

$$\nu_\ell(r) = N\, r^2 + S\, r + T \qquad (4.134)$$

$$\alpha_\ell(r) = L\, r^2 + U\, r + V$$

In order to determine the constants the following conditions are used

$$E_\ell(a) = E^f_T \quad \alpha_\ell(a) = \alpha^f_T \quad \nu_\ell(a) = \nu^f_T \quad \text{at} \quad r = a$$

$$E_\ell(b) = E^m \quad \alpha_\ell(b) = \alpha^m \quad \nu_\ell(b) = \nu^m \quad \text{at} \quad r = b \qquad (4.135)$$

Equations (4.134) can be written in terms of the radial coordinate and the parameters M, N, and L as

$$E_\ell(r) = M\, r^2 + \frac{(E^f_T - E^m) - M(a^2 - b^2)}{a - b}\, r + \frac{E^m a - E^f_T b + Mab(a-b)}{a - b}$$

$$\alpha_\ell(r) = L\, r^2 + \frac{(\alpha_T^f-\alpha^m)-L(a^2-b^2)}{a-b}\, r + \frac{\alpha^m a-\alpha_T^f b+Lab(a-b)}{a-b} \qquad (4.136)$$

$$\nu_\ell(r) = N\, r^2 + \frac{(\nu_T^f-\nu^m)-N(a^2-b^2)}{a-b}\, r + \frac{\nu^m a-\nu_T^f b+Nab(a-b)}{a-b}$$

It is shown in Figures 4.3 and 4.4 that if the parameters M, L, and N are equal to zero, the parabolic distribution reduces to a linear distribution. Whereas, when $M = M_{max} = \frac{E_T^f-E^m}{(a-b)^2}$, $L = L_{max} = \frac{\alpha_T^f-\alpha^m}{(a-b)^2}$, and $N = N_{max} = \frac{\nu_T^f-\nu^m}{(a-b)^2}$ the parabolic curve assures the smoothest transition of the thermal and elastic properties at the interphase-matrix interface. All the other variation relationships are approximately covered by the parabolic distribution by selecting a proper value to these parameters.

In this section the parabolic variation relationship is used to simulate the property gradients in the interphase. The differential equation in terms of displacements for the interphase is written as

$$p_1(r)\, u'' + r\, p_2(r)\, u' + r^2\, p_3(r)\, u + p_4(r) = 0 \qquad (4.137)$$

where $p_1(r)$, $p_2(r)$, and $p_3(r)$ are polynomials of order 8 and $p_4(r)$ of order 9. The expressions of these polynomials for parabolic distributions are too lengthy to include. However, several special cases are given in the Appendix I.

The solution for the above differential equation is found using the same method presented in Section 4.6. The expressions for the effective thermal expansion coefficients are the same as those given by equations (4.109) and (4.110).

4.8 NUMERICAL RESULTS AND DISCUSSION

The numerical results are presented for graphite-epoxy composites with properties E^m=3.5 GPA; ν^m=.35; α^m=65x10^{-6}/°C; E_A^f=214 GPA; ν_A^f=.25; K_T^f=8.83 GPA; G_T^f=5.83 GPA; α_A^f=-10^{-6}/°C; α_T^f=10.1x10^{-6}/°C (Sottos et al., 1989); G_A^f=8 GPA and for glass-plastics composites with properties E^m=3.4 GPA; ν^m=.38; α^m=66x10^{-6}/°C; E^f=69 GPA; ν^f=.2; α^f=5x10^{-6}/°C (Uemura et al., 1979). Both composites are treated as effectively transversely isotropic due to the geometry of the reinforcement, thus, five independent effective elastic constants (E_A^c, ν_A^c, K_T^c, G_A^c, and G_T^c) and two thermal expansion coefficients (α_A^c and α_T^c) are determined.

As discussed in the previous sections the interphase between the matrix and the fibers is assumed to be non-homogeneous but isotropic. In the numerical examples this fact is simulated by varying the two independent elastic properties (Young's modulus E and Poisson's ratio ν) and the thermal expansion coefficient in the radial direction. The power variation of the elastic modulus with a constant Poisson's ratio in the interphase gave a closed form for the effective elastic constants and the effective thermal expansion coefficients as discussed by Lekhnitskii (1981) and illustrated by Jayaraman et al. (1991). However, any other radial variation for both elastic and thermal properties requires infinite series for displacements, stresses, and thermoelastic constants solution. These solutions are obtained with the help of the symbolic manipulation program called MACSYMA.

Fig. 4.3 illustrates the parabolic variation in the interphase of the elastic and thermal properties written as $EP(r)=Ar^2+Br+C$. It is seen that the free parameter being properly selected gives a wide range of distributions. In fact, the zero value of this parameter A gives the linear variation and the value $A = 0.4\ A_{max}$ gives approximately the power variation. A_{max} is defined in Section 4.7.6.

Fig. 4.4 illustrates the linear, reciprocal, power, hyperbolic, and parabolic variation relationships adopted to simulate the variation of the elastic and thermal properties in the interphase. These variation relationships can be compared to the parabolic variation relationship provided that the free parameter in the latter is properly selected.

Figures 4.3 and 4.4 are done for a fiber radius a=1.0 and an interphase outer radius b=1.1. The elastic or thermal properties of the interphase are chosen to vary from the value 1.0 to the value 2.0.

Figures 4.5-4.18 illustrate the variation of the normalized effective elastic and thermal properties versus the fiber volume fraction. In these figures Poisson's ratio is assumed to be the average of Poisson's ratios of the matrix and the fiber, while, the elastic modulus and the thermal expansion coefficient if applicable are either constant or having a power variation in the interphase. When they are constant, they are taken as the average of equation (4.5) obtained by integration. The normalized thickness $t = (b-a)/a = 0.0$, 0.1 and 0.2, where a is the fiber radius and b is the interphase outer radius. It is seen that the effect of the non-homogeneous interphase is significant especially for high volume fraction of fibers and for thick interphases. These results agree with studies of Sullivan and Hashin (1990), Benveniste et al. (1989), and Tong and Jasiuk (1990) for the

homogeneous interphase case. Further investigations of the effect of Poisson's ratio value in the interphase on the effective elastic properties of the composite are made. It was shown that an interphase having a non-constant Poisson's ratio affects significantly the local stress fields and the effective elastic and thermal properties. The effective plane strain bulk modulus, axial shear and thermal expansion coefficients are chosen to be presented in Figures 4.19-4.26 because these properties are the most affected by the variable Poisson's ratio.

Figures 4.19-4.26 show the variation of the normalized effective plane strain bulk modulus, axial shear modulus and thermal expansion coefficients versus the fiber volume fraction. In these graphs the elastic modulus and Poisson's ratio are assumed to be changing in the radial direction, the variation is either linear or of power type. The normalized thickness is taken to be (b-a)/a = 0.1 . It is seen that the effect of non-constant Poisson's ratio on the effective elastic and thermal properties of the composite is considerable but less significant than the effect of the variable elastic modulus on the same properties.

Figures 4.27-4.30 show the distribution of the normalized radial stress $\sigma_{rr}/2K^{m}\epsilon^{o}_{rr}$ and the axial shear stress σ_{rz} in the radial direction for elastic modulus and Poisson's ratio having either linear or power variation in the radial direction. In these graphs the composite cylinders assemblage model is used, where the fiber radius a = 0.7, the interphase outer radius b = 0.8, and the matrix radius c = 1.0 which corresponds to fiber volume fraction f=0.49. These stresses for the case of ν=const. are the same as the stresses obtained by Jayaraman et al. (1991). It is clearly seen in these two graphs that

the smoother is the transition of the elastic properties values at the interphase-matrix interface the higher stress is transferred to the reinforcements and the lower is the stress carried by the matrix. Therefore, for design purposes it is a desirable result; composite may be used at its optimum.

Figures 4.31-4.34 show a distribution of the normalized radial stress $\sigma_{rr}/2K^{m}\epsilon^{o}_{rr}$ in the radial direction. These graphs are done using a parabolic variation relationship simulating the variation of the elastic modulus in the interphase. Poisson's ratio in the interphase is either constant or varies linearly in the radial direction. The free parameter of the parabolic variation relationship is chosen as A = 0, 0.4 A_{max}, and A_{max}. A = 0 represents the linear variation, the value A = 0.4 A_{max} represents approximately the power variation and the value A = A_{max} gives the smoothest transition of the elastic properties at the interphase-matrix interface. This is when the tangent vector to this curve at this interface is horizontal. The same conclusion as in Figures 4.27-4.30 is drawn. The radial stresses obtained previously using the power variation for the elastic modulus is very close to the radial stresses obtained using the parabolic variation for a value of the free parameter A = 0.4 A_{max}.

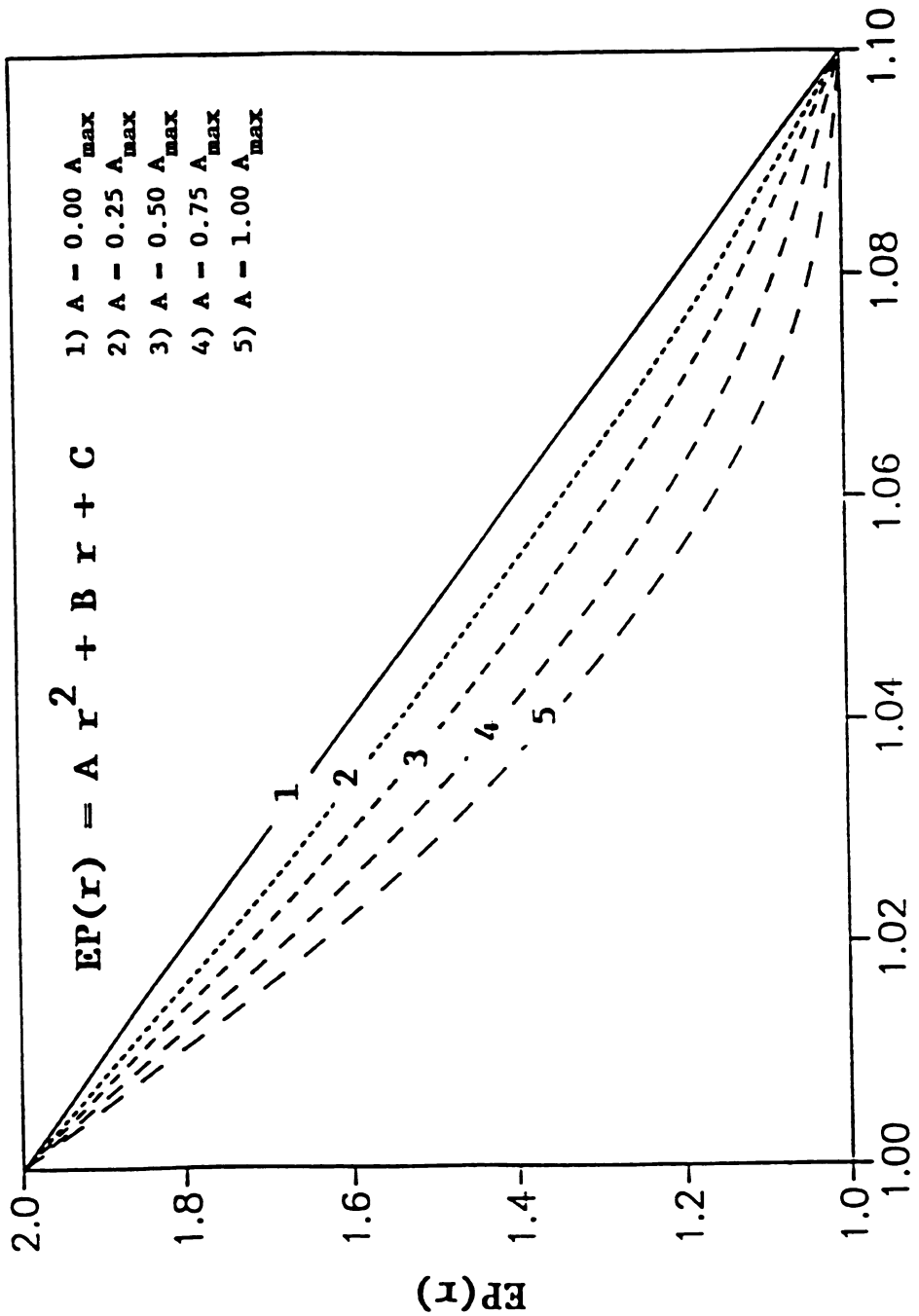

Fig. 4.3 Parabolic variation relationship for changing parameter.

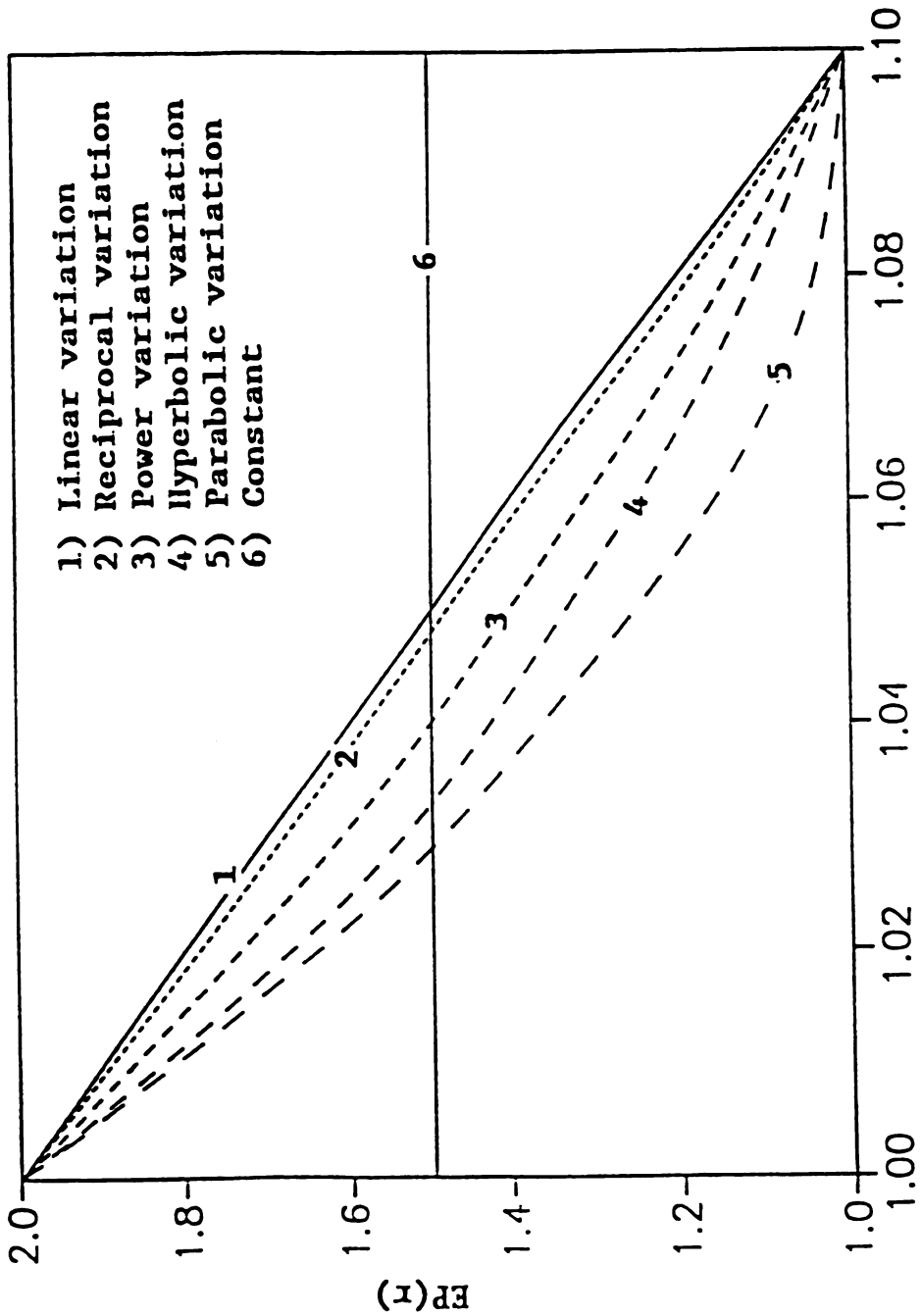

Fig. 4.4 Linear, reciprocal, power, hyperbolic, and parabolic variation relationship.

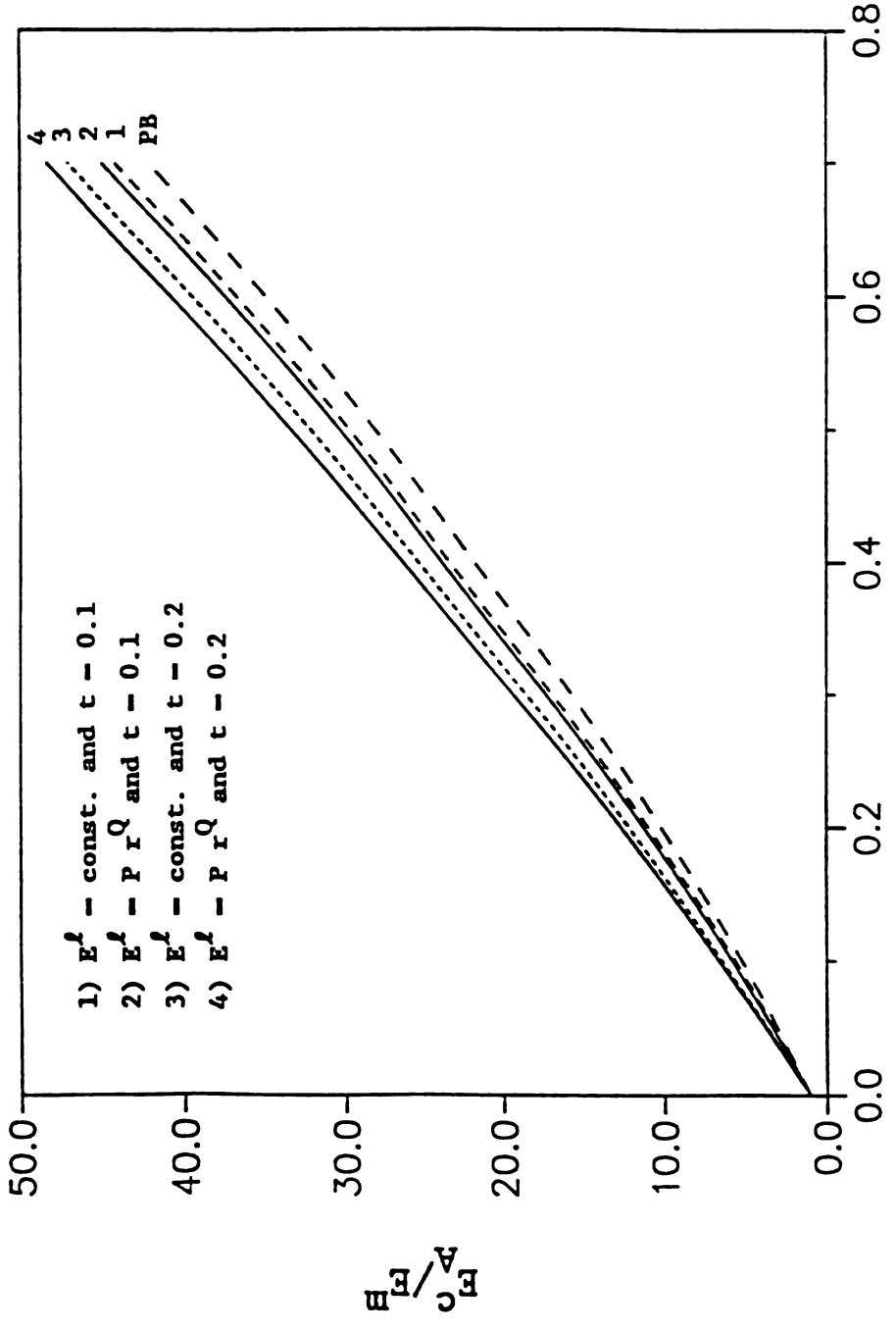

Fig. 4.5 E_A^C/E^m vs. f for graphite-epoxy composite for $\nu^\ell=(\nu^m+\nu_T^f)/2$ and changing $E^\ell(r)$ and t=(b-a)/a.

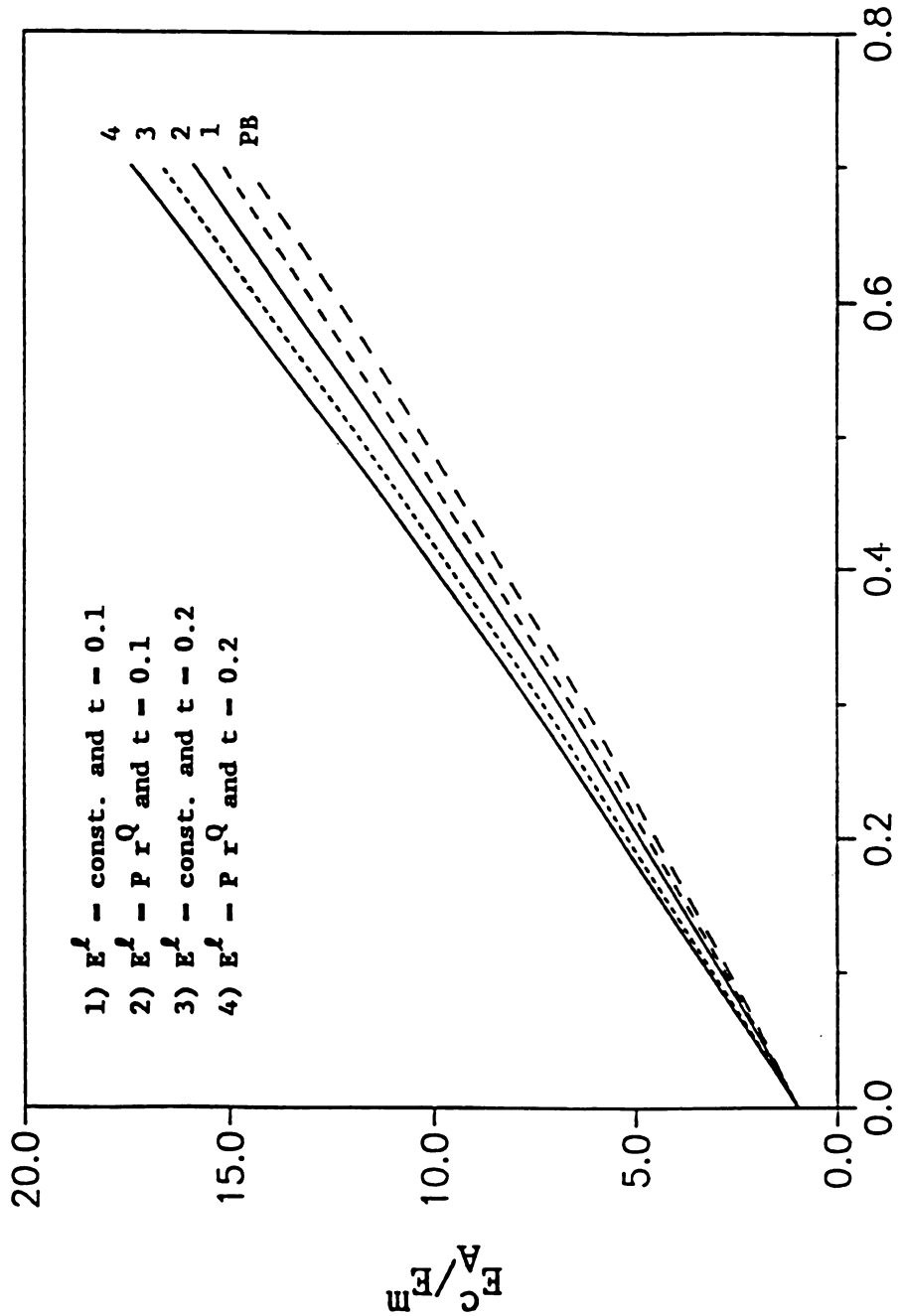

Fig. 4.6 E_A^c/E^m vs. f for glass-plastic composite for $\nu^f=(\nu^m+\nu_T^f)/2$ and changing $E^f(r)$ and t.

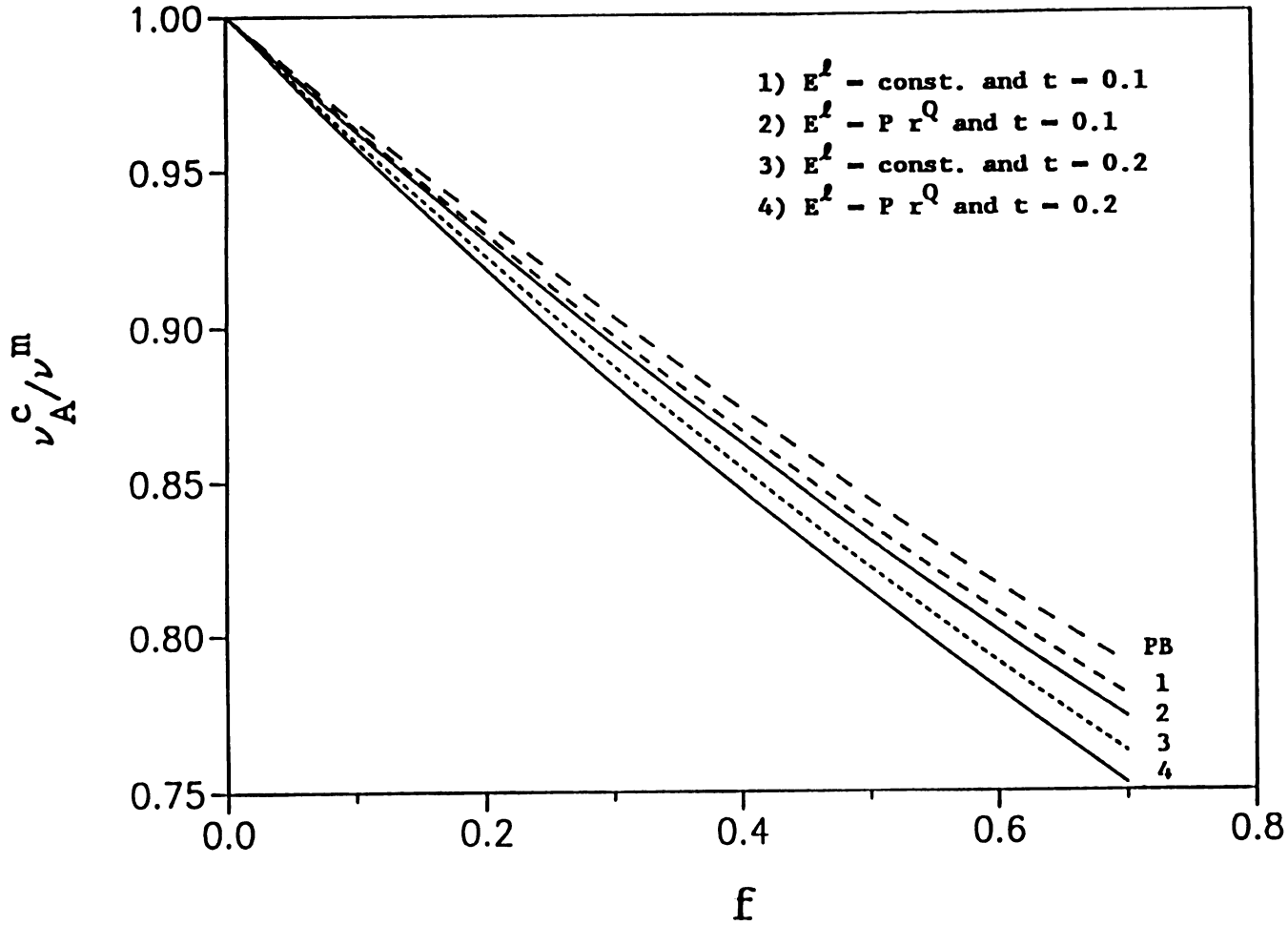

Fig. 4.7 ν_A^c/ν^m vs. f for graphite-epoxy composite for $\nu^\ell=(\nu^m+\nu_T^f)/2$ and changing $E^\ell(r)$ and t.

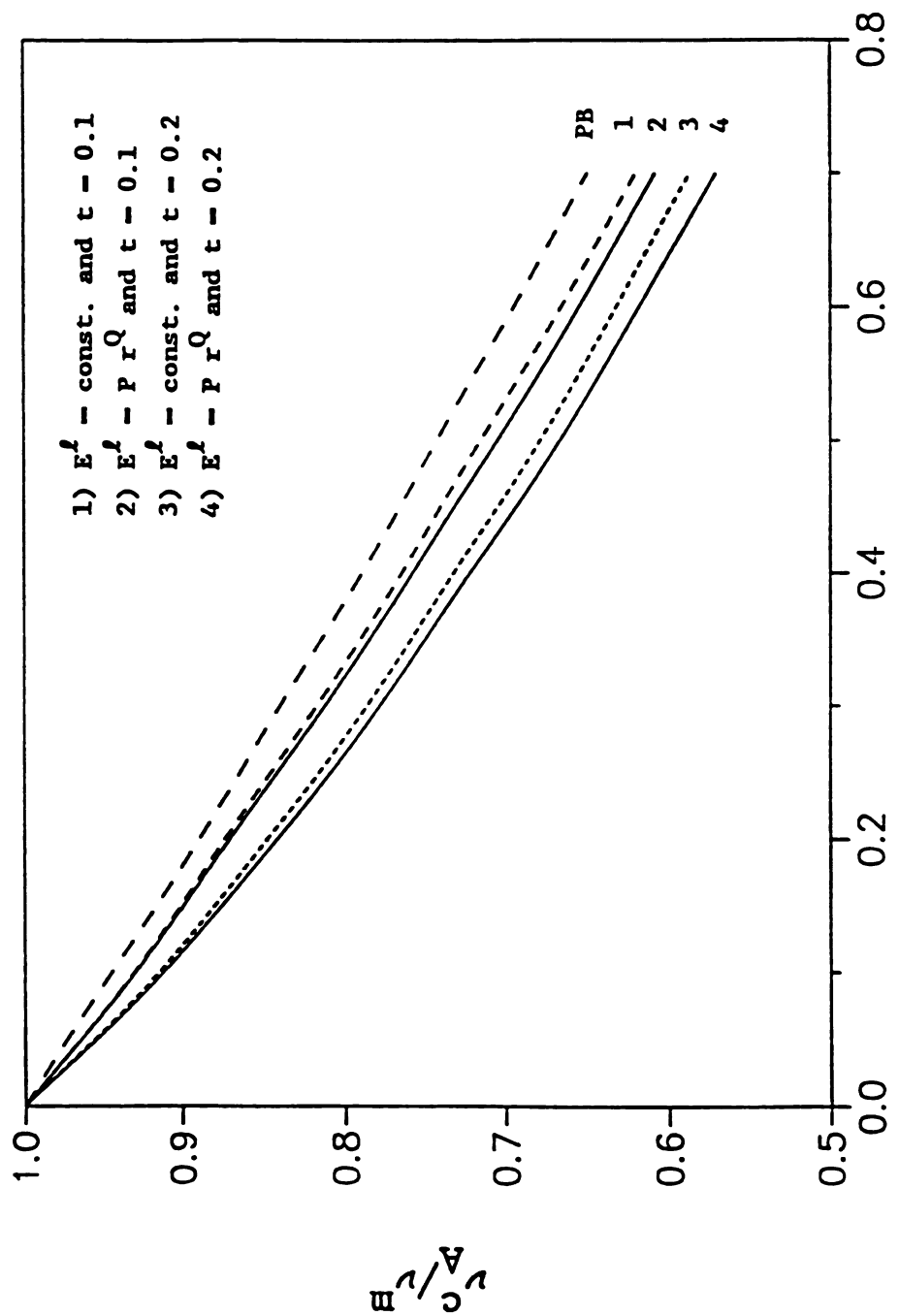

Fig. 4.8 ν_A^c/ν^m vs. f for glass-plastic composite for $\nu^{\ell}=(\nu^m+\nu_T^f)/2$ and changing $E^{\ell}(r)$ and t.

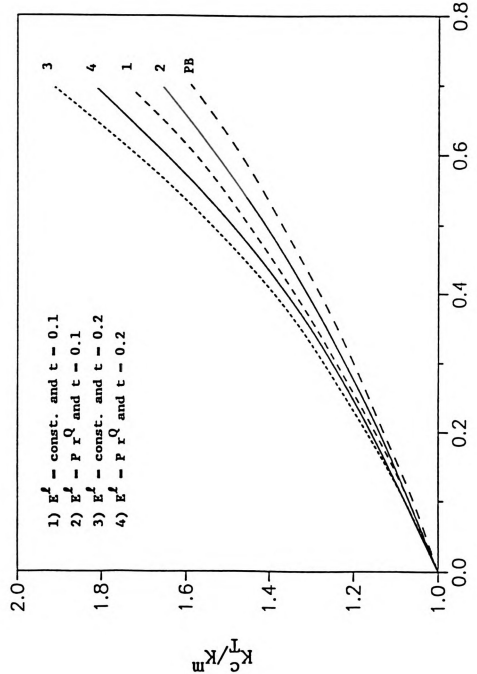

Fig. 4.9 K_T^c/K^m vs. f for graphite-epoxy composite for $\nu^f=(\nu^m+\nu_T^f)/2$ and changing $E^f(r)$ and t.

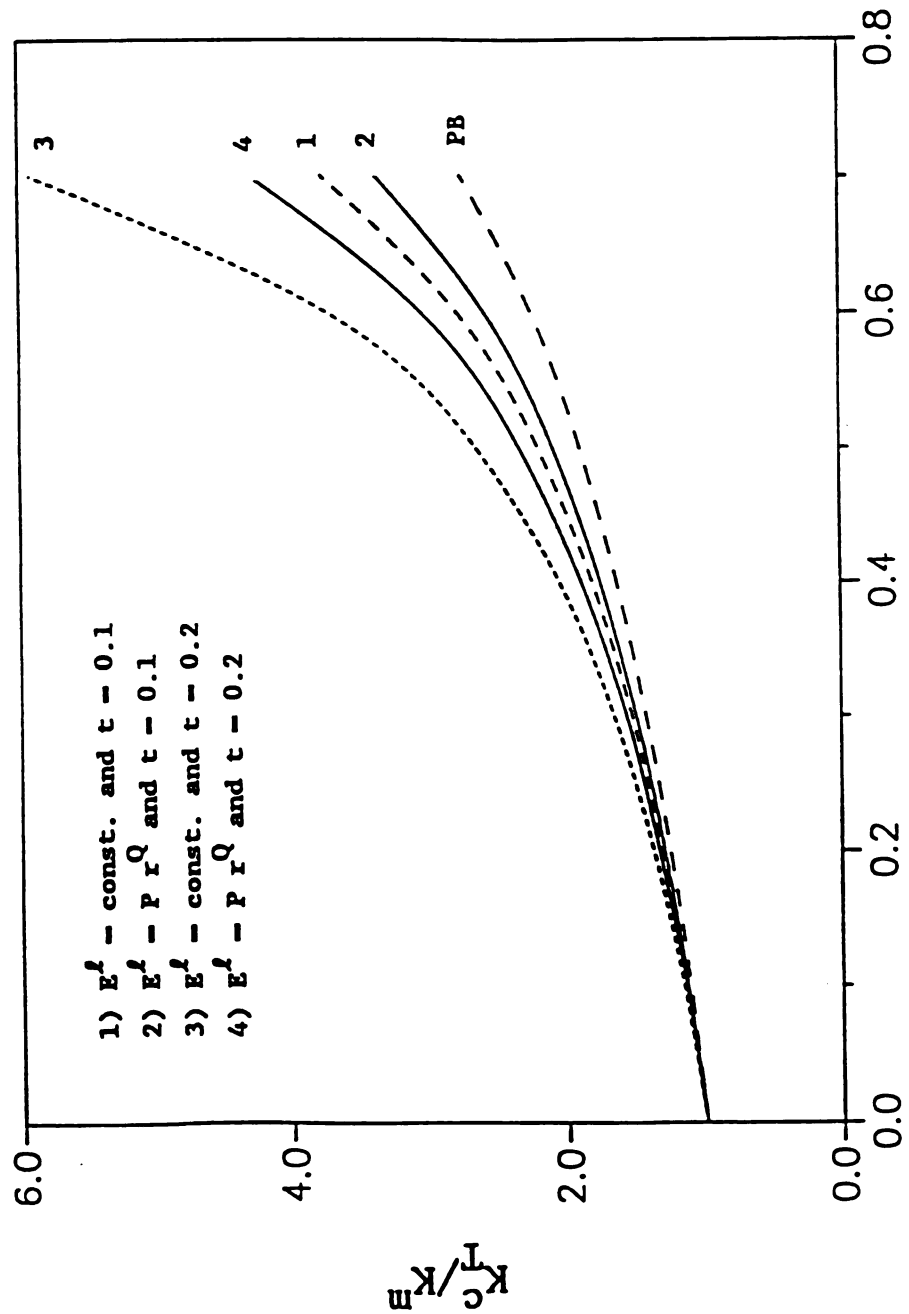

Fig. 4.10 K_T^C/K^m vs. f for glass-plastic composite for $\nu^{\ell}=(\nu^m+\nu_T^f)/2$ and changing $E^{\ell}(r)$ and t.

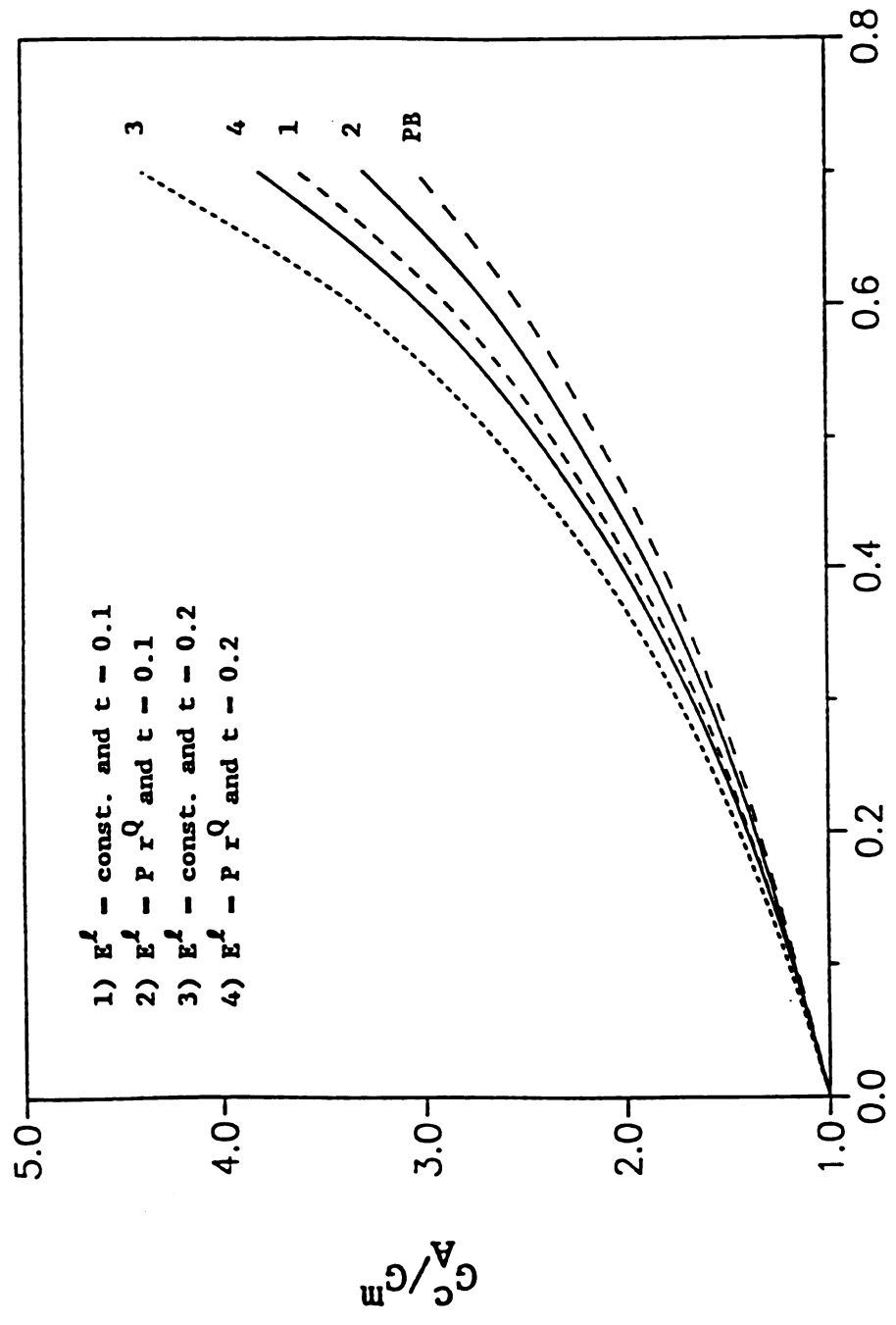

Fig. 4.11 G^c_A/G^m vs. f for graphite-epoxy composite for $\nu^f=(\nu^m+\nu^f_T)/2$ and changing $E^f(r)$ and t.

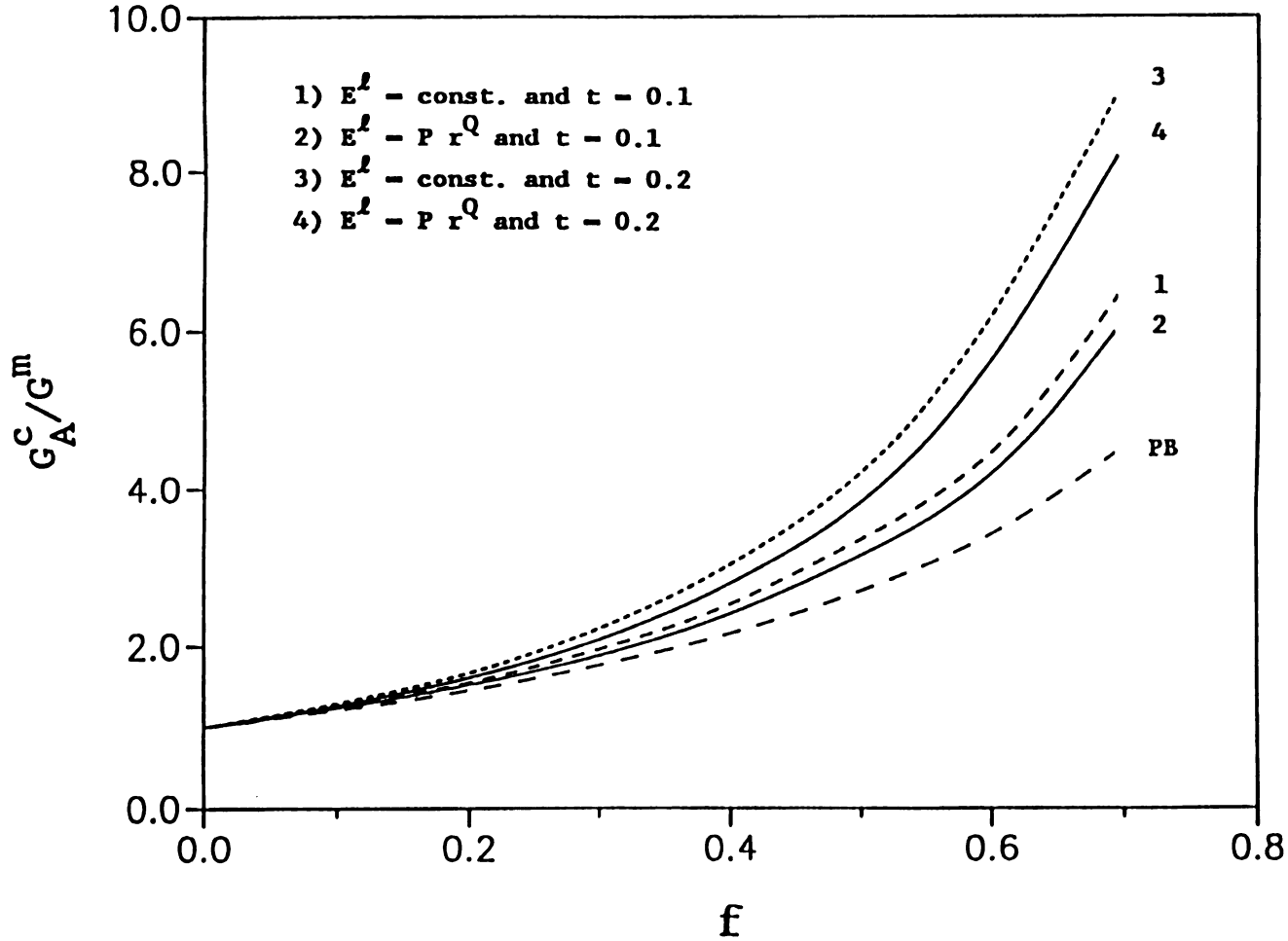

Fig. 4.12 G_A^c/G^m vs. f for glass-plastic composite for $\nu^{\ell}=(\nu^m+\nu_T^f)/2$ and changing $E^{\ell}(r)$ and t.

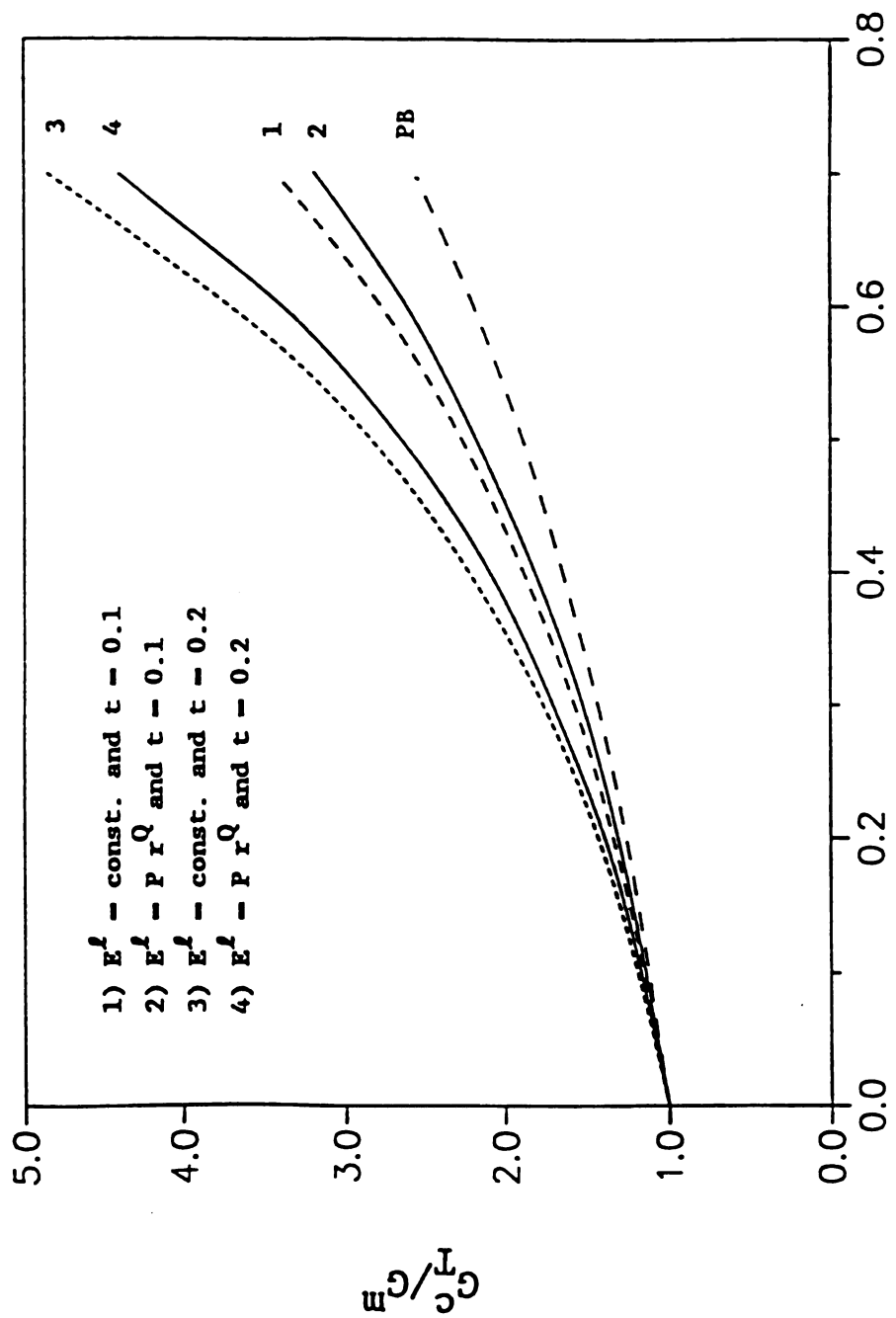

Fig. 4.13 G_T^c/G^m vs. f for graphite-epoxy composite for $\nu^f=(\nu^m+\nu_T^f)/2$ and changing $E^f(r)$ and t.

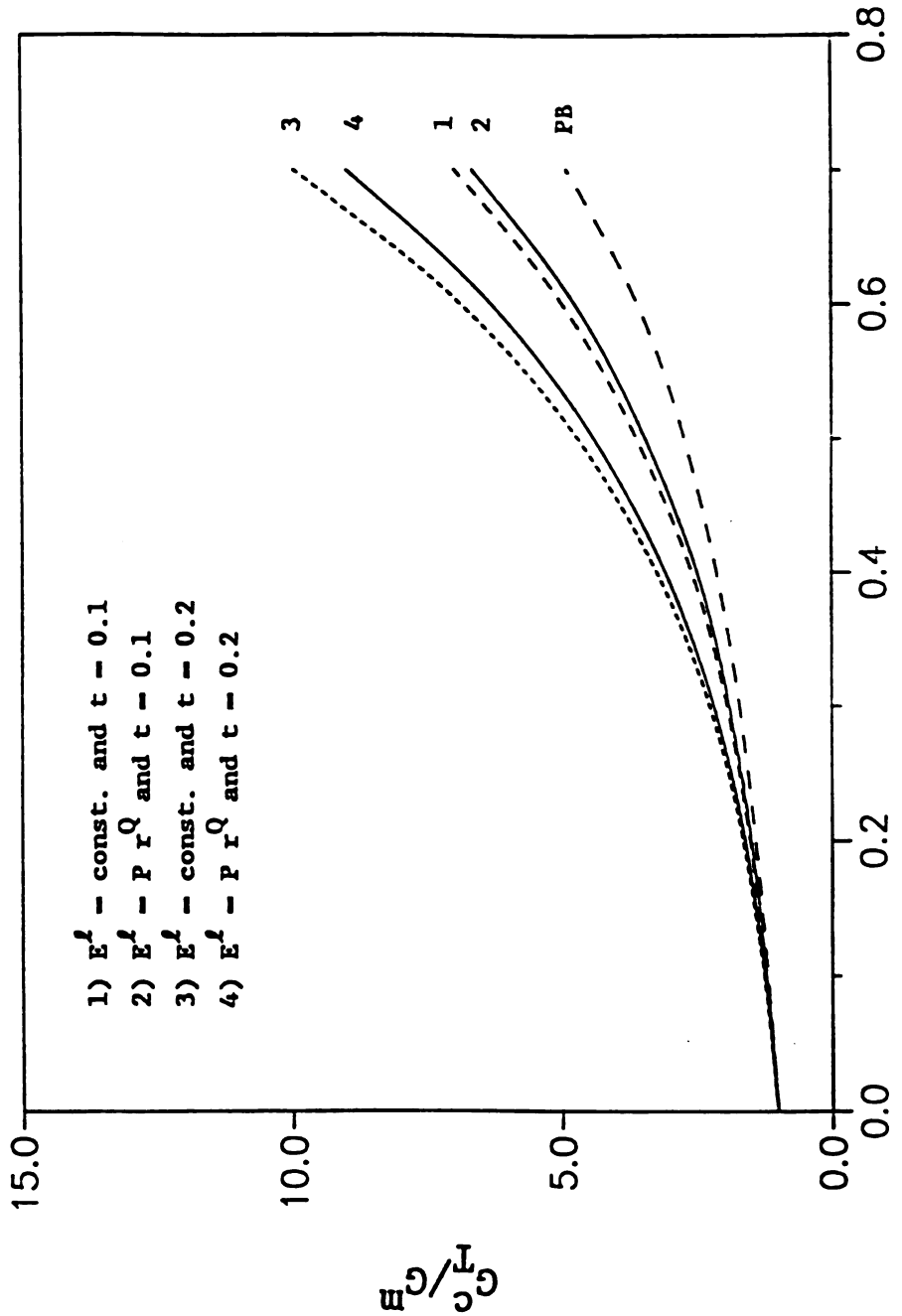

Fig. 4.14 G_T^C/G^m vs. f for glass-plastic composite for $\nu^{\ell}=(\nu^m+\nu_T^f)/2$ and changing $E^{\ell}(r)$ and t.

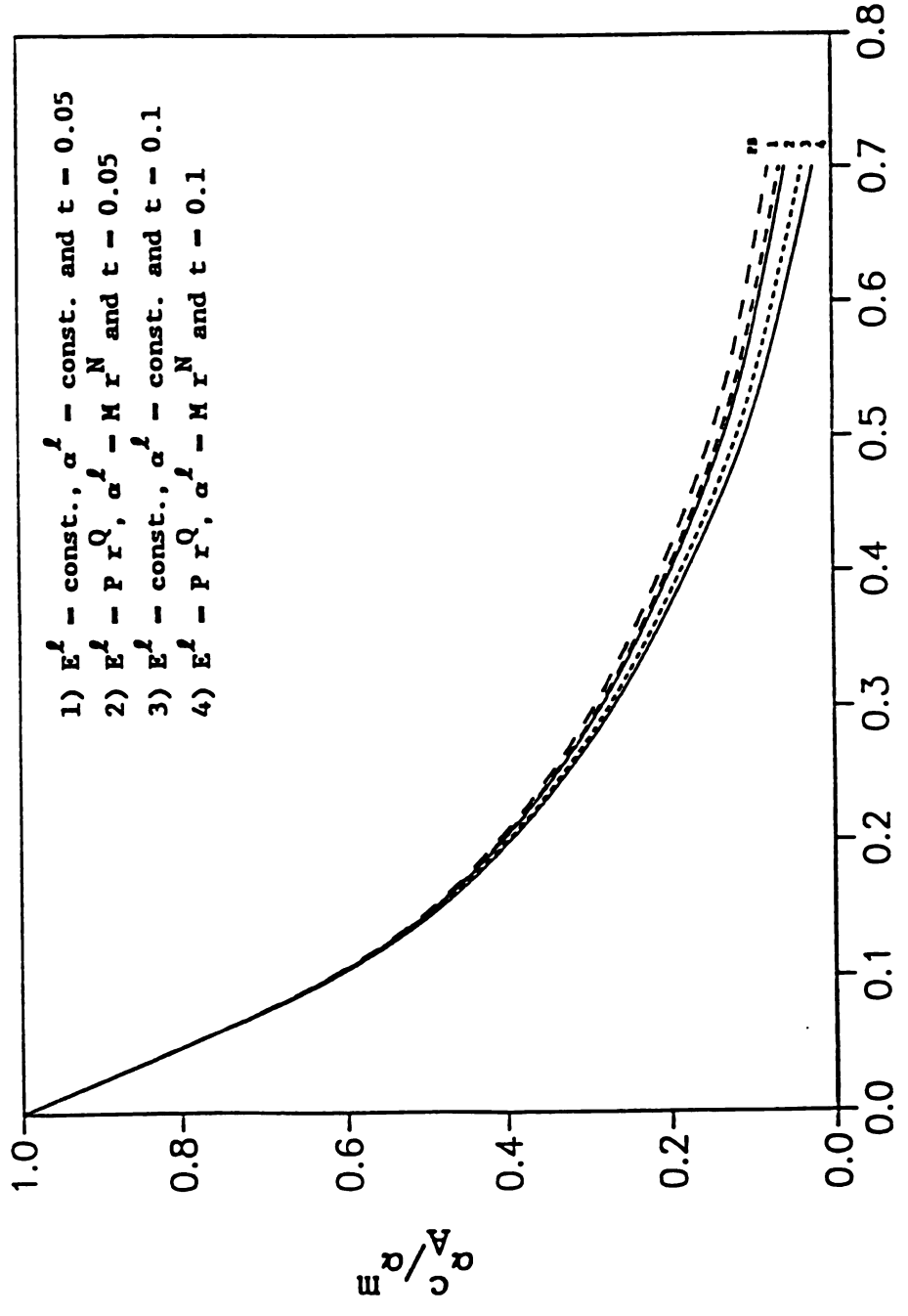

Fig. 4.15 α_A^c/α^m vs. f for graphite-epoxy composite for $\nu^f-(\nu^m+\nu_T^f)/2$, and changing $\alpha^f(r)$, $E^f(r)$ and t.

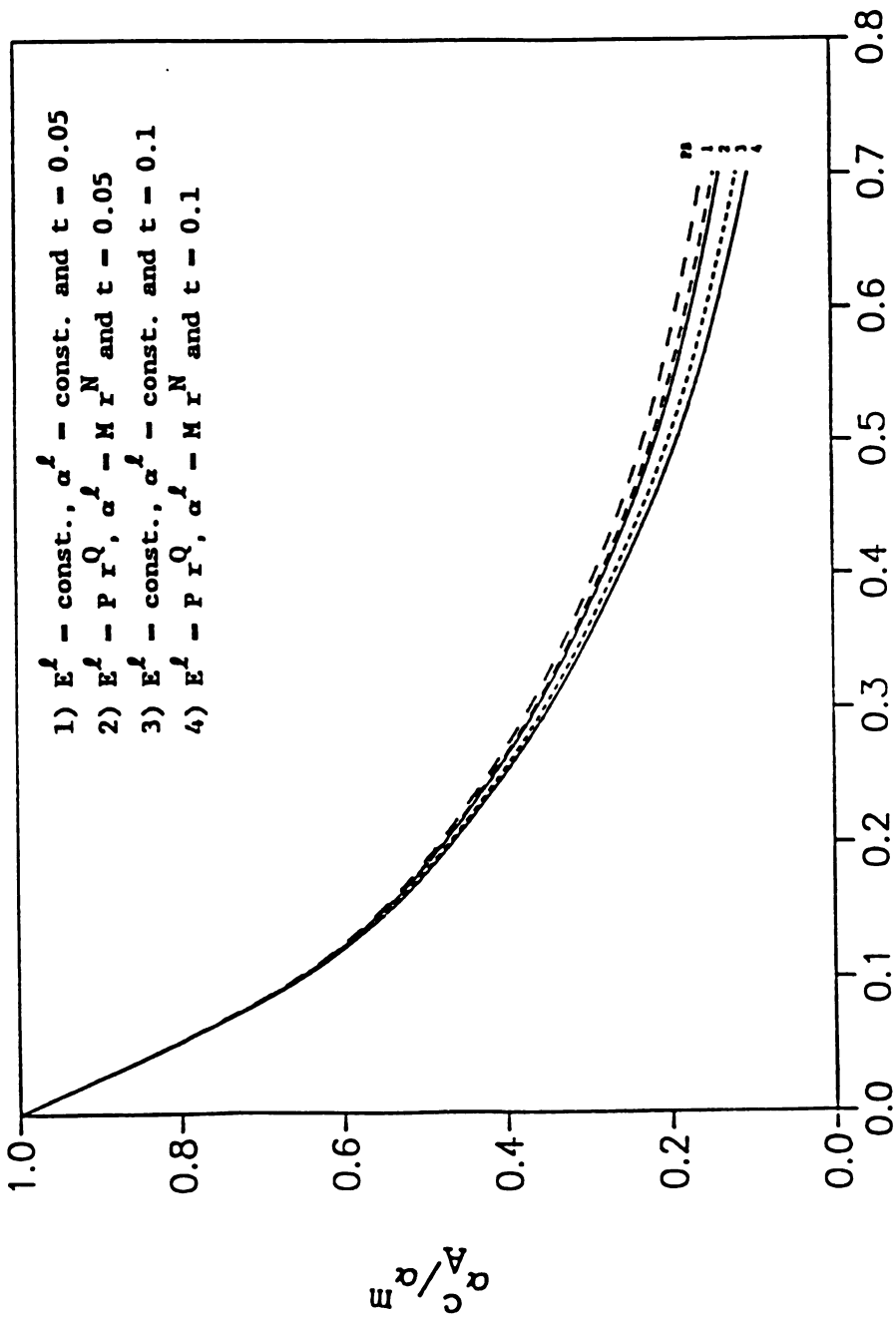

Fig. 4.16 α_A^c/α^m vs. f for glass-plastic composite for $\nu^{\ell}=(\nu^m+\nu_T^f)/2$, and changing $\alpha^{\ell}(r)$, $E^{\ell}(r)$ and t.

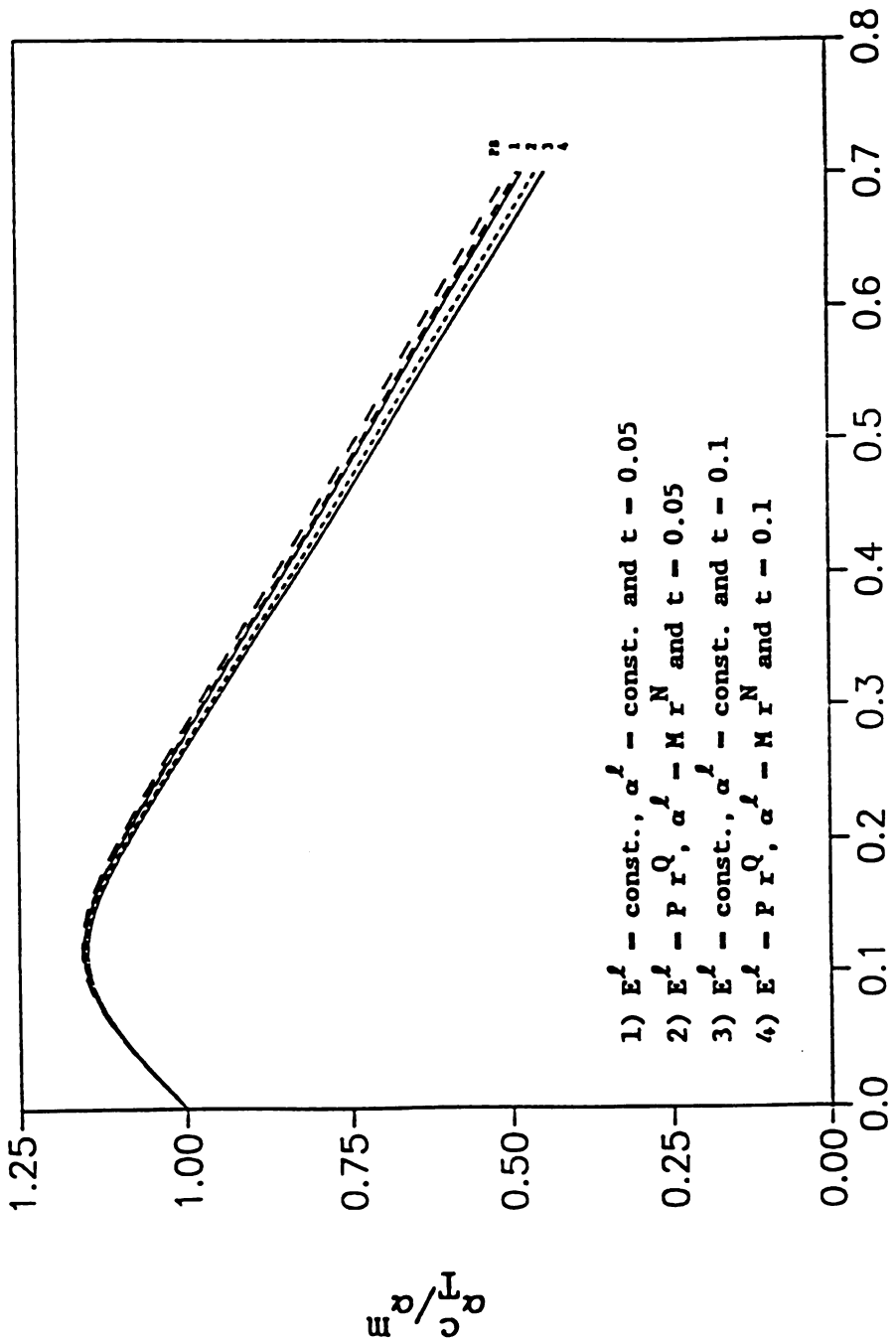

Fig. 4.17 α_T^c/α^m vs. f for graphite-epoxy composite for $\nu^{\ell}=(\nu^m+\nu_T^f)/2$, and changing $\alpha^{\ell}(r)$, $E^{\ell}(r)$ and t.

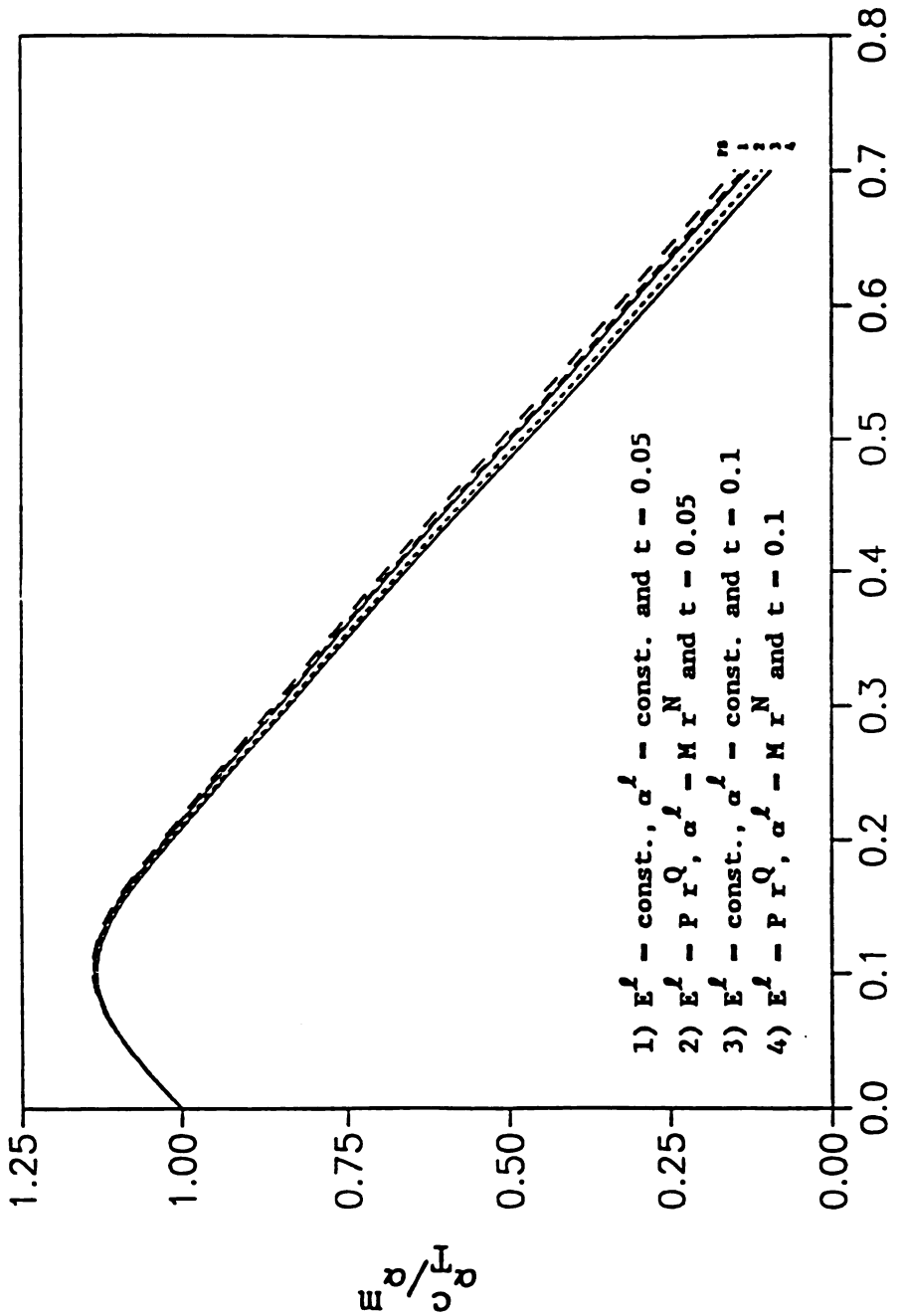

Fig. 4.18 α_T^c/α^m vs. f for glass-plastic composite for $\nu^f=(\nu^m+\nu_T^f)/2$, and changing $\alpha^f(r)$, $E^f(r)$ and t.

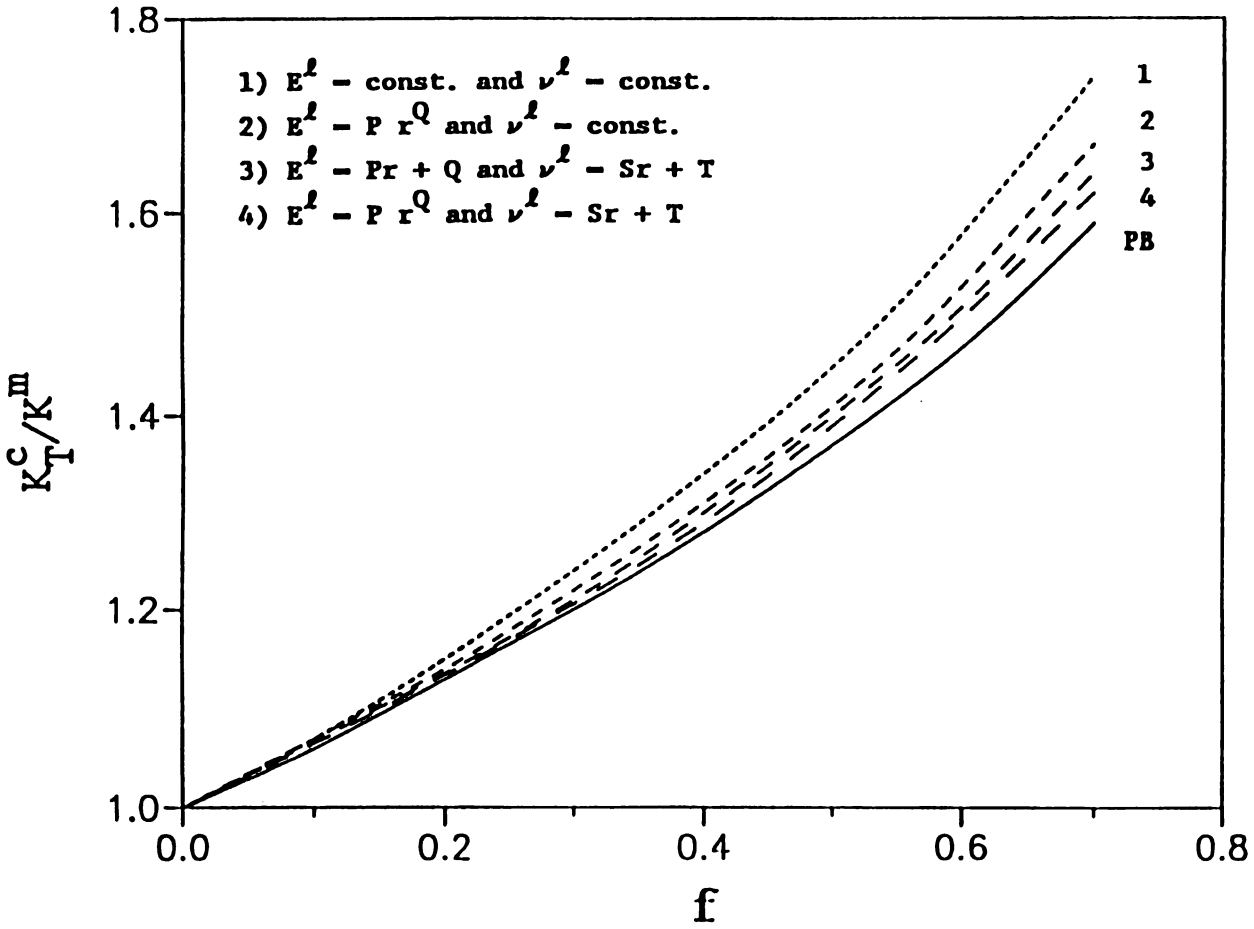

Fig. 4.19 K_T^c/K^m vs. f for graphite-epoxy composite for changing $E^{\ell}(r)$ and $\nu^{\ell}(r)$ when t = 0.1.

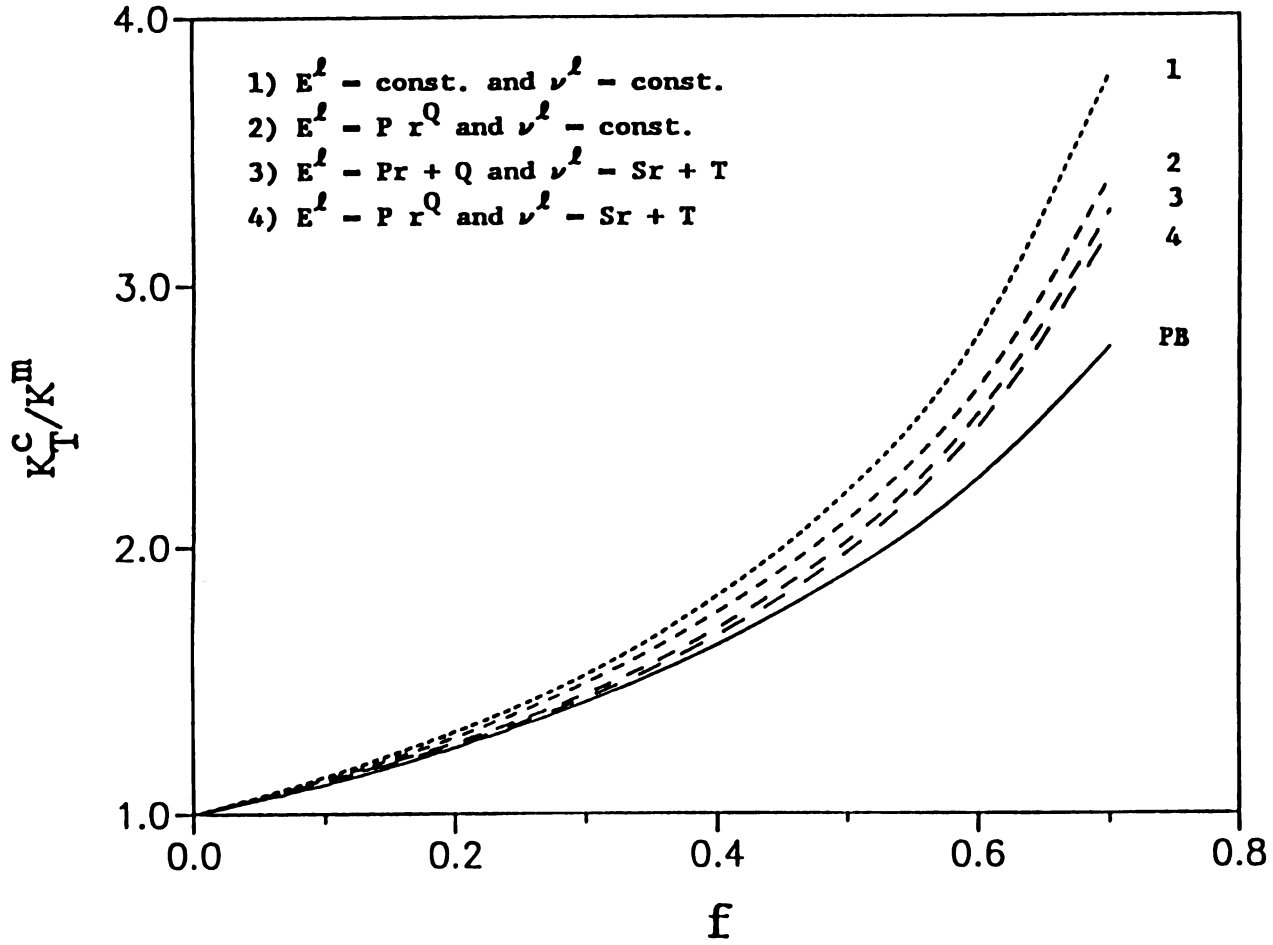

Fig. 4.20 K_T^c/K^m vs. f for glass-plastic composite for changing $E^\ell(r)$ and $\nu^\ell(r)$ when t = 0.1.

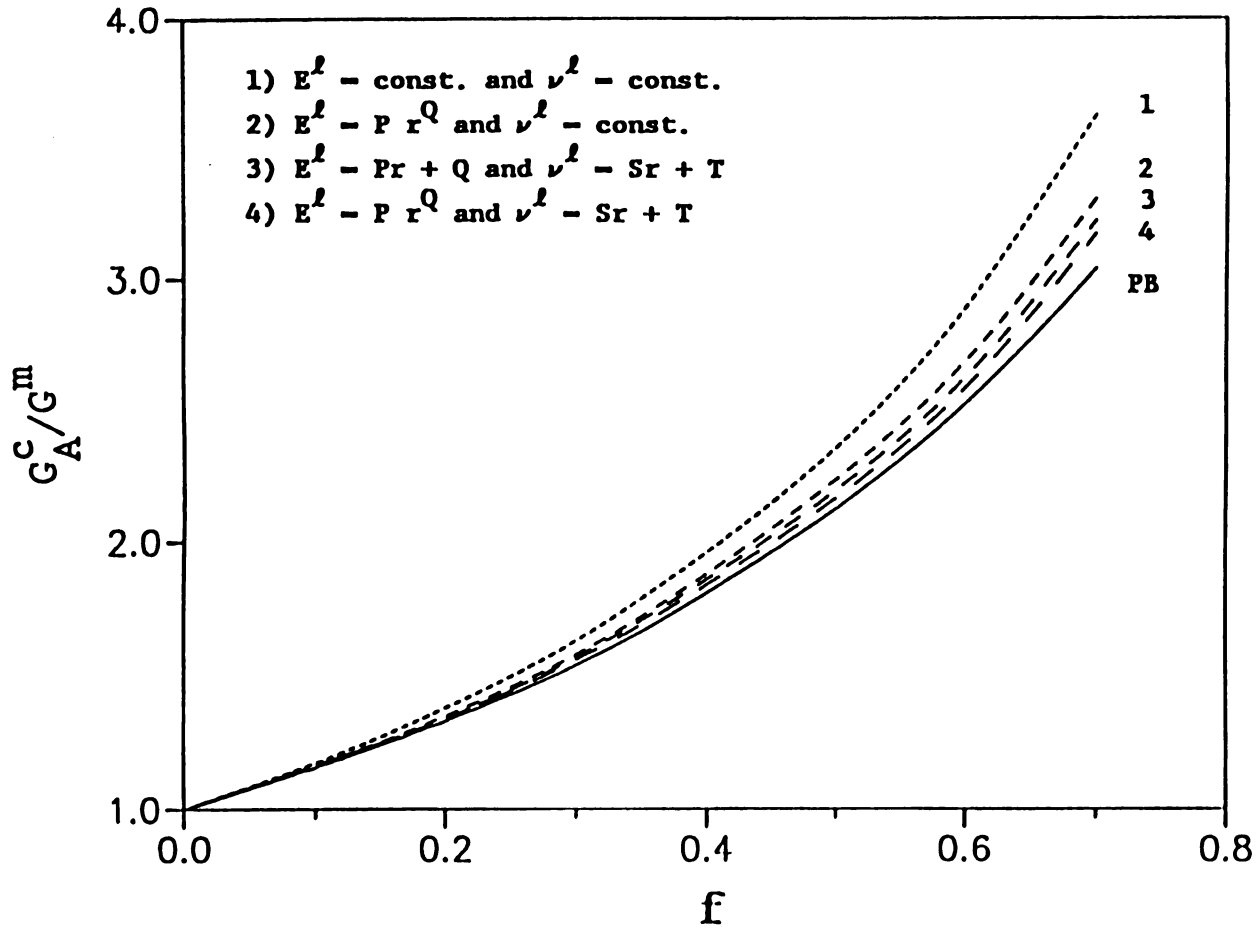

Fig. 4.21 G_A^c/G^m vs. f for graphite-epoxy composite for changing $E^{\ell}(r)$ and $\nu^{\ell}(r)$ when t = 0.1.

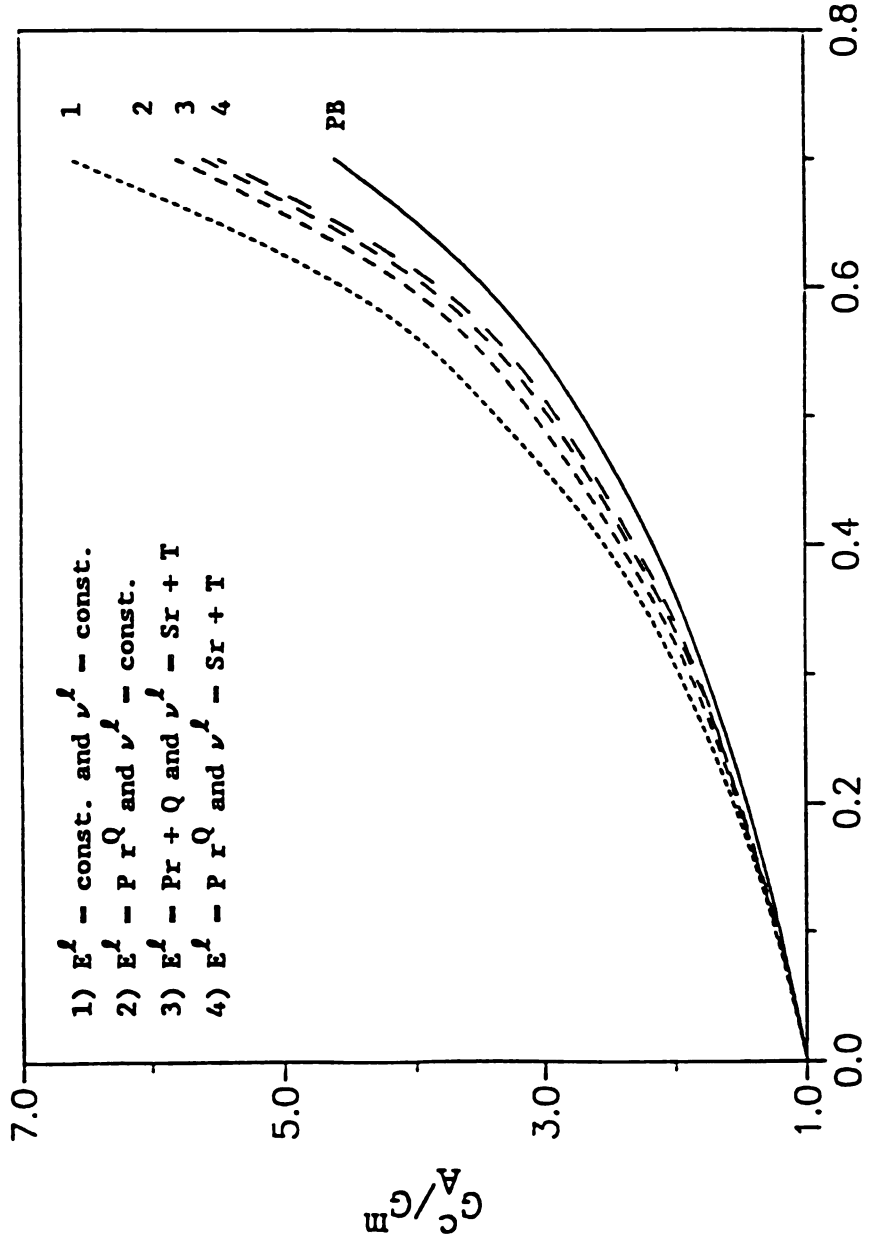

Fig. 4.22 G_A^C/G^M vs. f for glass-plastic composite for changing $E^{\ell}(r)$ and $\nu^{\ell}(r)$ when t = 0.1.

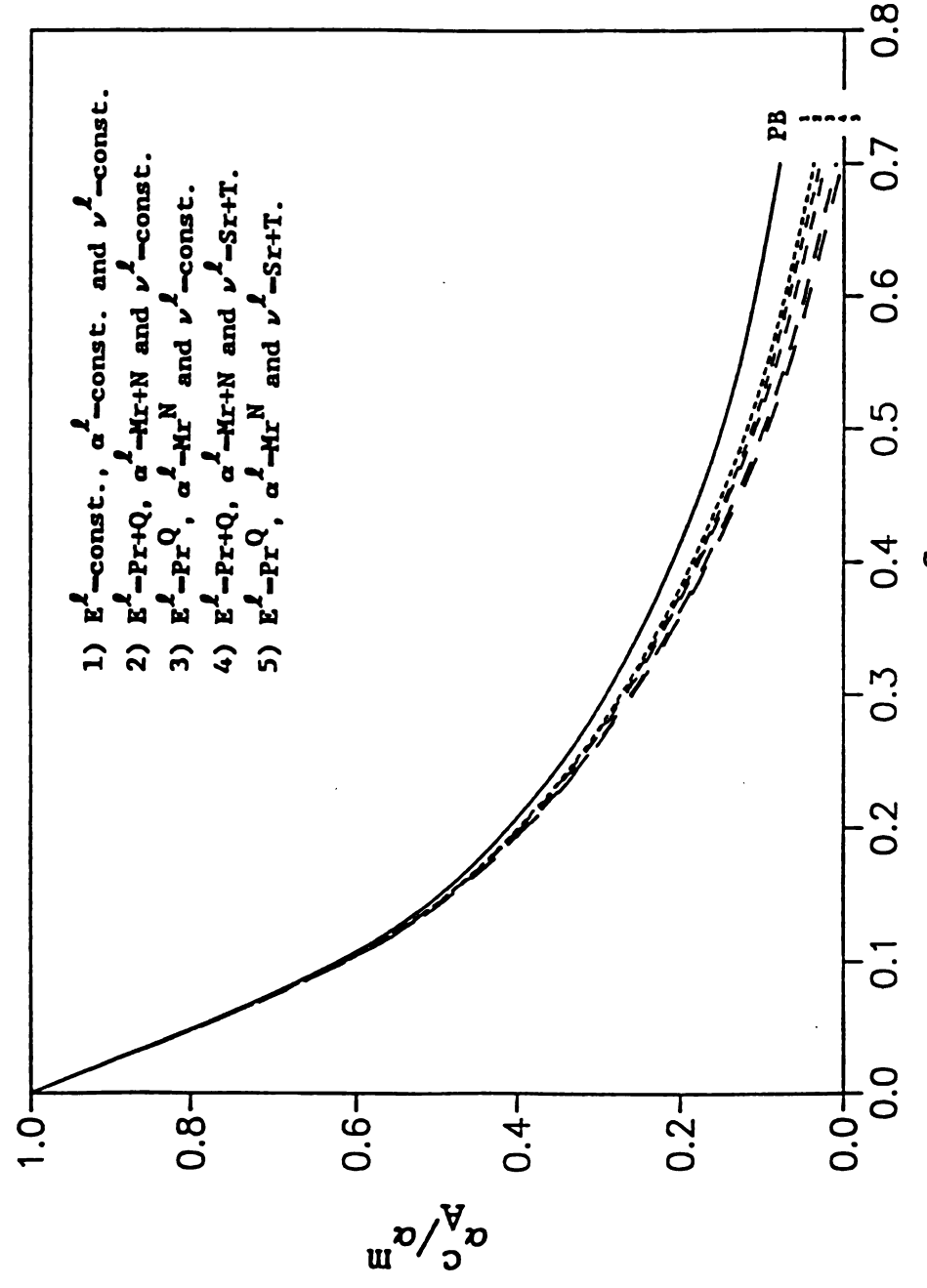

Fig. 4.23 α_A^c/α^m vs. f for graphite-epoxy composite for changing $E^f(r)$, $\alpha^f(r)$ and $\nu^f(r)$ when t = 0.1.

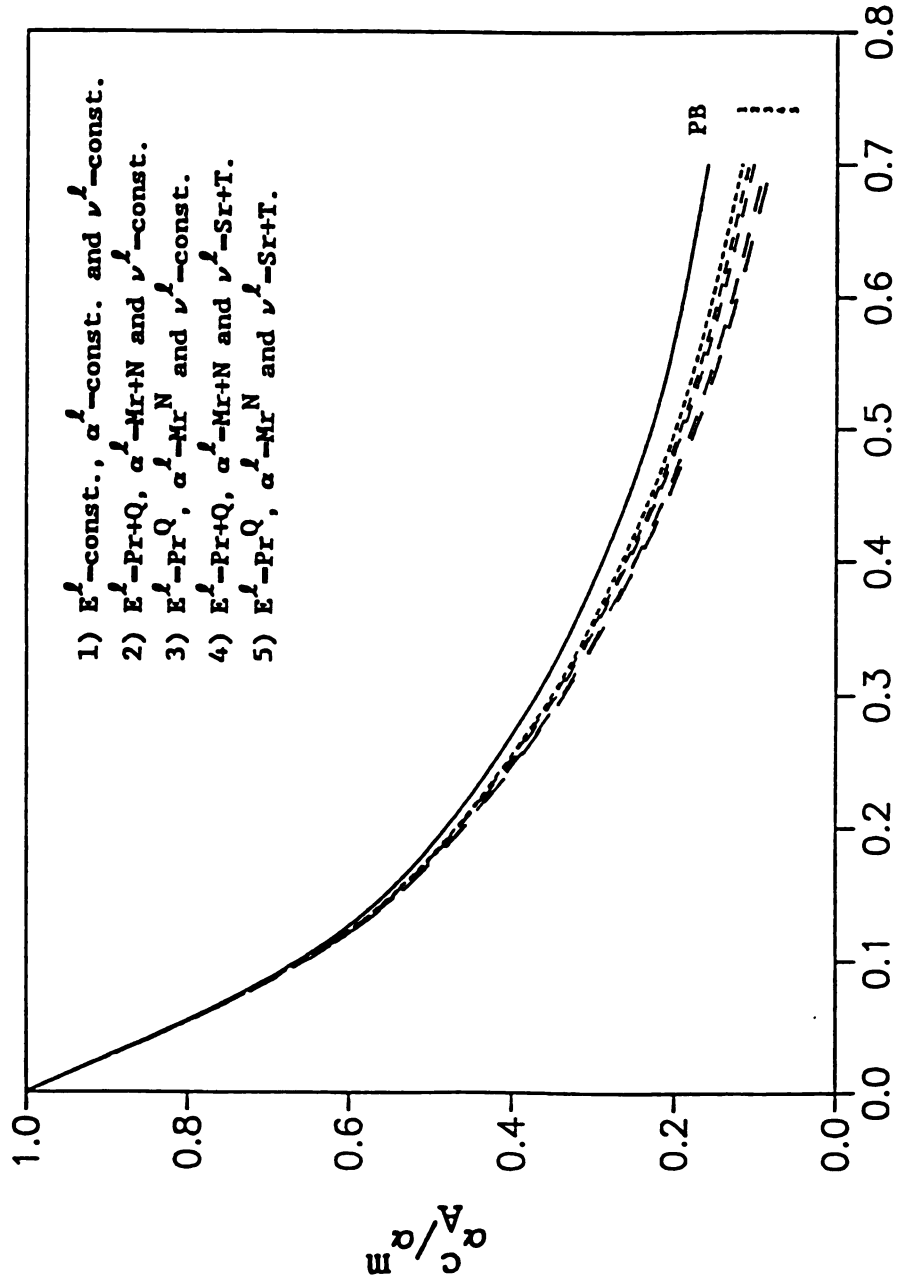

Fig. 4.24 α_A^c/α^m vs. f for glass-plastic composite for changing $E^{\ell}(r)$, $\alpha^{\ell}(r)$ and $\nu^{\ell}(r)$ when t = 0.1.

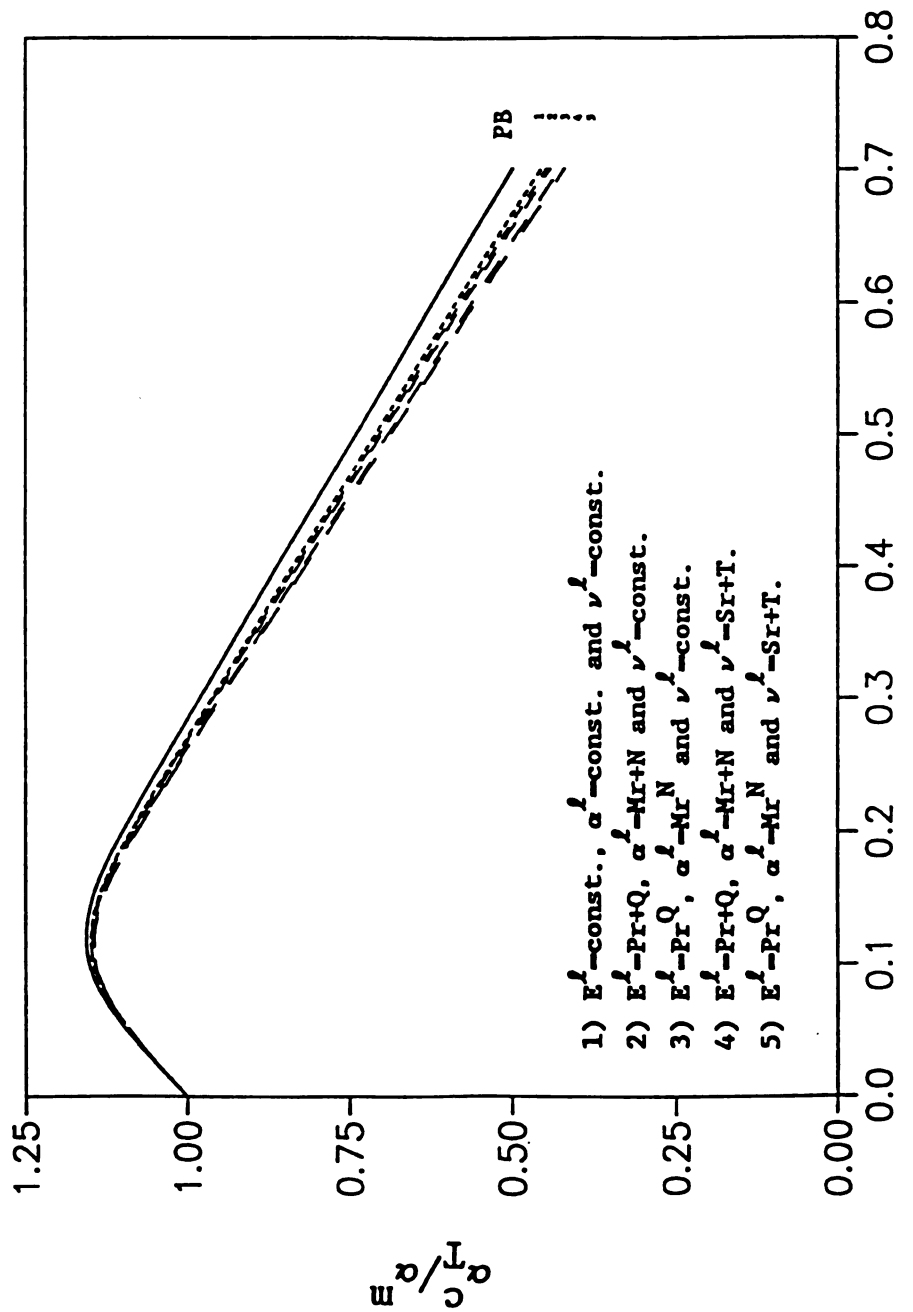

Fig. 4.25 α_T^c/α^m vs. f for graphite-epoxy composite for changing $E^f(r)$, $\alpha^f(r)$ and $\nu^f(r)$ when t = 0.1.

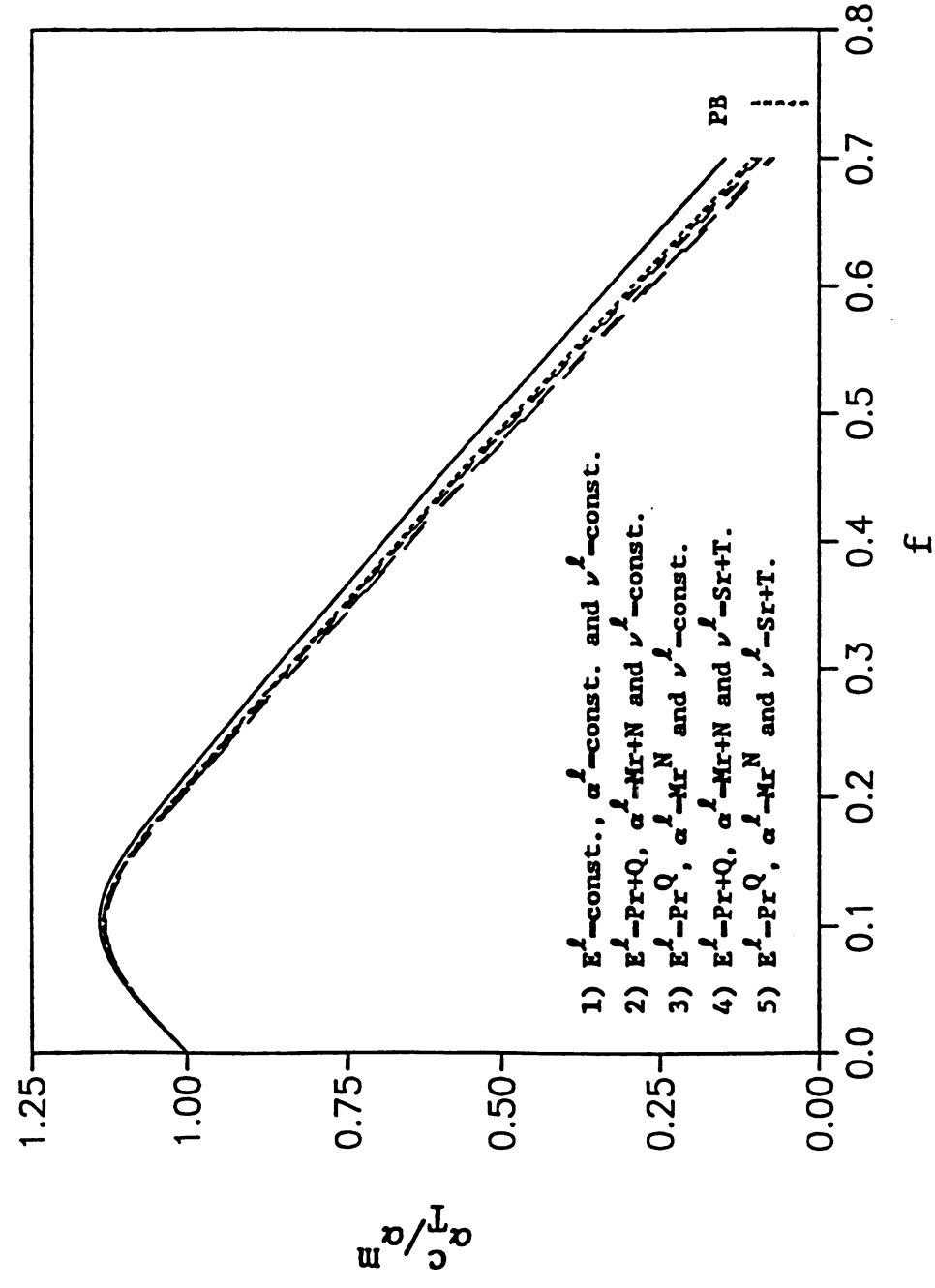

Fig. 4.26 α_T^c/α^m vs. f for glass-plastic composite for changing $E^f(r)$, $\alpha^f(r)$ and $\nu^f(r)$ when t = 0.1.

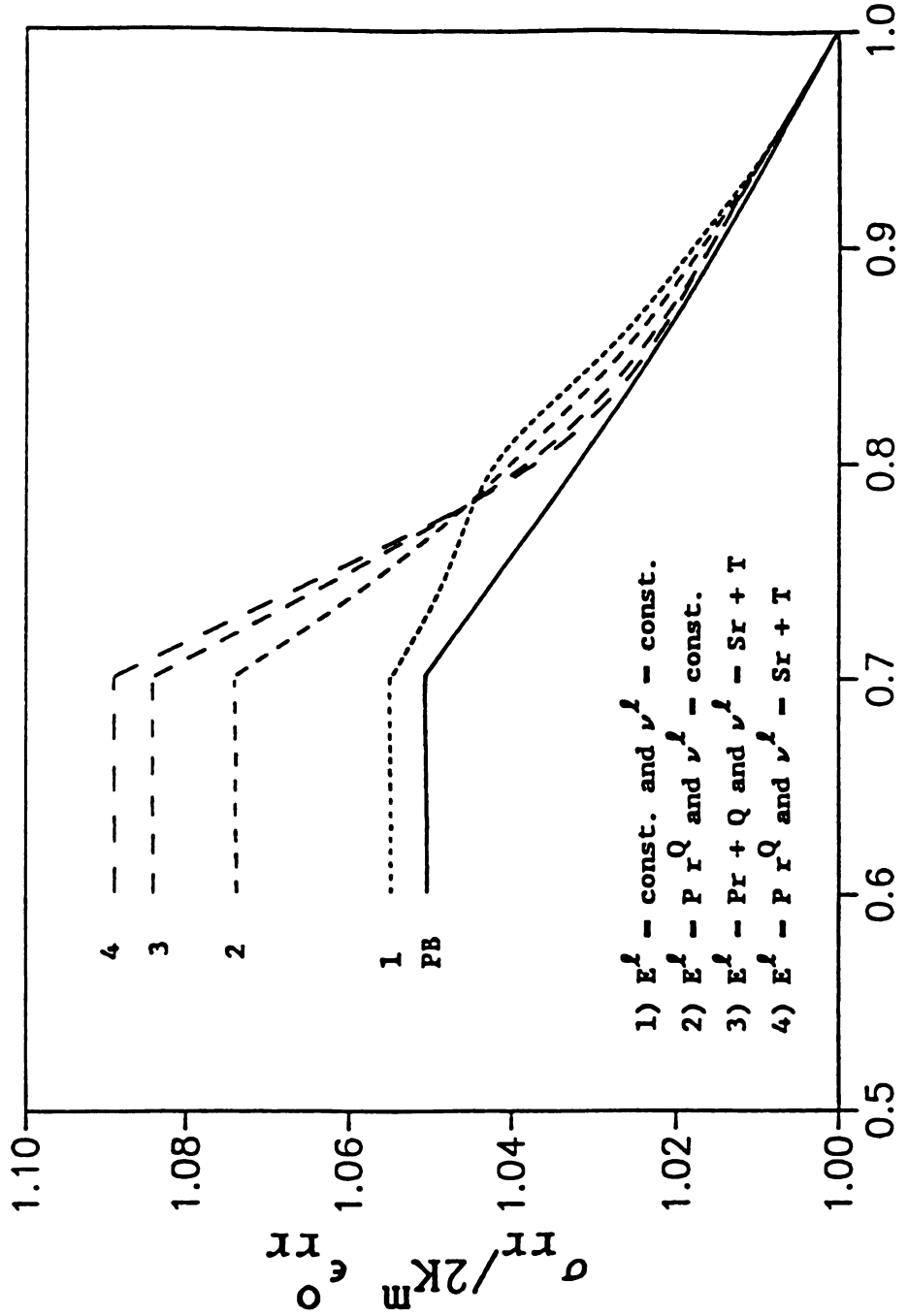

Fig. 4.27 Distribution of $\sigma_{rr}/2K^m\ \epsilon^o_{rr}$ along r for graphite-epoxy composite for changing $E^l(r)$ and $\nu^l(r)$.

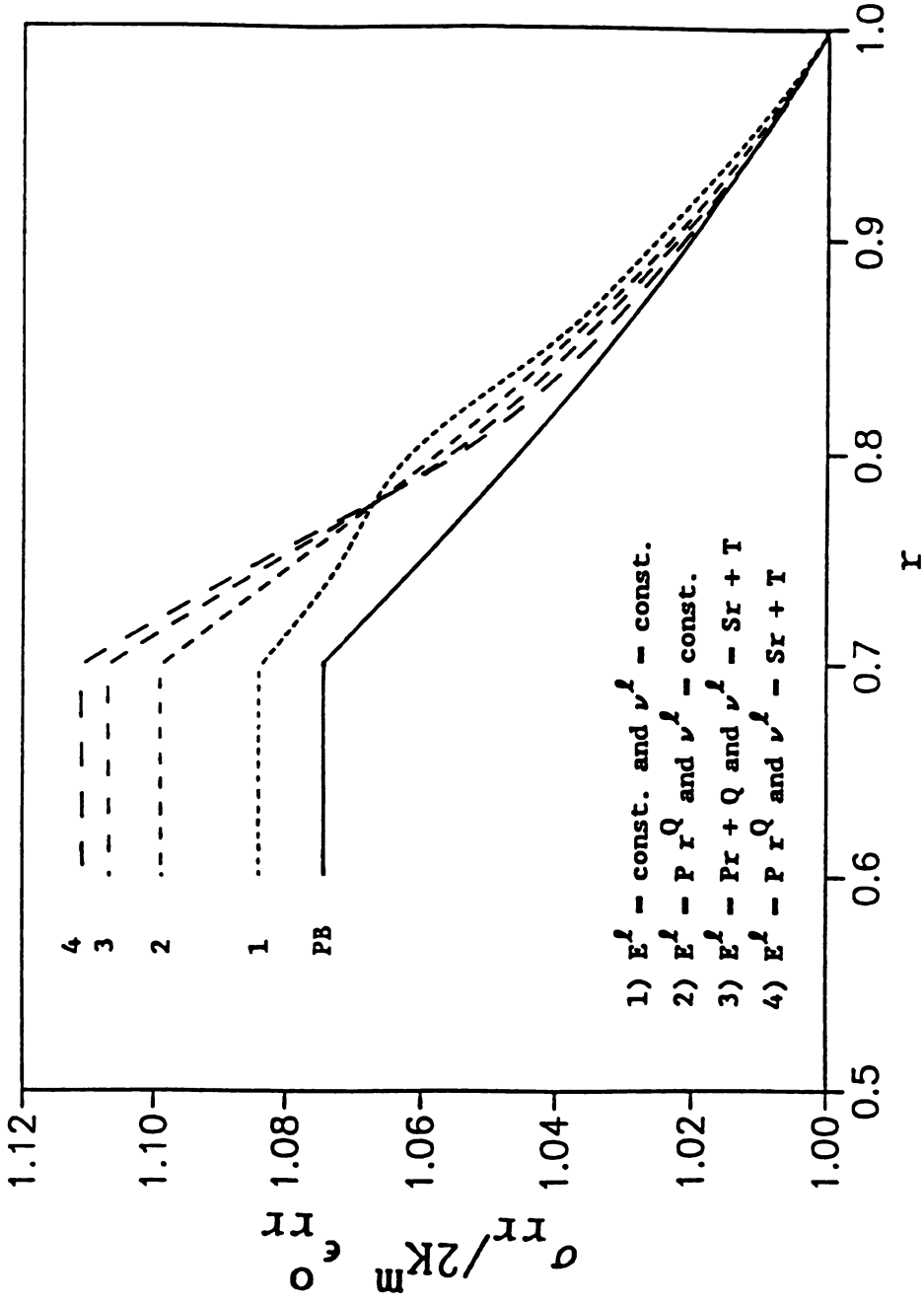

Fig. 4.28 Distribution of $\sigma_{rr}/2K^m\,\epsilon^o_{rr}$ along r for glass-plastic composite for changing $E^\ell(r)$ and $\nu^\ell(r)$.

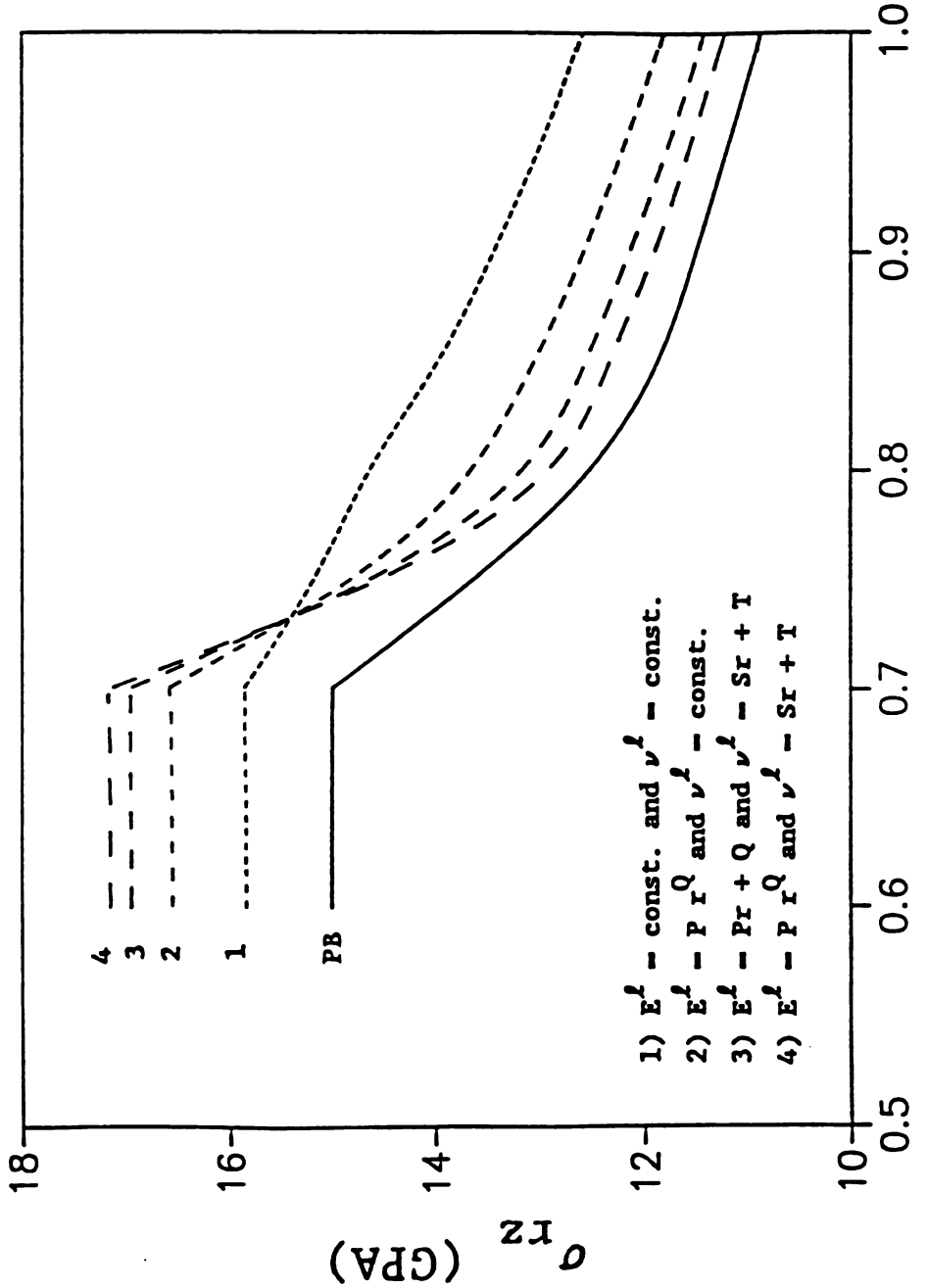

Fig. 4.29 Distribution of σ_{rz} (GPA) along r for graphite-epoxy composite for changing $E^{\ell}(r)$ and $\nu^{\ell}(r)$ when $\epsilon^{o}_{rz} = 1$.

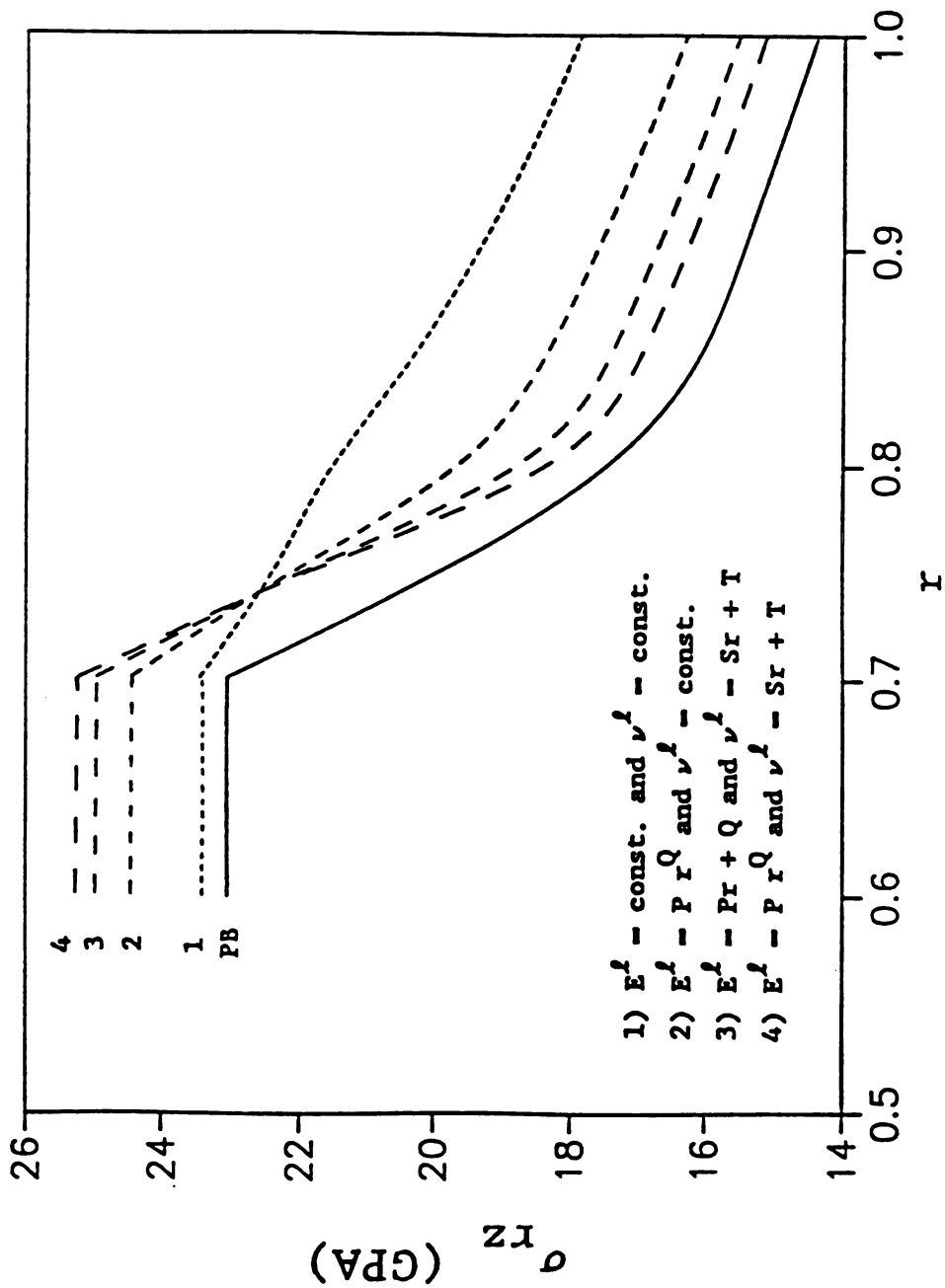

Fig. 4.30 Distribution of σ_{rz} (GPA) along r for glass-plastic composite for changing $E^{\ell}(r)$ and $\nu^{\ell}(r)$ when $\epsilon^{o}_{rz} = 1$.

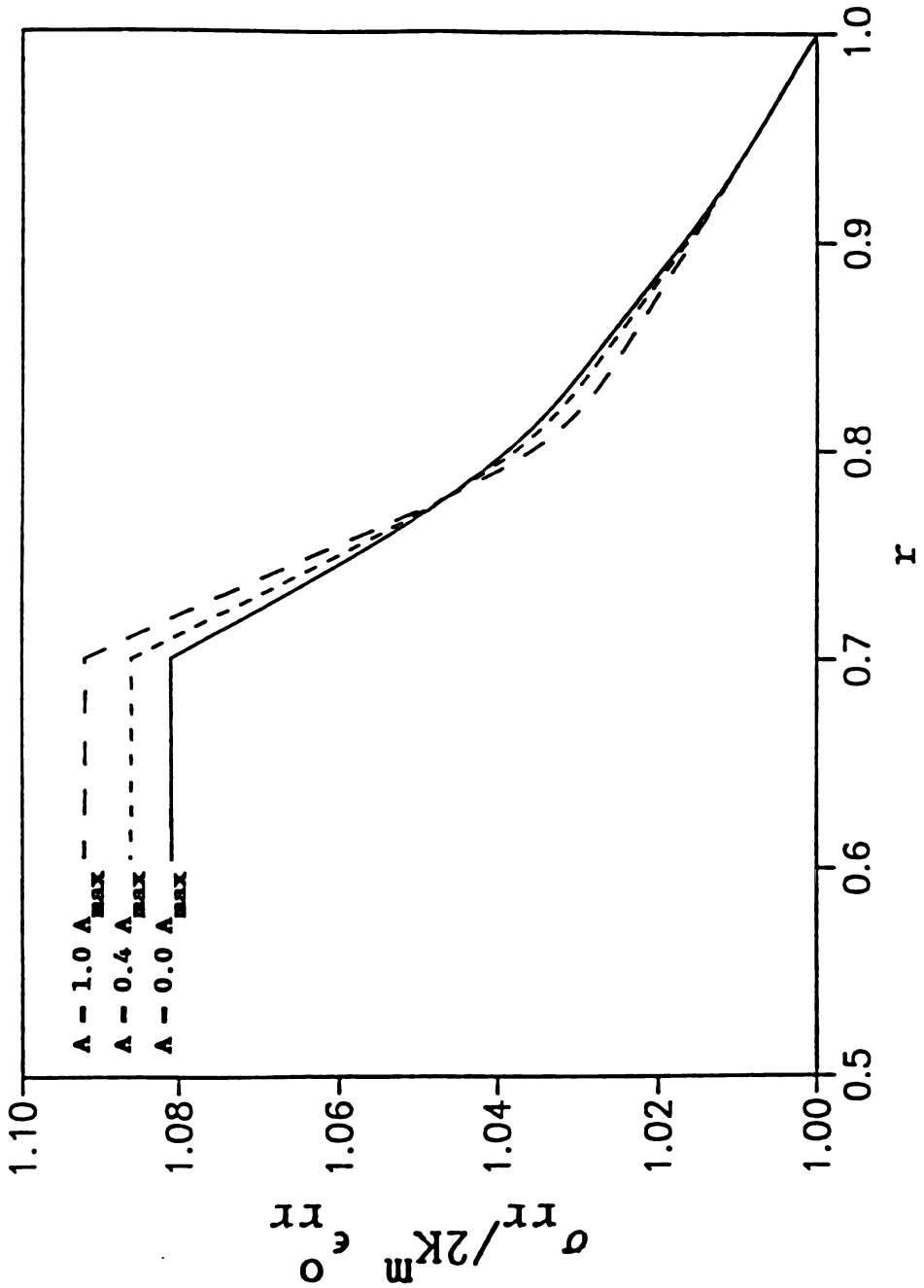

Fig. 4.31 Distribution of $\sigma_{rr}/2K^m\ \epsilon^o_{rr}$ along r for graphite-epoxy composite for $\nu^\ell=(\nu^m+\nu_T^f)/2$ and $E^\ell(r)=Ar^2+Br+C$.

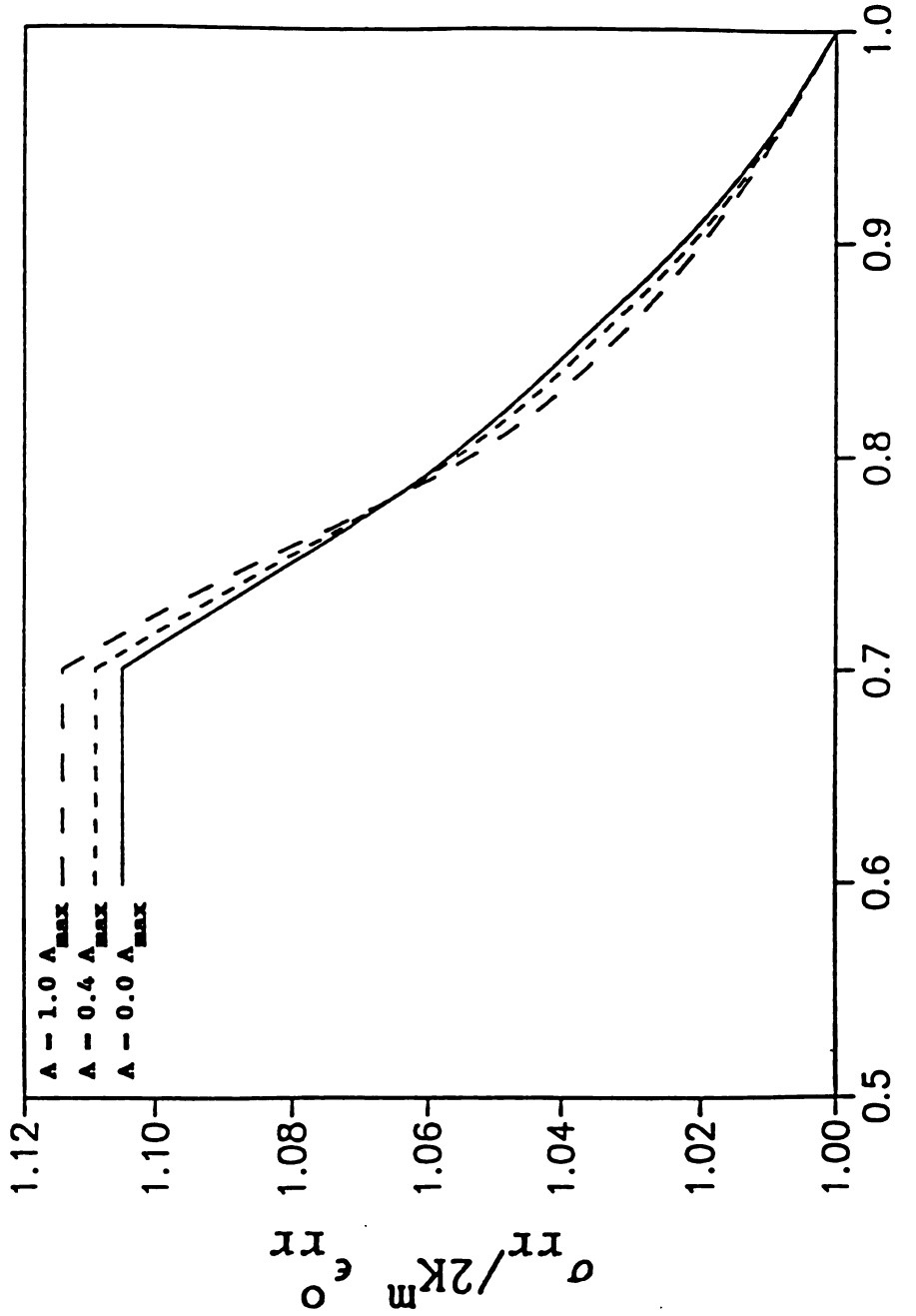

Fig. 4.32 Distribution of $\sigma_{rr}/2K^m\ \epsilon^o_{rr}$ along r for glass-plastic composite for $\nu^\ell=(\nu^m+\nu^f_T)/2$ and $E^\ell(r)=Ar^2+Br+C$.

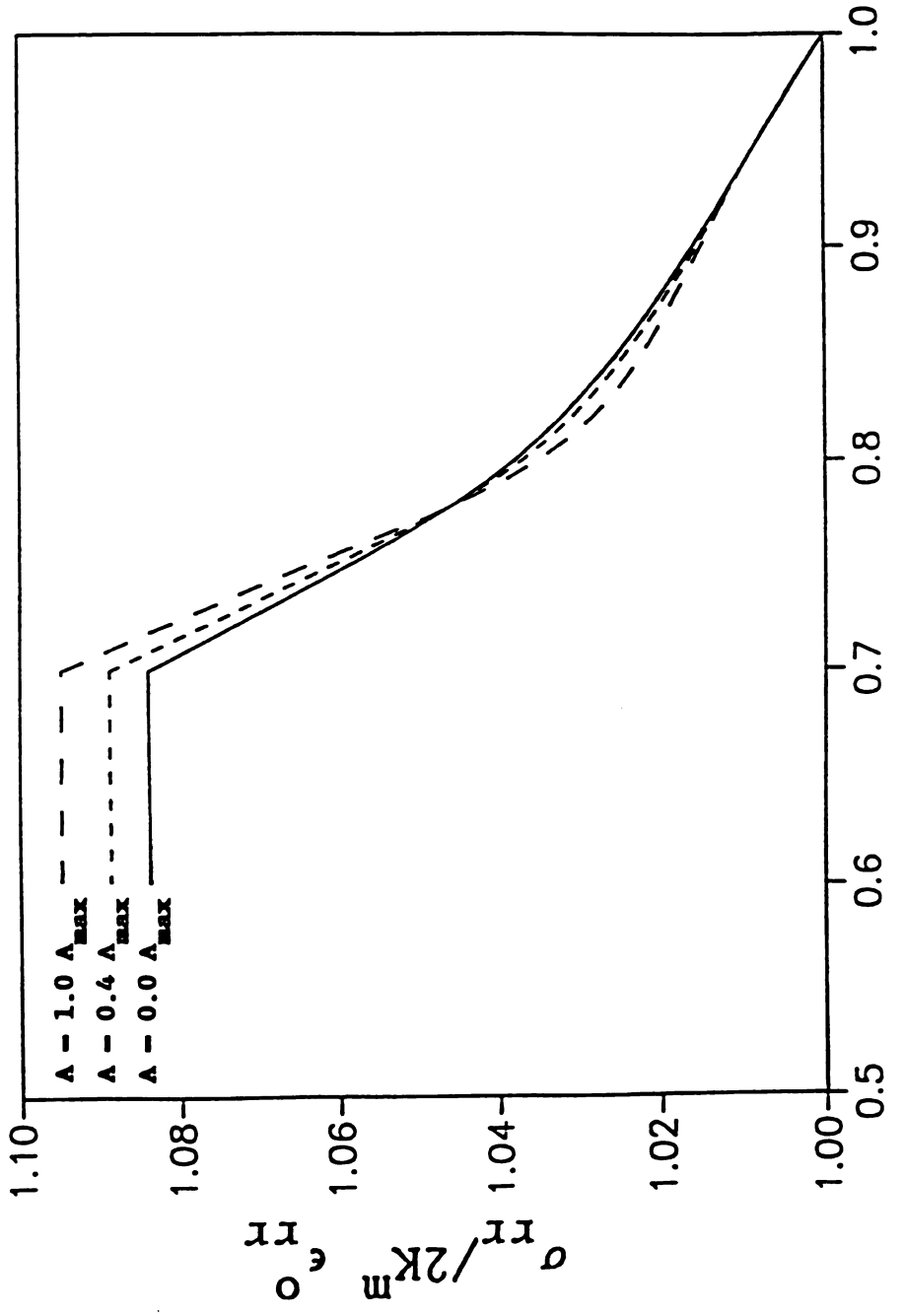

Fig. 4.33 Distribution of $\sigma_{rr}/2K^m\ \epsilon^o_{rr}$ along r for graphite-epoxy composite for $\nu^{\ell}(r)=Sr+T$ and $E^{\ell}(r)=Ar^2+Br+C$.

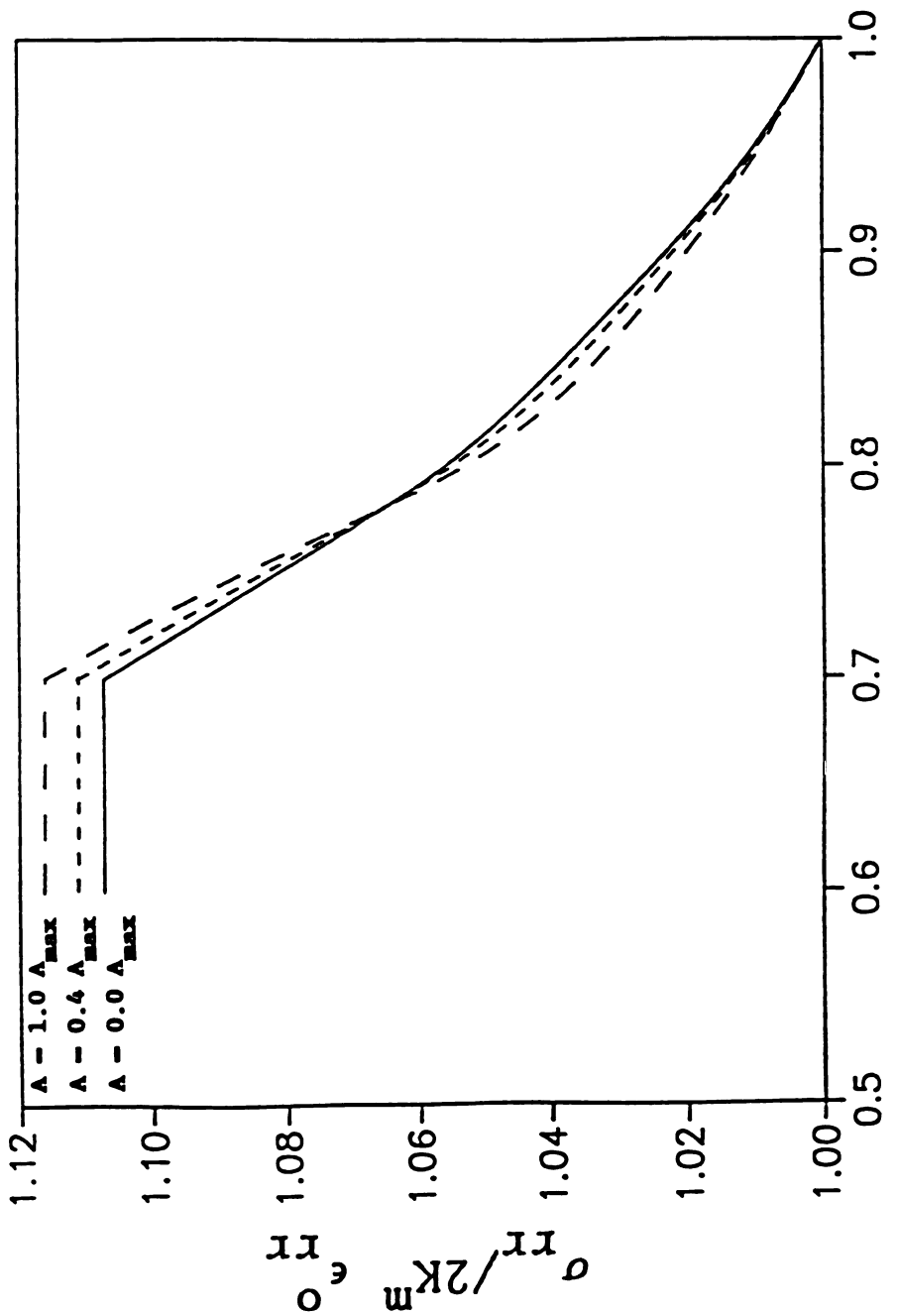

Fig. 4.34 Distribution of $\sigma_{rr}/2K^m\ \epsilon^o_{rr}$ along r for glass-plastic composite for $\nu^{\ell}(r)=Sr+T$ and $E^{\ell}(r)=Ar^2+Br+C$.

CHAPTER 5

CONCLUSIONS

In the first part of this dissertation (Chapter 3) the thermal stresses and thermal expansion coefficients of composites containing short fibers of spheroidal shape are obtained. The fibers are assumed to be either aligned or randomly oriented in 2-D and 3-D space. The sliding is allowed at the fiber-matrix interfaces such that shear tractions are specified to vanish. The same study is done for a composite with fibers perfectly bonded to the matrix, and the effect of interface is investigated by comparing the pure sliding case with the perfectly bonded case. The pure sliding interface is shown to affect considerably the thermal stresses and the thermal expansion coefficients of composites reinforced with fibers unidirectionally oriented and fibers misoriented in 2-D space, while, its effect on the same properties for composites reinforced with fibers misoriented in 3-D space is negligible. Also the misorientation of fibers in 2-D and 3-D space has a significant effect on the overall thermal expansion coefficients of composites.

In the second part (Chapter 4) the effective thermal and elastic properties of a composite reinforced with unidirectional long fibers of cylindrical shape are obtained. The composite is treated as effectively transversely isotropic and the interphase between fiber and matrix is assumed to be isotropic but non-homogeneous. This latter property is simulated by the elastic and thermal constants changing in the radial direction. It is shown that the variations of the elastic

modulus, Poisson's ratio, and thermal expansion coefficient in the interphase affect considerably the local stresses, displacements, and the effective elastic and thermal properties of the composite. However, the effect of variable Poisson's ratio on the effective properties of the composite is a little less significant than the effect of variable elastic modulus. It is also concluded that the smoother is the transition of the elastic properties at the interphase-matrix interface the higher is the stress transfered to the reinforcement and the lower is the stress carried by the matrix which is desirable from the design point of view.

APPENDICES

APPENDIX A

For the case of perfect bonding interfaces the quantities $\boldsymbol{\eta}$, $\boldsymbol{\gamma}$, $\boldsymbol{\beta}$ and $\boldsymbol{\lambda}$ used in our formulation are expressed by using Eshelby's tensor $\mathbf{S}$ as

$$\boldsymbol{\eta} = [(\mathbf{L}^f - \mathbf{L}^m)\mathbf{S} + \mathbf{L}^m]^{-1}\mathbf{L}^f(\boldsymbol{\alpha}^f - \boldsymbol{\alpha}^m) \tag{A.1}$$

$$\boldsymbol{\gamma} = \mathbf{L}^m(\mathbf{S} - \mathbf{I})[(\mathbf{L}^f - \mathbf{L}^m)\mathbf{S} + \mathbf{L}^m]^{-1}\mathbf{L}^f(\boldsymbol{\alpha}^f - \boldsymbol{\alpha}^m) \tag{A.2}$$

$$\boldsymbol{\beta} = [(\mathbf{L}^f - \mathbf{L}^m)\mathbf{S} + \mathbf{L}^m]^{-1}(\mathbf{L}^m - \mathbf{L}^f)\mathbf{M}^m \tag{A.3}$$

$$\boldsymbol{\lambda} = \mathbf{L}^m(\mathbf{S} - \mathbf{I})\ [(\mathbf{L}^f - \mathbf{L}^m)\mathbf{S} + \mathbf{L}^m]^{-1}(\mathbf{L}^m - \mathbf{L}^f)\mathbf{M}^m \tag{A.4}$$

APPENDIX B

The constants used to obtain the effective axial Young's modulus and the effective axial Poisson' ratio are

$$A_f = A_\ell a^{s_1-1} + B_\ell a^{s_2-1} - \epsilon^o_{zz}\nu^\ell \tag{B.1}$$

$$A_m = (1 - 2\nu^m)B_m/c^2 - \nu^m\epsilon^o_{zz} \tag{B.2}$$

$$B_m = \frac{[A_\ell b^{s_1} + B_\ell b^{s_2} + b\epsilon^o_{zz}(\nu^m - \nu^\ell)]\ c^2 b}{[(1 - 2\nu^m)b^2 + c^2]} \tag{B.3}$$

$$B_\ell = -A_\ell \frac{2K^f_T A_3 - A_{1f}}{2K^f_T A_3 - A_{2f}} a^{s_1-s_2} - \frac{2K^f_T \epsilon^o_{zz}(\nu^f_A - \nu^\ell)A_3}{2K^f_T A_3 - A_{2f}} \tag{B.4}$$

$$A_\ell = \frac{A_{\ell 1}}{A_{\ell 2}} \tag{B.5}$$

where

$$A_{\ell 1} = 2K^f_T\epsilon^o_{zz}(\nu^f_A-\nu^\ell)A_3(A_{2m}A_4-A_3A_5)b^{s_1-1} + \epsilon^o_{zz}(\nu^m-\nu^\ell)A_3A_5(2K^f_TA_3-A_{2f})b^{s_1-s_2}a^{s_2-1} \tag{B.6}$$

$$A_{\ell 2} = (2K_T^f A_3 - A_{2f})(A_{1m}A_4 - A_3A_5)b^{s_1 - s_2}a^{s_2 - 1}$$

$$- (2K_T^f A_3 - A_{1f})(A_{2m}A_4 - A_3A_5)a^{s_1 - 1} \tag{B.7}$$

$$A_{1m} = E^m[(1 - \nu^\ell)s_1 + \nu^\ell] \tag{B.8}$$

$$A_{2m} = E^m[(1 - \nu^\ell)s_2 + \nu^\ell] \tag{B.9}$$

$$A_{1f} = E_T^f[(1 - \nu^\ell)s_1 + \nu^\ell] \tag{B.10}$$

$$A_{2f} = E_T^f[(1 - \nu^\ell)s_2 + \nu^\ell] \tag{B.11}$$

$$A_3 = (1 - 2\nu^\ell)(1 + \nu^\ell) \tag{B.12}$$

$$A_4 = (1 + \nu^m)[(1 - 2\nu^m)b^2 + c^2] \tag{B.13}$$

$$A_5 = E^m(b^2 - c^2) \tag{B.14}$$

$$A_6 = (1 - 2\nu^m)(1 + \nu^m) \tag{B.15}$$

APPENDIX C

The constants used to obtain the effective plane strain bulk modulus are

$$A_f = A_\ell a^{s_1-1} + B_\ell a^{s_2-1} \tag{C.1}$$

$$A_m = \frac{A_6}{E^m} + (1 - 2\nu^m)\frac{B_m}{c^2} \tag{C.2}$$

$$B_m = \frac{[A_\ell b^{s_1} + B_\ell b^{s_2} - A_6 b/E^m]\, bc^2}{[(1 - 2\nu^m)b^2 + c^2]} \tag{C.3}$$

$$B_\ell = - A_\ell \frac{[2K_T^f A_3 - A_{1f}]}{[2K_T^f A_3 - A_{2f}]} a^{s_1-s_2} \tag{C.4}$$

$$A_\ell = \frac{A_{\ell 1}}{A_{\ell 2}} \tag{C.5}$$

where

$$A_{\ell 1} = A_3(2K_T^f A_3 - A_{2f})(A_4 - A_5 A_6/E^m) \tag{C.6}$$

$$A_{\ell 2} = (A_{1m}A_4 - A_3A_5)(2K_T^f A_3 - A_{2f})b^{s_1-1} \tag{C.7}$$

$$- (A_{2m}A_4 - A_3A_5)(2K_T^f A_3 - A_{1f})a^{s_1 - s_2} b^{s_2 - 1}$$

APPENDIX D

The constants used to obtain the effective axial shear modulus are

$$A_f = A_\ell a^{s_1-1} + B_\ell a^{s_2-1} - 1 \tag{D.1}$$

$$A_m = 1 - \frac{B_m}{c^2} \tag{D.2}$$

$$B_m = -[A_\ell s_1 b^{s_1-1} + B_\ell s_2 b^{s_2-1} - 2] \frac{b^2c^2}{b^2 + c^2} \tag{D.3}$$

$$B_\ell = - \frac{[b^2 + c^2 + s_1(c^2 - b^2)]b^{s_1}A_\ell - 4bc^2}{[b^2 + c^2 + s_2(c^2 - b^2)]b^{s_2}} \tag{D.4}$$

$$A_\ell = - \frac{4b^{1-s_2}c^2}{[b^2 + c^2 + s_2(c^2 - b^2)]A_{\ell 1}} \tag{D.5}$$

where

$$A_{\ell 1} = \frac{G_A^f - s_1 G_T^f}{G_A^f - s_2 G_T^f} a^{s_1-s_2} - \frac{b^2 + c^2 + s_1(c^2 - b^2)}{b^2 + c^2 + s_2(c^2 - b^2)} b^{s_1-s_2} \tag{D.6}$$

APPENDIX E

The constants used in the displacement component u(r) and v(r) for the transverse shear case are

$$Q_j = - \frac{C + \lambda_j(B + A(\lambda_j - 1))}{E + \lambda_j D} \quad ; j = 1, 2, 3 \text{ and } 4 \qquad (E.1)$$

where

$$A = 1 - \nu^{\ell} \qquad (E.2)$$

$$B = (Q + 1)(1 - \nu^{\ell}) \qquad (E.3)$$

$$C = [(Q + 5)\nu^{\ell} - 3] \qquad (E.4)$$

$$D = -1 \qquad (E.5)$$

$$E = - 2(Q + 2)\nu^{\ell} + 3 \qquad (E.6)$$

λ_j are the solutions of the following equation

$$\lambda^4 + 2Q\,\lambda^3 + (Q^2-2Qt-10)\,\lambda^2 - 2(Q^2t+5Q)\,\lambda + [3Q^2(1-2t)-6Qt+9] = 0 \qquad (E.7)$$

where $$t = \frac{1 - 2\nu^{\ell}}{2(1 - \nu^{\ell})} \tag{E.8}$$

It can be easily shown that in our case the fourth order equation gives either four real solutions or four complex solutions. In the case of four complex solutions λ_j is written in the form

$$\lambda_j = \alpha_j + i\beta_j \; ; \qquad j = 1, 2, 3 \text{ and } 4 \tag{E.9}$$

The displacement solutions are

$$\begin{aligned} u = {} & A_{\ell}\cos(\beta_1 \ln r) r^{\alpha_1} - B_{\ell}\sin(\beta_2 \ln r) r^{\alpha_2} \\ & + C_{\ell}\cos(\beta_3 \ln r) r^{\alpha_3} - D_{\ell}\sin(\beta_4 \ln r) r^{\alpha_4} \end{aligned} \tag{E.10}$$

$$\begin{aligned} v = {} & A_{\ell}[\alpha_1' \cos(\beta_1 \ln r) - \beta_1' \sin(\beta_1 \ln r)] r^{\alpha_1} \\ & - B_{\ell}[\alpha_2' \sin(\beta_2 \ln r) + \beta_2' \cos(\beta_2 \ln r)] r^{\alpha_2} \\ & + C_{\ell}[\alpha_3' \cos(\beta_3 \ln r) - \beta_3' \sin(\beta_3 \ln r)] r^{\alpha_3} \\ & - D_{\ell}[\alpha_4' \sin(\beta_4 \ln r) + \beta_4' \cos(\beta_4 \ln r)] r^{\alpha_4} \end{aligned} \tag{E.11}$$

where

$$\alpha_j' = \frac{\alpha_{j1}\alpha_{j2} + \beta_{j1}\beta_{j2}}{\alpha_{j2}^2 + \beta_{j2}^2} \qquad j = 1, 2, 3, \text{ and } 4 \qquad \text{(E.12)}$$

$$\beta_j' = \frac{\beta_{j1}\alpha_{j2} - \alpha_{j1}\beta_{j2}}{\alpha_{j2}^2 + \beta_{j2}^2} \qquad j = 1, 2, 3, \text{ and } 4 \qquad \text{(E.13)}$$

$$\alpha_{j1} = - C - \alpha_j[B + A(\alpha_j - 1)] + A\beta_j^2 \qquad \text{(E.14)}$$

$$\alpha_{j2} = E + \alpha_j D \qquad \text{(E.15)}$$

$$\beta_{j1} = -(\beta_j[B + A(\alpha_j - 1)] + \alpha_j\beta_j A) \qquad \text{(E.16)}$$

$$\beta_{j2} = \beta_j D \qquad \text{(E.17)}$$

$j = 1, 2, 3, \text{ and } 4$

APPENDIX F

The constants used to obtain a closed form for the effective thermal expansion coefficients are

$$A_f = A_\ell a^{s_1-1} + B_\ell a^{s_2-1} - \epsilon^o_{zz}\nu^\ell + A_7 a^T \tag{F.1}$$

$$A_m = -(1-\nu^m)\epsilon^o_{zz}/2\nu^m + (1+\nu^m)\alpha^m \Delta T/2\nu^m \tag{F.2}$$

$$B_m = -b^2 A_6 (B_{m1}+A_9)/E^m(1-2\nu^m) \tag{F.3}$$

$$B_{m1} = A_\ell \frac{A_{1m}}{A_3} b^{s_1-1} + B_\ell \frac{A_{2m}}{A_3} b^{s_2-1} + (1-\nu^m-2\nu^{m\,2})E^m\epsilon^o_{zz}/2\nu^m A_6 \tag{F.4}$$

$$A_\ell = -A_{12}B_\ell/A_{11} - A_{13}\epsilon^o_{zz}/A_{11} - A14/A11 \tag{F.5}$$

$$B_\ell = -A_{18}\epsilon^o_{zz}/A_{17} - A19/A17 \tag{F.6}$$

$$\epsilon^o_{zz} = (A_{20}A_{19} - A_{22}A_{17})/(A_{21}A_{17} - A_{20}A_{18}) \tag{F.7}$$

where the constants A_{1f}, A_{2f}, A_{1m}, A_{2m}, A_3 and A_6 are given in appendix B

$$A_7 = \frac{(S(Q+T)\Delta T \frac{1+\nu^{\ell}}{1-\nu^{\ell}})}{T^2 + 2T + QT + Q\frac{1}{1-\nu^{\ell}}} \qquad \text{(F.8)}$$

$$A_{88} = -\frac{E_T}{A_3}([1+T(1-\nu^{\ell})]A_7 a^T - \alpha_T^f(1+\nu^{\ell})\Delta T) \qquad \text{(F.9)}$$

$$A_8 = 2K_T^f(A_7 a^T - \alpha_T^f \Delta T - \nu_A^f \alpha_A^f \Delta T) + A_{88} \qquad \text{(F.10)}$$

$$A_{99} = -\frac{E^m}{A_3}([1+T(1-\nu^{\ell})]A_7 b^T - \alpha^m(1+\nu^{\ell})\Delta T) \qquad \text{(F.11)}$$

$$A_9 = -\frac{1+\nu^m}{A_6}\alpha^m \Delta T E^m(1-2\nu^m)/2\nu^m + A_{99} \qquad \text{(F.12)}$$

$$A_{10} = A_7 b^T - (1+\nu^m)\alpha^m \Delta T/2\nu^m \qquad \text{(F.13)}$$

$$A_{11} = [1 + \frac{A_6 A_{1m}}{E^m(1-2\nu^m)A_3}]\, b^{s_1-1} \qquad \text{(F.14)}$$

$$A_{12} = [1 + \frac{A_6 A_{2m}}{E^m(1-2\nu^m)A_3}]\, b^{s_2-1} \qquad \text{(F.15)}$$

$$A_{13} = (\frac{1-\nu^m}{2\nu^m} - \nu^{\ell}) + (\frac{1-\nu^m}{2\nu^m} - \nu^m)/(1-2\nu^m) \qquad \text{(F.16)}$$

$$A_{14} = A_{10} + \frac{A_6 A_9}{E^m(1-2\nu^m)} \tag{F.17}$$

$$A_{15} = E^m(2\nu^{m\,2}+\nu^m-1)(c^2/b^2 - 1)/2\nu^m A_6 \tag{F.18}$$

$$A_{16} = c^2 E^m(1-\nu^m-2\nu^{m\,2})/2\nu^m \alpha^m \Delta T b^2 A_6 + A_9 \tag{F.19}$$

$$A_{17} = \frac{A_{2m}}{A_3} b^{s_2-1} - \frac{A_{12}A_{1m}}{A_{11}A_3} b^{s_1-1} \tag{F.20}$$

$$A_{18} = A_{15} - \frac{A_{13}A_{1m}}{A_{11}A_3} b^{s_1-1} \tag{F.21}$$

$$A_{19} = A_{16} - \frac{A_{14}A_{1m}}{A_{11}A_3} b^{s_1-1} \tag{F.22}$$

$$A_{20} = (2K_T^f - \frac{A_{2f}}{A_3}) a^{s_2-1} - \frac{A_{12}}{A_{11}} (2K_T^f - \frac{A_{1f}}{A_3}) a^{s_1-1} \tag{F.23}$$

$$A_{21} = 2K_T(\nu_A^f - \nu^\ell) - \frac{A_{13}}{A_{11}} (2K_T^f - \frac{A_{1f}}{A_3}) a^{s_1-1} \tag{F.24}$$

$$A_{22} = A_8 - \frac{A_{14}}{A_{11}} (2K_T^f - \frac{A_{1f}}{A_3}) a^{s_1-1} \tag{F.25}$$

APPENDIX G

The variation models used to simulate the interphase property gradients are as follow

Linear variation model

$$y = c_1 r + c_2 \tag{G.1}$$

Power variation model

$$y = c_1 r^{c_2} \tag{G.2}$$

Hyperbolic variation model

$$y = c_1 + \frac{c_2}{r} \tag{G.3}$$

Reciprocal variation model

$$y = \frac{c_1}{r - c_2} \tag{G.4}$$

parabolic variation model

$$y = c_1 r^2 + c_2 r + c_3 \tag{G.5}$$

where y is any property of the composite material, r the radial coordinate, c_1 and c_2 are two constants to be determined easily using the assumed boundary conditions

Property(r=a) = Property(fiber)

Property(r=b) = Property(matrix)

c_3 is used only in the parabolic variation model, it is a free parameter which gives a wide range of distributions being properly selected.

APPENDIX H

The functions M(r) and N(r) of the differential equation in section 4.7 are given in this appendix for each model.

Model 1

$$M(r) = \frac{1}{r} \frac{A_2 r^3+B_2 r^2+C_2 r+D_2}{A_1 r^3+B_1 r^2+C_1 r+D_1} \tag{H.1}$$

$$N(r) = \frac{1}{r^2} \frac{A_3 r^3+B_3 r^2+C_3 r+D_3}{A_1 r^3+B_1 r^2+C_1 r+D_1} \tag{H.2}$$

where

$$\begin{aligned} A_1 &= 2S^3 \\ B_1 &= S^2(6T - 1) \\ C_1 &= 2S(3T^2 - T - 1) \\ D_1 &= 2T^3 - T^2 - 2T + 1 \end{aligned} \tag{H.3}$$

$$\begin{aligned} A_2 &= 2QS^3 \\ B_2 &= S^2[2(3Q+1)T + (3-Q)] \\ C_2 &= 2S[(3Q+2)T^2 + (Q-1)T - (Q+1)] \\ D_2 &= (Q+1)(2T^3 - T^2 - 2T + 1) \end{aligned} \tag{H.4}$$

$$A_3 = -2QS^3$$

$$B_3 = S^2[-2(3Q+1)T + (1-Q)]$$

$$C_3 = S[-2(3Q+2)T^2 + 2(1-Q)T + (Q+3)] \qquad \text{(H.5)}$$

$$D_3 = -2(Q+1)T^3 + (1-Q)T^2 + (Q+2)T - 1$$

Model 2

$$M(r) = \frac{1}{r} \frac{A_2r^3+B_2r^2+C_2r+D_2}{A_1r^3+B_1r^2+C_1r+D_1} \qquad \text{(H.6)}$$

$$N(r) = \frac{1}{r^2} \frac{A_3r^3+B_3r^2+C_3r+D_3}{A_1r^3+B_1r^2+C_1r+D_1} \qquad \text{(H.7)}$$

where

$$A_1 = 2S^3 - S^2 - 2S + 1$$

$$B_1 = 2(3S^2 - S - 1)T$$

$$C_1 = (6S-1)T^2 \qquad \text{(H.8)}$$

$$D_1 = 2T^3$$

$$A_2 = (Q+1)(2S^3 - S^2 - 2S + 1)$$

$$B_2 = 2[(3Q+4)S^2 - (Q+3)S - 2(Q+1)]T$$

$$C_2 = [2(3Q+5)S - (Q+5)]T^2 \qquad (H.9)$$

$$D_2 = 2(Q+2)T^3$$

$$A_3 = -2(Q+1)S^3 + (1-Q)S^2 + (Q+2)S - 1$$

$$B_3 = [-2(3Q+4)S^2 + 2(1-Q)S + (Q+1)]T$$

$$C_3 = [-2(3Q+5)S - (Q-1)]T^2 \qquad (H.10)$$

$$D_3 = -2(Q+2)T^3$$

Model 3

$$M(r) = \frac{1}{r} \frac{A_2r^4+B_2r^3+C_2r^2+D_2r+E_2}{A_1r^4+B_1r^3+C_1r^2+D_1r+E_1} \qquad (H.11)$$

$$N(r) = \frac{1}{r^2} \frac{A_3r^4+B_3r^3+C_3r^2+D_3r+E_3}{A_1r^4+B_1r^3+C_1r^2+D_1r+E_1} \qquad (H.12)$$

where

$$A_1 = 1$$

$$B_1 = -2(2T+S)$$

$$C_1 = 6T^2 + 6ST - S^2 \qquad (H.13)$$

$$D_1 = 2(-2T^3 - 3ST^2 + S^2T + S^3)$$

$$E_1 = (T^3 + 2ST^2 - S^2T - 2S^3)T$$

$$A_2 = Q+1$$

$$B_2 = -(Q+1)(4T + 2S)$$

$$C_2 = 6(Q+1)T^2 + 6(Q+1)ST - (Q+5)S^2 \qquad \text{(H.14)}$$

$$D_2 = 2[-2(Q+1)T^3 - 3(Q+1)ST^2 + (Q+3)S^2T + (Q+2)S^3]$$

$$E_2 = (Q+1)(T^3 + 2ST^2 - S^2T - 2S^3)T$$

$$A_3 = -1$$

$$B_3 = 4T + (Q+1)S$$

$$C_3 = -6T^2 - (3Q+1)ST + (1-Q)S^2 \qquad \text{(H.15)}$$

$$D_3 = 4T^3 + (3Q+5)ST^2 + 2(Q-1)S^2T - 2(Q+2)S^3$$

$$E_3 = [-T^3 - (Q+2)ST^2 + (1-Q)S^2T + 2(Q+1)S^3]T$$

Model 4

$$M(r) = \frac{1}{r} \frac{A_2r^6+B_2r^5+C_2r^4+D_2r^3+E_2r^2+F_2r+G_2}{A_1r^6+B_1r^5+C_1r^4+D_1r^3+E_1r^2+F_1r+G_1} \qquad \text{(H.16)}$$

$$N(r) = \frac{1}{r^2} \frac{A_3r^6+B_3r^5+C_3r^4+D_3r^3+E_3r^2+F_3r+G_3}{A_1r^6+B_1r^5+C_1r^4+D_1r^3+E_1r^2+F_1r+G_1} \qquad \text{(H.17)}$$

where

$$A_1 = 2S^3$$

$$B_1 = 6S^2T$$

$$C_1 = S[6T^2 + (6W-1)S]$$

$$D_1 = T[2T^2 + 2(6W-1)S] \qquad \text{(H.18)}$$

$$E_1 = (6W-1)T^2 + 2(3W^2-W-1)S$$

$$F_1 = 2(3W^2 - W - 1)T$$

$$G_1 = 2W^3 - W^2 - 2W + 1$$

$$A_2 = 2(Q-1)S^3$$

$$B_2 = 2(3Q-2)S^2T$$

$$C_2 = S\{2(3Q-1)T^2 + [(6W-1)Q-2W+7]S\}$$

$$D_2 = T\{2QT^2 + 2[(6W-1)Q+5]S\} \qquad \text{(H.19)}$$

$$E_2 = [(6W-1)Q+2W+3]T^2 + 2[(3W^2-W-1)Q+W^2+3W-1]S$$

$$F_2 = 2[(3W^2-W-1)Q + 2W^2 + W - 1]T$$

$$G_2 = (2W^3-W^2-2W+1)Q + 2W^3 - W^2 - 2W + 1$$

$$A_3 = 2(1-Q)S^3$$

$$B_3 = 2(2-3Q)S^2T$$

$$C_3 = S\{2(1-3Q)T^2 + [-(6W+1)Q+2W+1]S\}$$

$$D_3 = T\{2[-(6W+1)Q+1]S - QT^2\} \qquad \text{(H.20)}$$

$$E_3 = [-(6W+1)Q-2W+1]T^2 + [-(6W^2+2W-1)Q - 2W^2 + 2W +4]S$$

$$F_3 = [(-6W^2-2W+1)Q - 4W^2 + 2W + 3]T$$

$$G_3 = W(-2W^2-W+1)Q - 2W^3 + W^2 + 2W - 1$$

Model 5

$$M(r) = \frac{1}{r} \frac{A_2r^4+B_2r^3+C_2r^2+D_2r+E_2}{A_1r^4+B_1r^3+C_1r^2+D_1r+E_1} \tag{H.21}$$

$$N(r) = \frac{1}{r^2} \frac{A_3r^4+B_3r^3+C_3r^2+D_3r+E_3}{A_1r^4+B_1r^3+C_1r^2+D_1r+E_1} \tag{H.22}$$

where

$$A_1 = 2PS^3$$

$$B_1 = (6PT + 2QS - P)S^2$$

$$C_1 = [6PT^2 + 2(QS-2P)T - QS - 2P]S \tag{H.23}$$

$$D_1 = 2PT^3 + (6QS-P)T^2 - 2(QS+P)T - 2QS + P$$

$$E_1 = (2T^3 - T^2 - 2T + 1)Q$$

$$A_2 = 2PS^3$$

$$B_2 = 2PS^2(4T + 1)$$

$$C_2 = S(10PT^2 + 2QST + 3QS - 4P) \tag{H.24}$$

$$D_2 = 4PT^3 + 2(2QS-P)T^2 + 2(QS-2P)T - 2QS + 2P$$

$$E_2 = Q(2T^3 - T^2 - 2T + 1)$$

$$A_3 = -2PS^3$$

$$B_3 = -8PS^2T$$

$$C_3 = S(-10PT^2 - 2QST + QS + 4P) \qquad \text{(H.25)}$$

$$D_3 = -4PT^3 - 4QST^2 + (2QS+3P)T + 3QS - P$$

$$E_3 = Q(-2T^3 + T^2 + 2T - 1)$$

Model 6

$$M(r) = \frac{1}{r} \frac{A_2r^4+B_2r^3+C_2r^2+D_2r+E_2}{A_1r^4+B_1r^3+C_1r^2+D_1r+E_1} \qquad \text{(H.26)}$$

$$N(r) = \frac{1}{r^2} \frac{A_3r^4+B_3r^3+C_3r^2+D_3r+E_3}{A_1r^4+B_1r^3+C_1r^2+D_1r+E_1} \qquad \text{(H.27)}$$

where

$$A_1 = P(2S^3 - S^2 - 2S + 1)$$

$$B_1 = 2(S^2-S-1)PT + Q(2S^3-S^2-2S+1)$$

$$C_1 = T[(6S-1)PT + 2Q(3S^2-S-1)] \qquad \text{(H.28)}$$

$$D_1 = T^2[2PT + Q(6S-1)]$$

$$E_1 = 2QT^3$$

$$A_2 = 2P(2S^3 - S^2 - 2S + 1)$$

$$B_2 = 2PT(7S^2-4S-2) + Q(2S^3-S^2-2S+1)$$

$$C_2 = 2PT^2(8S-3) + 2QT(4S^2-3S-1) \qquad \text{(H.29)}$$

$$D_2 = T^2[6PT + 5Q(2S-1)]$$

$$E_2 = 4QT^3$$

$$A_3 = P(4S^3 + 3S - 1)$$

$$B_3 = 2PT(1-7S^2) - Q(2S^3+S^2+2S-1)$$

$$C_3 = T[Q(-8S^2+2S+1) - 16PST] \qquad \text{(H.30)}$$

$$D_3 = T^2[Q(1-10S) - 6PT]$$

$$E_3 = -4QT^3$$

Model 7

$$M(r) = \frac{1}{r} \frac{A_2r^5+B_2r^4+C_2r^3+D_2r^2+E_2r+F_2}{A_1r^5+B_1r^4+C_1r^3+D_1r^2+E_1r+F_1} \qquad \text{(H.31)}$$

$$N(r) = \frac{1}{r^2} \frac{A_3r^5+B_3r^4+C_3r^3+D_3r^2+E_3r+F_3}{A_1r^5+B_1r^4+C_1r^3+D_1r^2+E_1r+F_1} \qquad \text{(H.32)}$$

where

$$A_1 = P$$

$$B_1 = -4PT - 2PS + Q$$

$$C_1 = 6PT^2 + 2(3PS-2Q)T - PS^2 - 2QS \qquad \text{(H.33)}$$

$$D_1 = -4PT^3 + 6(Q-PS)T^2 + 2S(PS+3Q)T + S^2(2PS-Q)$$

$$E_1 = PT^4 + 2T^3(PS-2Q) - ST^2(PS+6Q) + 2S^2T(Q-PS) + 2QS^3$$

$$F_1 = QT(T^3 + 2ST^2 - S^2T - 2S^3)$$

$$A_2 = 2P$$

$$B_2 = -8PT - 4PS + Q$$

$$C_2 = 12PT^2 + 4T(3PS-Q) - 2S(3PS+Q) \qquad \text{(H.34)}$$

$$D_2 = -8PT^3 + 6T^2(Q-2PS) + 2ST(4PS+3Q) + S^2(6PS-5Q)$$

$$E_2 = 2PT^4 + 4T^3(PS-Q) - 2ST^2(PS+3Q) + 2S^2T(3Q-2PS) + 4QS^3$$

$$F_2 = QT(T^3 + 2ST^2 - S^2T^2 - 2S^3$$

$$A_3 = -P$$

$$B_3 = 4PT + 2PS - Q$$

$$C_3 = -6PT^2 + (4Q-7PS)T + QS \qquad \text{(H.35)}$$

$$D_3 = 4PT^3 + 2T^2(4PS-3Q) - 4QST - 6PS^3 + QS^2$$

$$E_3 = -PT^4 + (4Q-3PS)T^3 + 5QST^2 + 2S^2(2PS-Q)T - 4QS^3$$

$$F_3 = QT(-T^3 - 2ST^2 + S^2T + 2S^3)$$

Model 8

$$M(r) = \frac{1}{r} \frac{A_2r^4+B_2r^3+C_2r^2+D_2r+E_2}{A_1r^4+B_1r^3+C_1r^2+D_1r+E_1} \tag{H.36}$$

$$N(r) = \frac{1}{r^2} \frac{A_3r^4+B_3r^3+C_3r^2+D_3r+E_3}{A_1r^4+B_1r^3+C_1r^2+D_1r+E_1} \tag{H.37}$$

where

$$\begin{aligned} A_1 &= P(2S^3 - S^2 - 2S + 1) \\ B_1 &= 2PT(3S^2-S-1) + Q(2S^3-S^2-2S+1) \\ C_1 &= PT^2(6S-1) + 2QT(3S^2-S-1) \\ D_1 &= T^2[2PT + Q(6S-1)] \\ E_1 &= 2QT^3 \end{aligned} \tag{H.38}$$

$$\begin{aligned} A_2 &= P(2S^3 - S^2 - 2S + 1) \\ B_2 &= 2PT(4S^2-3S-1) \\ C_2 &= T[5PT(2S-1) + 2QST(S-2)] \end{aligned} \tag{H.39}$$

$$D_2 = 4T^2[PT + Q(S-1)]$$

$$E_2 = 2QT^3$$

$$A_3 = -P(2S^3 - S^2 - 2S + 1)$$

$$B_3 = -[PT(8S^2-2S-1) - Q(2S^2+S-1)]$$

$$C_3 = -T[PT(10S-1) + 2QS(S-2)] \qquad \text{(H.40)}$$

$$D_3 = -2T^2[2PT + 2Q(2S-1)]$$

$$E_3 = -2QT^3$$

Model 9

$$M(r) = \frac{1}{r} \frac{A_2r^5+B_2r^4+C_2r^3+D_2r^2+E_2r+F_2}{A_1r^5+B_1r^4+C_1r^3+D_1r^2+E_1r+F_1} \qquad \text{(H.41)}$$

$$N(r) = \frac{1}{r^2} \frac{A_3r^5+B_3r^4+C_3r^3+D_3r^2+E_3r+F_3}{A_1r^5+B_1r^4+C_1r^3+D_1r^2+E_1r+F_1} \qquad \text{(H.42)}$$

where

$$A_1 = 2PS^3$$

$$B_1 = S^2(6PT + 2QS - P)$$

$$C_1 = S[2T(3PT + 3QS - P) + 2RS^2 - QS - 2P] \qquad \text{(H.43)}$$

$$D_1 = 2PT^3 + (6QS-P)T^2 + 2(3RS^2-QS-P)T - RS^2 - 2QS + P$$

$$E_1 = 2QT^3 + (6RS-Q)T^2 - 2(SR+Q)T - 2RS + Q$$

$$F_1 = R(2T^3 - T^2 - 2T + 1)$$

$$A_2 = 4PS^3$$

$$B_2 = S^2(14PT + 2QS + P)$$

$$C_2 = 2S[8PT^2 + (4QS-P)T + QS - 3P] \qquad \text{(H.44)}$$

$$D_2 = 6PT^3 + (10QS-3P)T^2 + 2T(RS^2-3P) + 3RS^2 - 4QS +3P$$

$$E_2 = 4QT^3 + 2T^2(2RS-Q) + 2T(RS-2Q) - 2(RS-Q)$$

$$F_2 = R(2T^3 - T^2 - 2T + 1)$$

$$A_3 = -4PS^3$$

$$B_3 = -S^2(14PT + 2QS + P)$$

$$C_3 = S(-16PT^2 - 2(4QS+POT + 5P) \qquad \text{(H.45)}$$

$$D_3 = -6PT^3 - T^2(10QS+P) + 2T(2P-RS^2) + RS^2 + 4QS - P$$

$$E_3 = -4QT^3 - 4RST^2 + (2RS+3Q)T + 3RS - Q$$

$$F_3 = R(-2T^3 + T^2 + 2T -1)$$

Model 10

$$M(r) = \frac{1}{r} \frac{A_2 r^2 + B_2 r + C_2}{A_1 r^2 + B_1 r + C_1} \tag{H.46}$$

$$N(r) = \frac{1}{r^2} \frac{A_3 r^2 + B_3 r + C_3}{A_1 r^2 + B_1 r + C_1} \tag{H.47}$$

where

$$\begin{aligned} A_1 &= (2S^3 - S^2 - 2S + 1)R \\ B_1 &= (2S^3 - S^2 - 2S + 1)P \\ C_1 &= (2S^3 - S^2 - 2S + 1)Q \end{aligned} \tag{H.48}$$

$$\begin{aligned} A_2 &= (6S^3 - 3S^2 - 6S + 3)R \\ B_2 &= 2(2S^3 - S^2 - 2S + 1)P \\ C_2 &= (2S^3 - S^2 - 2S + 1)Q \end{aligned} \tag{H.49}$$

$$\begin{aligned} A_3 &= (-6S^3 - S^2 + 4S - 1)R \\ B_3 &= (-4S^3 + 3S - 1)P \\ C_3 &= (-2S^3 + S^2 + 2S - 1)Q \end{aligned} \tag{H.50}$$

APPENDIX I

The coefficients $p_1(r)$, $p_2(r)$, $p_3(r)$, and $p_4(r)$ in the differential equation (4.137) are given for special cases of $E^{\ell}(r)$, $\alpha^{\ell}(r)$, and $\nu^{\ell}(r)$ given by equation (4.134).

Case 1 N = 0

$$p_1(r) = A_1r^5 + B_1r^4 + C_1r^3 + D_1r^2 + E_1r + F_1$$

$$p_2(r) = A_2r^5 + B_2r^4 + C_2r^3 + D_2r^2 + E_2r + F_2 \qquad \text{(I.1)}$$

$$p_3(r) = A_3r^5 + B_3r^4 + C_3r^3 + D_3r^2 + E_3r + F_3$$

$$p_4(r) = A_4r^6 + B_4r^5 + C_4r^4 + D_4r^3 + E_4r^2 + F_4r + G_4$$

where

$$A_1 = 2MS^3$$

$$B_1 = 6MS^2T + 2PS^3 - MS^2$$

$$C_1 = 6MST^2 + (6PS^2-2MS)T + 2QS^3 - PS^2 - 2MS \qquad \text{(I.2)}$$

$$D_1 = 2MT^3 + (6PS-M)T^2 + (6QS^2-2PS-2M)T - QS^2 - 2PS + M$$

$$E_1 = 2PT^3 + (6QS-P)T^2 - 2(QS+P)T - 2QS + P$$

$$F_1 = Q(2T^3 - T^2 - 2T + 1)$$

$$A_2 = 4MS^3$$

$$B_2 = S^2(14MT + 2PS + M)$$

$$C_2 = 16MST^2 + 2ST(4PS - M) + 2PS^2 - 6MS \qquad \text{(I.3)}$$

$$D_2 = 6MT^3 + (10PS-3M)T^2 + 2T(QS^2-3M) + 3QS^2 - 4PS + 3M$$

$$E_2 = 4PT^3 + 2T^2(2QS-P) + 2T(QS-2P) - 2QS + 2P$$

$$F_2 = Q(2T^3 - T^2 - 2T + 1)$$

$$A_3 = -MS^3$$

$$B_3 = -S^2(14MT + 2PS + M)$$

$$C_3 = -16MST^2 - 2ST(4PS+M) + 5MS \qquad \text{(I.4)}$$

$$D_3 = -6MT^3 - (10PS+M)T^2 + 2T(2M-QS^2) + QS^2 + 4PS - M$$

$$E_3 = -4PT^3 - 4QST^2 + (2QS+3P)T + 3QS - P$$

$$F_3 = Q(-2T^3 + T^2 + 2T - 1)$$

$$A_4 = 6LMS^3\Delta T$$

$$B_4 = 4S^2\Delta T(MSU + 5LMT + LPS + 2LM)$$

$$C_4 = 2MS^3\Delta T + US^2\Delta T(14MT+2PS+5M) + 22LMST^2\Delta T + \qquad \text{(I.5)}$$

$$2LST\Delta T(7PS+10M) + 2S^3(LQ\Delta T - \epsilon^o_{zz}M) + LS\Delta T(5PS-2M)$$

$$D_4 = 2MS^2V\Delta T(4T+1) + (16MST^2\Delta T + 2ST\Delta T(4PS+7M) + 2PS^2\Delta T$$

$$- 2MS\Delta T)U + 8LMT^3\Delta T + 4LT^2\Delta T(4PS+3M) + (8S^2(LQ\Delta T-\epsilon^o_{zz}M)$$

$$+ 14LPS\Delta T)T + 2S^2(LQ\Delta T-\epsilon^o_{zz}M) - 2LPS\Delta T - 4LM\Delta T$$

$$E_4 = (10MST^2\Delta T + 2ST\Delta T(PS+4M) - 2QS^3\Delta T - PS^2\Delta T - 2MS\Delta T)V +$$

$$(6MT^3\Delta T + (10PS\Delta T+9M\Delta T)T^2 + 2ST\Delta T(QS+4P) - QS^2\Delta T - 2PS\Delta T$$

$$- 3M\Delta T)U + 6LPT^3\Delta T + (10(LQ\Delta T-\epsilon^o_{zz}M)S + 9LP\Delta T)T^2$$

$$+ (4S(2L\Delta T- \epsilon^o_{zz}M) - 2\epsilon^o_{zz}PS^2)T + \epsilon^o_{zz}S^2(2QS-P)$$

$$+ (3\epsilon^o_{zz}M-2LQ\Delta T)S - 3LP\Delta T$$

$$F_4 = (4MT^3\Delta T + 2T^2\Delta T(2PS+3M) + 2ST\Delta T(P-2QS)$$

$$- 2\Delta T(2QS^2+PS+M))V + (4PT^3\Delta T + 2T^2\Delta T(2QS+3P)$$

$$+ 2\Delta T(QST-QS-P))U + 4T^3(LQ\Delta T-\epsilon^o_{zz}M) + 2T^2(-2\epsilon^o_{zz}PS+3LQ\Delta T$$

$$-\epsilon^o_{zz}M) + 2T\epsilon^o_{zz}(2QS^2-PS+M) + 2\epsilon^o_{zz}PS - 2LQ\Delta T$$

$$G_4 = (2PT^3\Delta T + T^2\Delta T(3P-2QS) - (4QST+2QS+P)\Delta T)V +$$

$$QU\Delta T(2T^3+3T^2-1) + \epsilon^o_{zz}(-2PT^3+(2QS-P)T^2+PT+QS)$$

Case 2 $N = S = 0$

$$p_1(r) = A_1r^2 + B_1r + C_1$$

$$p_2(r) = A_2r^2 + B_2r + C_2$$

(I.6)

$$p_3(r) = A_3 r^2 + B_3 r + C_3$$

$$p_4(r) = A_4 r^3 + B_4 r^2 + C_4 r + D_4$$

where

$$\begin{aligned} A_1 &= M(2T^3 - T^2 + 1) \\ B_1 &= P(2T^3 - T^2 - 2T + 1) \\ C_1 &= Q(2T^3 - T^2 - 2T + 1) \end{aligned} \tag{I.7}$$

$$\begin{aligned} A_2 &= 3M(2T^3 - T^2 - 2T + 1) \\ B_2 &= 2P(2T^3 - T^2 - T + 1) \\ C_2 &= Q(2T^3 - T^2 - 2T + 1) \end{aligned} \tag{I.8}$$

$$\begin{aligned} A_3 &= -M(6T^3 + T^2 - 4T + 1) \\ B_3 &= -P(4T^3 - 3T + 1) \\ C_3 &= Q(-2T^3 + T^2 + 2T - 1) \end{aligned} \tag{I.9}$$

$$\begin{aligned} A_4 &= 4LM\Delta T(2T^3 + 3T^2 - 1) \\ B_4 &= 3(MU + LP)\Delta T(2T^3 + 3T^2 - 1) \\ C_4 &= 2(MV + PU)\Delta T(2T^3 + 3T^2 - 1) + 4T^3(LQ\Delta T - \epsilon^o_{zz}M) \end{aligned} \tag{I.10}$$

$$+ 2T^2(3LQ\Delta T - \epsilon^o_{zz}M) + 2(\epsilon^o_{zz}MT - LQ\Delta T)$$

$$D_4 = (VP + QU)\Delta T(2T^3 + 3T^2 - 1) - \epsilon^o_{zz}PT(2T^2 + T - 1)$$

Case 3 $M = N = L = 0$

$$p_1(r) = A_1r^4 + B_1r^3 + C_1r^2 + D_1r + E_1$$

$$p_2(r) = A_2r^4 + B_2r^3 + C_2r^2 + D_2r + E_2 \qquad \text{(I.11)}$$

$$p_3(r) = A_3r^4 + B_3r^3 + C_3r^2 + D_3r + E_3$$

$$p_4(r) = A_4r^5 + B_4r^4 + C_4r^3 + D_4r^2 + E_4r + F_4$$

where

$$A_1 = 2PS^3$$

$$B_1 = S^2(6PT + 2QS - P)$$

$$C_1 = S(6PT^2 + 2(3QS-P)T - QS - 2P \qquad \text{(I.12)}$$

$$D_1 = 2PT^3 + (6QS-P)T^2 - 2(QS+P)T - 2QS + P$$

$$E_1 = Q(2T^3 - T^2 - 2T + 1)$$

$$A_2 = 2PS^3$$

$$B_2 = 2PS^2(4T + 1)$$

$$C_2 = S(2P(5T^2 - 2) + Q(2T + 3)) \qquad \text{(I.13)}$$

$$D_2 = T(4PT^2 + 2(2QS - P)T + 2(QS - P)) - 2(QS - P)$$

$$E_2 = Q(2T^3 - T^2 - 2T + 1)$$

$$A_3 = -2PS^3$$

$$B_3 = -8PS^2T$$

$$C_3 = S(2P(-5T^2 + 2) - QS(2T - 1)) \qquad \text{(I.14)}$$

$$D_3 = -4T^2(PT - QS) + (2QS + 3P)T + 3QS - P$$

$$E_3 = Q(-2T^3 + T^2 + 2T - 1)$$

$$A_4 = 2PS^3U\Delta T$$

$$B_4 = 2PUS^2\Delta T(4T + 1)$$

$$C_4 = S^2V\Delta T(2PT - 2QS - P) + (2TS\Delta T(5PT + (QS+4P)) \qquad \text{(I.15)}$$

$$- S\Delta T(QS+2P))U - \epsilon^o_{zz}S^2(2PT-2QS+P)$$

$$D_4 = (2ST\Delta T(2PT + P - 2QS) - 2S\Delta T(2QS + P))V$$

$$+ (2T^2\Delta T(2PT + 2QS + 3P) + 2\Delta T(QST - QS - P))U$$

$$- 2\epsilon^o_{zz}S(2PT^2 - (2QS - P)T - P)$$

$$E_4 = \Delta T((2PT^3 + (3P - 2QS)T^2 - 4QST - 2QS - P)V + Q(2T^3$$

$$+ 3T^2 - 1)U) + \epsilon^o_{zz}(T(-2PT^2 + (2QS - P)T + P) + QS)$$

Case 4 M = N = L = S = 0

$$p_1(r) = A_1 r + B_1$$

$$p_2(r) = A_2 r + B_2 \qquad \text{(I.16)}$$

$$p_3(r) = A_3 r + B_3$$

$$p_4(r) = A_4 r + B_4$$

where

$$A_1 = P(2T^3 - T^2 - 2T + 1) \qquad \text{(I.17)}$$

$$B_1 = Q(2T^3 - T^2 - 2T + 1)$$

$$A_2 = 2P(2T^3 - T^2 - 2T + 1) \qquad \text{(I.18)}$$

$$B_2 = Q(2T^3 - T^2 - 2T + 1)$$

$$A_3 = P(-4T^3 + 3T - 1) \qquad \text{(I.19)}$$

$$B_3 = Q(-2T^3 + T^2 + 2T - 1)$$

$$A_4 = 2PU\Delta T(2T^3 + 3T^2 - 1) \qquad \text{(I.20)}$$

$$B_4 = \Delta T(PV + QU)(2T^3 + 3T^2 - 1) + \epsilon^{o}_{zz} PT(-2T^2 - T + 1)$$

BIBLIOGRAPHY

BIBLIOGRAPHY

Aboudi, J., 1987, "Damage in Composite-Modeling of Imperfect Bonding," Composites Science and Technology, Vol. 28, pp. 103-128.

Achenbach, J.D. and Zhu, H., 1989, "Effect of Interfacial Zone on Mechanical Behavior and Failure of Fiber-Reinforced Composites," Journal of the Mechanics and Physics of Solids, Vol. 37, pp. 381-393.

Achenbach, J.D. and Zhu, H., 1990, "Effect of Interphases on Micro and Macromechanical Behavior of Hexagonal-Array Fiber Composites," Journal of Applied Mechanics, Vol. 57, pp. 956-963.

Benveniste, Y., 1984, "On the Effect of Debonding of the Overall Behavior of Composite Materials," Mechanics of Materials, Vol. 3, pp. 349-358.

Benveniste, Y., 1985, "The Effective Mechanical Behavior of Composite Materials with Imperfect Contact Between the Constituents", Mechanics of Materials, Vol. 4, pp. 197-208.

Benveniste, Y., 1987, "A New Approach to the Application of Mori-Tanka's Theory in Composites Materials," Mechanics of Materials, Vol. 6, pp. 147-157.

Benveniste, Y., Dvorak, G.J., and Chen T., 1989, "Stress Fields in Composites with Coated Inclusions," Mechanics of Materials, Vol. 7, pp. 305-317.

Broutman, L.J. and Agarwal, B.D., 1974, "A Theoretical Study of the Effect of an Interfacial Layer on the Properties of Composites," Polymer Engineering Science, Vol. 14, pp. 581-588.

Budiansky, B., 1965, "On the Elastic Moduli of Some Heterogeneous Materials," Journal of the Mechanics and Physics of Solids, Vol. 13, pp. 223-227.

Budiansky, B., 1970, "Thermal and Thermoelastic Properties of Isotropic Composites," Journal of Composite Materials, Vol. 4, pp. 286-295.

Chatterjee, S.N. and Kibler, J.J., 1979, "An Analytical Model for Three Dimensionally Reinforced Graphite Composites," Vinson, J.R., ed., in Modern Developments in Composite Materials and Structures, ASME, pp. 269-287.

Chen, T., Dvorak, G.J., and Benveniste, Y., 1990, "Stress Field in Composite Reinforced by Coated Cylindrically Orthotropic Fibers," Mechanics of Materials, Vol. 9, pp. 17-32.

Christensen, R.M. and Waals,F.M., 1972, "Effective Stiffness of Randomly Oriented Fiber Composites," Journal of Composite Materials, Vol. 6, pp. 518-532.

Christensen, R.M., 1979, Mechanics of Composite Materials, J. Wiley & Sons Publishers, New York.

Christensen, R.M. and Lo, K.H., 1979, "Solutions for Effective Shear Properties in Three Phase Sphere and Cylinder Models," Journal of the Mechanics and Physics of Solids, Vol. 27, pp. 315-330.

Christensen, R.M., 1990, "A Critical Evaluation for a Class of Micro-Mechanics Models," Journal of the Mechanics and Physics of Solids, Vol. 38, pp. 379-404.

Craft, W.J. and Christensen, R.M., 1984, "Coefficient of Thermal Expansion for Composites with Randomly Oriented Fibers," in Environmental Effects on Composite Materials, George, S., ed., Springer Technomic Publishing Company, Inc., Vol. 2, pp. 330-347.

Cooper, G.A., 1965, "Orientation Effects in Fiber-Reinforced Metals," Journal of the Mechanics and Physics of Solids, Vol. 14, pp. 103-111.

Dekker, M.E.J., 1985, "The Deformation Behavior of Glass Bead-Filled Glassy Polymer," Ph.D. Dissertation, De Technische Hogeschool Eindhoven, Geboren Te Tilburg.

Drzal, L.T., 1983, "Composite Interphase Characterization," SAMPE Jounal, Sep/Oct, pp. 7-13.

Drzal, L.T., 1986, "The Interphase in Epoxy Composites," Advances in Polymer Science, Vol. 75, pp. 1-32.

Drzal, L.T., 1987, "Interface Considerations in Composite Materials," in Proceedings of The Workshop Held at Stanford Sierra Camp. Stanford University, pp. (4-39)-(4-48).

Dvorak, G.J. and Chen, T., 1989, "Thermal Expansion of Three-Phase Composite Materials," Journal of Applied Mechanics, Vol. 56, pp.418-422.

Dvorak, G.J., 1990, ed., Inelastic Deformation of Composite Materials, Springer-Verlag, New York.

Eshelby, J.D., 1957, "The Determination of the Elastic Field of an Ellipsoidal Inclusion, and Related Problems," Proceedings of the Royal Society, London, Series A, Vol. 241, pp. 376-396.

Ferrari, M., and Johnson, G.C., 1989, "Effective Elasticities of Short-Fiber Composites with Arbitrary Orientation Distribution," Mechanics of Materials, Vol. 8, pp. 67-73.

Hashin, Z., 1962, "The Elastic Moduli of Heterogeneous Materials," Journal of Applied Mechanics, Vol. 29, pp. 143-150.

Hashin, Z. and Shtrikman, S., 1963, "A Variational Approach to the Theory of the Elastic Behavior of Multiphase Materials," Journal of the Mechanics and Physics of Solids, Vol. 11, pp. 127-140.

Hashin, Z. and Rosen, B.W., 1964, "The Elastic Moduli of Fiber-Reinforced Materials," Journal of Applied Mechanics, Vol. 31, pp. 223-232.

Hashin, Z., 1983, "Analysis of Composite Materials- A Survey," Journal of Applied Mechanics, Vol. 50, pp. 481-505.

Hashin, Z., 1990a, "Thermoelastic Properties and Conductivity of Carbon/Carbon Fiber Composites," Mechanics of Materials, Vol. 8, pp. 293-308.

Hashin, Z., 1990b, "Thermoelastic properties of Fiber Composites with Imperfect Interface," Mechanics of Materials, Vol. 8, pp. 333-348.

Hashin, Z., 1991, "The Spherical Inclusion with Imperfect Interface," Journal of Applied Mechanics, Vol. 58, pp. 444-449.

Hatta, H. and Taya, M., 1985, "Effective Thermal Conductivity of a Misoriented Short Fiber Composite," Journal of Applied Physics, Vol. 58, pp. 2478-2486.

Hill, R., 1965, "A Self-Consistent Mechanics of Composite Materials," Journal of the Mechanics and Physics of Solids, Vol. 13, pp. 213-222.

Hughes, J.D.H., 1991, "The Carbon fiber/Epoxy Interface- A Review," Composites Science and Technology, Vol. 41, pp. 13-45.

Ishikawa, T., Koyama, K., and Kobayashi, S., 1978, "Thermal Expansion Coefficients of Unidirectional Composites," Journal of Composite Materials, Vol. 12, pp. 153-168.

Jasiuk, I., Mura, T., and Tsushida, E., 1988, "Thermal Stresses and Thermal Expansion Coefficients of Short Fiber Composites with Sliding Interfaces," Journal of Engineering Materials and Technology, Vol. 10, pp. 96-100.

Jasiuk, I. and Tong, Y., 1989, "The Effect of Interface on the Elastic Stiffness of Composites," in Mechanics of Composite Materials and Structures, eds. J.N. Reddy and J.L. Teply, ASME, New York, pp. 49-54.

Jasiuk, I., Chen, T., and Thorpe, M.F., 1989, "The Effect of Interface on the Elastic Properties of Fiber Composites with Rigid Inclusions," in Proceedings of the American Society for Composites, Technomic Publishing Co., Lancaster, PA, pp. 513-522.

Jasiuk, I., Chen, J. and Thorpe, M.F., 1992, "Elastic Moduli of Composites with Rigid Sliding Inclusions," Journal of the Mechanics and Physics of Solids, in press.

Jayaraman, K. and Reifsnider, K.L., 1990, "Micromechanical Stress Analysis of Continuous Fiber Composites with Local Material Property ," in Achievement in Composites in Japan and the united state, A. Kobayashi, ed., Kokon Shoin Co., Tokyo, pp. 421-428.

Jayaraman, K., Gao, Z., and Reifsnider, K.L., 1991, "Stress Fields in Continuous Fiber Composites with Interphasial Property Gradients," in Proceedings of the Sixth Technical Conference of the American Society for Composites, Technomic Publishing Co., Lancaster, PA, pp. 759-768.

Johnson, D.E., and Johnson, J.R., 1982, Mathematical Methods in Engineering and Physics, Prentice-Hall, Inc., Englewood Cliffs, New Jersey, pp. 42-50.

Jones, J.P., and Whittier, J.S., 1967, "Waves at a Flexibly Bonded Interface," Journal of Applied Mechanics, Vol. 34, pp. 905-909.

Jones, R.M., 1975, Mechanics of Composite Materials, McGraw-Hill, New York.

Kaplan, W., 1980, Advanced Mathematics for Engineers, Adison-Wesley Publishing Company, Reading, Massachusetts.

Kerans, R.J., Hay, R.S., Pagano, N.J., and Parthasarathy, T.A., 1989, "The Role of the Fiber-Matrix Interface in Ceramic Composites," Ceramic Bulletin, Vol. 68, pp. 429-442.

Kerner, E.H., 1956, "The Elastic and Thermoelastic Properties of Composite Media," Proceedings of the Physical Society, Vol. 69, pp. 807-808.

Laws, N., 1973, "On the Thermostatics of Composite Materials," Journal of the Mechanics and Physics of Solids, Vol. 21, pp. 9-17.

Lekhnitskii, S.G., 1963, Theory of Elasticity of an Anisotropic Elastic Body, Holden-day, Inc., San Francisco.

Lene, F., and Leguillon, D., 1982, "Homogenized Constitutive Law for a Partially Cohesive Composite Material," International Journal of Solids and Structures, Vol. 18, pp. 443-458.

Luo, H.A., and Weng, G.J., 1987, "On Eshelby's Inclusion Problem in a Three-Phase Spherically Concentric Solid, and a Modification of Mori-Tanaka's Method," Mechanics of Materials, Vol. 6, pp. 347-361.

Luo, H.A., and Weng, G.J., 1989, "On Eshelby's S-Tensor in a Three Phase Cylindrically Concentric Solid, and the Elastic Moduli of Fiber-Reinforced Composites," Mechanics of Materials, Vol. 8, pp. 77-88.

Macsyma, 1990, Vax Unix Macsyma Reference Manual, Version 11, Symbolics Inc., Michigan State University.

Mal, A.K. and Bose, S.K., 1974, "Dynamic Elastic Moduli of a Suspension of Imperfectly Bonded Spheres," in Proceedings of the Cambridge Philosophical Society, New York, Vol. 76, pp. 587-600.

Maurer, F.H.J., Simha, R., and Jain, R.K., 1986, "On the Elastic Moduli of Particulate Composites: Interlayer Versus Molecular Model," in Composite Interfaces, H. Ishida, ed., Elsevier, New York, pp. 367-375.

Maurer, F.H.J., Papazoglou, E., and Simha, R., 1988, "On the Theory of Particulate Composites: Interlayer vs. Molecular Model. II Thermal Expansivity," in Interfaces in Polymer, Ceramic, and Metal Matrix Composites, H. Ishida, ed., Elsevier, New York, pp. 747-755.

Maurer, F.H.J., 1990, "An Interlayer Model to Describe the Physical Properties of Particulate Composites," in Controlled Interphase in Composite Materials, H. Ishida, ed., Elsevier, New york, pp. 491-504.

Mikata, Y. and Taya, M., 1985, "Stress Field in a Coated Continuous Fiber Composite Subjected to Thermo-Mechanical Loadings," Journal of Composite Materials, Vol. 19, pp. 554-578.

Mikata, Y. and Taya, M., 1986, "Thermal Stress in a Coated Short Fiber Composite," ASME Journal of Applied Mechanics, Vol. 53, pp. 681-689.

Mori, T. and Tanaka, K., 1973, "Average Stress in Matrix and Average Elastic Energy of Materials with Misfitting Inclusions," Acta Metallurgica, Vol. 21, pp. 571-574.

Mori, T. and Wakashima, K., 1990, "Successive Iteration Method in the Evaluation of Average Fields in Elastically Inhomogeneous Materials," in Micromechanics and Inhomogeneity, G.J. Weng, M. Taya and H. Abe, eds, Spring-Verlag, New York, pp. 269-282.

Mura, T., 1982, Micromechanics of Defects in Solids, Martinus Nijhoff Publishers, Hague.

Mura, T. and Furuhashi, R., 1984, "The Elastic Inclusion with a Sliding Interface," Journal of Applied Mechanics, Vol. 51, pp. 308-310.

Mura, T., Jasiuk, I., and Tsushida, E., 1985, "The Stress Field of a Sliding Inclusion," International Journal of Solids and Structures, Vol. 12, pp. 1165-1179.

Norris, A.N., 1989, "An Examination of the Mori-Tanaka Effective Medium Approximation for Multiphase Composites," Journal of Applied Mechanics, Vol. 56, pp. 53-88.

Pagano, N.J., and Tandon, G.P., 1988, "Elastic Response of Multi-directional Coated Fiber Composites," Composite Science and Technology, Vol. 31, pp. 273-293.

Papanicolaou, G.C., Messinis, S.S., and Karakatsanidis, 1989, "The Effect of Interfacial Conditions on the Elastic-Longitudinal Modulus of Fiber Reinforced Composites," Journal of Material Science, Vol. 24, pp. 395-401.

Rosen, B.W. and Hashin, Z., 1970, "Effective Thermal Expansion Coefficients and Specific Heats of Composite Materials," Journal of the Mechanics and Physics of Solids, Vol. 8, pp. 157-173.

Shibata, S., Jasiuk, I., Mori, T., and Mura, T., 1990, "Successive Iteration Method Applied to Composite Containing Sliding Inclusions: Effective Modulus and Anelasticity," Mechanics of Materials, Vol. 9, pp.229-243.

Sideridis, E., 1988, "The In-Plane Shear Modulus of Fiber Reinforced Composites as Defined by the Concept of Interphase," Composites Science and Technology, Vol. 31, pp. 35-53.

Sottos, N.R., MaCullough, R.L., and Guceri, S.I., 1989, "Thermal Stresses due to Property Gradients at the Fiber-Matrix Interface," in Mechanics of Composite Materials and Structures, J.N. Reddy and J.L. Teply, eds., ASME, New York, pp.11-20.

Steif, P.S. and Hoysan, S.F., 1987, "An Energy Method for Calculating the Stiffness of Aligned Short-Fiber Composites," Mechanics of Materials, Vol. 6, pp. 197-210.

Steif, P.S. and Hoysan, S.F., 1988, "Longitudinal Shearing of a Weakly Bonded Fiber Composite," Journal of Applied Mechanics, Vol. 55, pp. 618-623.

Sullivan, B.J. and Hashin, Z., 1990, "Determination of Mechanical Properties of Interfacial Region Between Fiber and Matrix in Organic Matrix Composite," in Controlled Interphases in Composite Materials, H. Ishida, ed., Elsevier, New York, pp. 521-537.

Takahashi, K. and Chou, T., 1988, "Transverse Elastic Moduli of Unidirectional Fiber Composite with Interfacial Debonding," Metallurgical Transactions A, Vol. 19A, pp. 129-135.

Takao, Y., Chou, T.W., and Taya, M., 1982, "Effective Longitudinal Young's Modulus of Misoriented Short Fiber Composites," Journal of Applied Mechanics, Vol. 49, pp. 536-540.

Takao, Y., 1985, "Thermal Expansion Coefficients of Misoriented Short-Fiber Reinforced Composites," American Society for Testing and Materials, ed., Vinson,J.R. and Taya, M., pp. 685-699.

Takao, Y. and Taya, M., 1985, "Thermal Expansion Coefficients and Thermal Stresses in an Aligned Short Fiber Composite with Application to a Short Carbon Fiber/Aluminum," Journal of Applied Mechanics, Vol. 52, pp. 806-810.

Tandon, G.P. and Weng, G.L., 1986a, Stress Distribution in and Around Spheroidal Inclusions and Voids at Finite Concentration," Journal of Applied Mechanics, Vol. 53, pp. 511-518.

Tandon, G.P. and Weng, G.J., 1986b, "Average Stress in the Matrix and Effective Moduli of Randomly Oriented Composites," Composites Science and Technology, Vol. 27, pp. 111-132.

Taya, M. and Chou, T.W., 1981, "On Two Kinds of Ellipsoidal Inhomogeneities in an Infinite Elastic Body: An Application to a Hybrid Composite," International Journal of Solids and Structures, Vol. 17, pp. 553-563.

Taya, M. and Mura, T., 1981, "On Stiffness and Strength of an Aligned Short-Fiber Reinforced Composite Containing Fiber-End Cracks Under Uniaxial Applied Stress," Journal of Applied Mechanics, Vol. 48, pp. 361-367.

Taya, M. and Arsenault, R., 1989, Metal Matrix Composites, Pergamon Press, Inc., New York.

Taya, M., Dunn, M., Derby, B., and Walker, J., 1990, "Thermal Residual Stress in a Two-Dimensional In-Plane Misoriented Short Fiber Composite," Applied Mechanics Reviews, Vol. 43, pp. S294-S303.

Theocaris, P.S., 1983, "Interface-Interphase in Composite Materials," in Proceedings of the International Conference, J. Liegeois and S. Okuda eds., SPE publication, pp. t1-t28.

Theocaris, P.S., 1984, "The Adhesion Quality and the Extent of the Mesophase in Particulates," Journal of Reinforced Plastics and Composites, Vol. 3, pp. 204-231.

Theocaris, P.S., 1986, "The Concept and Properties of Mesophase in Composites," in Composite Interfaces, H. Ishida and J.L. Koenig, eds., North-Halland, pp. 329-349.

Theocaris, P.S., 1987, The Concept of Mesophase in Composites, Springer Verlag, Berlin.

Tong, Y. and Jasiuk, I., 1988, "The Effect of Interface on the Mechanical Properties of Composites," in Interfaces in Polymer, Ceramic and Metal Matrix Composites, H. Ishida, ed., Elsevier, pp. 757-764.

Tong, Y., 1990, "The Effect of Interface on Thermo-Mechanical Properties of Composites," Ph.D. Dissertation, Michigan State University, East Lansing, Michigan.

Tong, Y. and Jasiuk, I., 1990a, "Thermal Stresses and Thermal Expansion Coefficients of Composites Reinforced with Coated Spherical Particles," in Controlled Interphases in Composite Materials, H. Ishida, ed., Elsevier, New York, pp. 539-548.

Tong, Y. and Jasiuk, I., 1990b, "Transverse Elastic Moduli of Composites Reinforced with Cylindrical Coated Fibers: Successive Iteration Method," in Proceedings of the American Society for Composites, Technomic, Lancaster, PA, pp. 117-126

Uemura, M., Iyama, H., and Yamaguchi, Y., 1979, "Thermal Residual Stresses in Filament-Wound Carbon-Fiber-Reinforced Composites," Journal of Thermal Stresses, Vol. 2, pp. 393-412.

Vedula, M., Pangborn, R.N., and Queeney, R.A., 1988, "Modification of Residual Thermal Stress in a Metal-Matrix Composite with the Use of a Tailored Interfacial Region," Composites, Vol. 19, pp. 133-137.

Von Mises, R., 1928, "Mechanik der Plastischen Formanderung Von Kristallen," Zeit. Angew. Math. Mech., Vol. 8, pp. 161-185.

Wakashima, K., Otsuka, M., and Umekawa, S., 1974, "Thermal Expansions of Heterogeneous Solids Containing Aligned Ellipsoidal Inclusions," Journal of Composite Materials, Vol. 8, pp. 391-404.

Weng, G.J., 1984, "Some Elastic Properties of Reinforced Solids, with Special Reference to Isotropic Ones Containing Spherical Inclusions," International Journal of Engineering Science, Vol. 22, pp. 845-856.

Wu, T.T., 1966, "The Effect of Inclusion Shape on the Elastic Moduli of a Two-Phase Material," International Journal of Solids and Structures, Vol. 2, pp. 1-8.

Zhao, Y.H., Tandon, G.P., and Weng, G.J., 1988, "Elastic Moduli for a Class of Porous Materials," Acta Mechanica, Vol. 76, pp. 105-131.